Turun yliopisto
University of Turku

INTEGRATIVE REGULATION OF MAJOR BIOENERGETIC PATHWAYS IN *SYNECHOCYSTIS* SP. PCC 6803

Tuomas Huokko

TURUN YLIOPISTON JULKAISUJA – ANNALES UNIVERSITATIS TURKUENSIS
Sarja – ser. AI osa – tom. 576 | Astronomica – Chemica – Physica – Mathematica | Turku 2018

Turun yliopisto
University of Turku

INTEGRATIVE REGULATION OF MAJOR BIOENERGETIC PATHWAYS IN *SYNECHOCYSTIS* SP. PCC 6803

Tuomas Huokko

TURUN YLIOPISTON JULKAISUJA – ANNALES UNIVERSITATIS TURKUENSIS
Sarja - ser. A I osa - tom. 576 | Astronomica - Chemica - Physica - Mathematica | Turku 2018

University of Turku

Faculty of Science and Engineering
Department of Biochemistry
Laboratory of Molecular Plant Biology

Supervised by

Academician Eva-Mari Aro
Laboratory of Molecular Plant Biology
Department of Biochemistry
University of Turku, FI-20014
Turku, Finland

Dr. Natalia Battchikova
Laboratory of Molecular Plant Biology
Department of Biochemistry
University of Turku, FI-20014
Turku, Finland

Assoc. Prof. Yagut Allahverdiyeva
Laboratory of Molecular Plant Biology
Department of Biochemistry
University of Turku, FI-20014
Turku, Finland

Reviewed by

Prof. Julian Eaton-Rye
Department of Biochemistry
University of Otago
New Zealand

Dr. Kirstin Gutekunst
Botanical Institute
Christian-Albrechts University of Kiel
Germany

Opponent

Prof. Nir Keren
Department of Plant and Environmental Sciences
The Alexander Silberman Institute of Life Sciences
Hebrew University of Jerusalem
Israel

ISBN 978-951-29-7146-6 (PRINT)
ISBN 978-951-29-7147-3 (PDF)
ISSN 0082-7002 (Print)
ISSN 2343-3175 (Online)
Painosalama Oy - Turku, Finland 2018

LIST OF ORIGINAL PUBLICATIONS

This thesis is composed of the following scientific articles, referred to in the text by their Roman numerals.

I. Ermakova M*, Huokko T*, Richaud P, Bersanini L, Howe CJ, Lea-Smith DJ, Peltier G, Allahverdiyeva Y (2016) Distinguishing the roles of thylakoid respiratory terminal oxidases in the cyanobacterium *Synechocystis* sp. PCC 6803. Plant Physiology 171: 1307–1319. *=equal contribution

II. Kämäräinen J*, Huokko T*, Kreula S*, Jones PR, Aro EM, Kallio P (2017) Pyridine nucleotide transhydrogenase PntAB is essential for optimal growth and photosynthetic integrity under low-light mixotrophic conditions in *Synechocystis* sp. PCC 6803. New Phytologist 214: 194–204. *=equal contribution

III. Huokko T, Muth-Pawlak D, Battchikova N, Allahverdiyeva Y, Aro EM (2017) Role of type 2 NAD(P)H dehydrogenase NdbC in regulation of carbon allocation in Synechocystis 6803. Plant Physiology 174: 1863-1880.

IV. Huokko T, Muth-Pawlak D, Aro EM. Thylakoid localized type 2 NAD(P)H dehydrogenase NdbA optimizes light-activated heterotrophic growth of *Synechocystis* sp. PCC 6803. Manuscript.

Other publications related to the topic:

Georg J, Kostova G, Vuorijoki L, Schön V, Kadowaki T, Huokko T, Baumgartner D, Müller M, Klähn S, Allahverdiyeva Y, Hihara Y, Futschik ME, Aro EM, Hess WR (2017) Acclimation of Oxygenic Photosynthesis to Iron Starvation Is Controlled by the sRNA IsaR1. Current Biology 27: 1425-1436.

TABLE OF CONTENTS

ABBREVIATIONS

ABC	adenosine triphosphate binding cassette
ACN	acetonitrile
ATP	adenosine triphosphate
ARTO	alternative respiratory terminal oxidase
BG-11	growth medium for cyanobacteria
Bp	basepair
CA	carbonic anhydrase
CBB	Calvin-Benson-Bassham cycle
CCM	carbon concentrating mechanisms
CET	cyclic electron transport
Chl *a*	chlorophyll *a*
Cox	cytochrome *c* oxidase
Cyd	cytochrome *bd* quinol oxidase
Cyt b_6f	cytochrome b_6f complex
Cyt c_6	cytochrome c_6
DBMIB	2,5-dibromo-6-isopropyl-3-methyl-1,4-benzoquinone
DCBQ	2,5-dichloro-1,4-benzoquinone
DCMU	3-(3,4-dichlorophenyl)-1,1-dimethylurea
DDA	data-dependent acquisition
DNA	deoxyribonucleic acid
DPOR	light-independent protochlorophyllide reductase
ED	Entner–Doudoroff pathway
EMP	Embden–Meyerhof–Parnas pathway
ETC	electron transfer chain
F_0	the mimimal fluorescence from dark-adapted samples
FA	formic acid

FAD	flavin adenine dinucleotide
FC	fold change
Fd	ferredoxin
FDP, Flv	flavoprotein
Fdx	flavodoxin
FL	fluctuating light conditions
F_m'	the maximum level of fluorescence under actinic light
F_m^D	the maximum level of fluorescence without actinic light
F_m^{FR}	the maximum level of fluorescence after far-red illumination
FMN	flavin mononucleotide
FNR $_{(L/S)}$	ferredoxin:$NADP^+$ oxidoreductase (long/short form)
FR	far-red
FRP	fluorescence recovery protein
F_S	the steady state fluorescence
F_v	variable fluorescence, (F_m-F_0)
F_v/F_m	the maximum quantum yield of PSII
GA3P	glyceraldehyde 3-phosphate
GL	growth light
HC	high CO_2 conditions (3% CO_2)
HEPES	4-(2-hydroxyethyl)-1-piperazineethanesulfonic acid
HL	high light conditions
HQNO	2-heptyl-4-hydroxyquinoline n-oxide
KCN	potassium cyanide
LAHG	light-activated heterotrophic growth conditions
LC	low CO_2 conditions, ambient CO_2 level
LC-MS/MS	liquid chromatography-tandem mass spectrometry
LET	linear electron transport
LED	light emitting diode

LICS	light-independent chlorophyll synthesis
MIMS	membrane inlet mass spectrometry
NADH	nicotinamide adenine dinucleotide (reduced)
NADPH	nicotinamide adenine dinucleotide phosphate (reduced)
NDH-1	type 1 NAD(P)H dehydrogenase
NDH-2	type 2 NAD(P)H dehydrogenase
NPQ	non-photochemical quenching
OCP	orange carotenoid protein
OD_{750}	optical density at 750 nm
2-OG	2-oxoglutarate
OEC	oxygen-evolving complex
OM	outer membrane
OPP	oxidative pentose phosphate pathway
ORF	open reading frame
P680/$P680^+$	primary electron donor of PSII (reduced/oxidized)
P700/$P700^+$	primary electron donor of PSI (reduced/oxidized)
PBP	phycobiliprotein
PBS	phycobilisomes
PC	plastocyanin
PCR	polymerase chain reaction
2-PG	2-phosphoglycolate
3-PGA	3-phosphoglycerate
pH	negative logarithm of proton concentration
PM	plasma membrane
P_m	the maximum level of oxidizable P700
P_m'	the maximum level of oxidizable P700 under actinic light
Pmf	proton motive force

PQH_2/PQ	plastoquinol/plastoquinone
PSI	photosystem I
PSII	photosystem II
Q_A	the primary electron-accepting plastoquinone of PSII
Q_B	the secondary electron-accepting plastoquinone of PSII
RNA	ribonucleic acid
ROS	reactive oxygen species
RTO	respiratory terminal oxidase
RT-qPCR	real-time quantitative polymerase chain reaction
Rubisco	ribulose 1,5-bisphosphate carboxylase/oxygenase
RuBP	ribulose 1,5-bisphosphate
ROS	reactive oxygen species
SDH	succinate dehydrogenase
SRM	selected reaction monitoring
TCA	tricarboxylic acid
TEM	transmission electron microscopy
TES	2-{[1,3-Dihydroxy-2-(hydroxymethyl)-2-propanyl]amino}ethanesulfonic acid
TM	thylakoid membrane
UV	ultraviolet
Y(I)	the effective quantum yield of PSI
Y(II)	the effective quantum yield of PSII
Y(NA)	the acceptor side limitation of PSI
Y(ND)	the donor side limitation of PSI

ABSTRACT

Cyanobacterial photosynthetic and respiratory electron transport chains are both located in the thylakoid membrane producing ATP and reducing agent NADPH. The other major cellular reducing equivalent, NADH, is mainly produced in catabolic reactions in the cytosol. In this thesis work, I took biophysical, biochemical and proteomic approaches to analyze the crosstalk between these two bioenergetic networks in the thylakoids of the cyanobacterium *Synechocystis* sp. PCC 6803 (hereafter, *Synechocystis*). Furthermore, novel proteins with a potential function in regulation of the NAD(P)H/NAD(P)$^+$ balance in this organism were addressed.

Canonical respiratory reactions are completed by respiratory terminal oxidases (RTO), and two of them, Cox and Cyd, reside in the thylakoid membrane of *Synechocystis*. In this work, I show that thylakoid-located RTOs function not only in darkness but also under illumination, alleviating the redox poise of the photosynthetic electron transfer chain by donating electrons to O_2. However, they do not have a high capacity to accept electrons under light as demonstrated for the flavodiiron proteins Flv1 and Flv3. Cyd is the main RTO performing O_2 photoreduction by electrons derived from the PQ pool and originating from Photosystem (PS) II mediated water splitting. Cox, on the other hand, is the most important RTO in dark respiration, but it can compete with PSI for electrons deriving from water splitting by PSII under high light if Cyd is absent.

In addition to providing energy, the regulation of NAD(P)H/ NAD(P)$^+$ redox homeostasis, which allows the interplay between anabolic and catabolic metabolism, becomes extremely important when cyanobacteria switch from one growth mode to the other. Pyridine nucleotide transhydrogenase PntAB is an integral membrane protein complex coupling the oxidation of NADH and concurrent reduction of NADP$^+$ to proton translocation across the membrane. I demonstrate that PntAB, which is located in the thylakoid membrane, is indispensable for the growth of *Synechocystis* under low-light mixotrophy, being the major source for NADPH under these conditions. Furthermore, PntAB has an indirect effect on the maintenance of the photosynthetic machinery under low-light mixotrophic conditions. The second group of enzymes functioning in pyridine nucleotide redox reactions is type 2 NAD(P)H dehydrogenases (NDH-2), which catalyze electron transport from NAD(P)H to quinones without simultaneous proton translocation or major effect on respiration. *Synechocystis* has three NDH-2s: NdbA, NdbB and NdbC. I show that under photoautotrophic conditions the absence of the plasma membrane located NdbC causes downregulation of glycolytic enzymes, likely due to the elevated NADH/NAD$^+$ ratio, which provokes modulations in several metabolic pathways and in cell morphology. Nevertheless, the Δ*ndbC* mutant showed growth retardation only upon light-activated heterotrophic growth (LAHG). On the other hand, NdbA, which resides in the thylakoid membrane, is required for optimal growth of *Synechocystis* under LAHG conditions by regulating photosynthetic functionality as well as inorganic carbon uptake.

Results presented in this thesis provide a better means to design cyanobacteria-based living factories where both the direction of the maximum amount of electrons to desired end products, and optimal regulation of the NAD(P)H/NAD(P)$^+$ ratio, are essential for the maximal productivity.

TIIVISTELMÄ

Syanobakteerien energia-aineenvaihdunta koostuu fotosynteesin valoreaktioiden ja soluhengityksen elektroninsiirtoreaktioista, jotka tapahtuvat pääosin tylakoidikalvolla, sekä niiden vuorovaikutuksesta soluliman hapetus-pelkistysreaktioiden kanssa. Väitöskirjatyössäni selvitin kahden tylakoidikalvon bioenergeettisten elektroninsiirtoverkoston yhteistoimintaa *Synechocystis* sp. PCC 6803 – syanobakteerissa sekä karakterisoin ”uusia” proteiineja, jotka mahdollisesti osallistuvat soluliman NADPH- ja NADH-molekyylien hapetus-pelkistystasapainon säätelyyn.

Terminaalioksidaasit (RTO) ovat proteiinikomplekseja, jotka päättävät pimeässä tapahtuvan soluhengityksen elektroninsiirtoreaktiot. Kaksi niistä, Cox ja Cyd, sijaitsevat *Synechocystis*-syanobakteerin tylakoidikalvossa. Osoitin, että nämä RTO:t eivät toimi pelkästään pimeässä vaan myös valossa, jolloin ne estävät fotosynteettisen elektroninsiirtoketjun liiallista pelkistymistä ja vaurioitumista luovuttamalla ylimääräisiä elektroneja hapelle. Cyd on tärkein valossa toimiva RTO ja välittää valoreaktio (PS) II:den hajottamasta vedestä peräisin olevia elektroneja PQ-poolista hapelle. Cox taas on tärkein RTO soluhengityksessä, mutta se kykenee myös valossa kilpailemaan elektroneista PS I:den kanssa, jos Cyd puuttuu.

NAD(P)H/NAD(P)$^+$ -tasapainon säätely mahdollistaa anabolisten ja katabolisten aineenvaihduntareittien sujuvan yhtäaikaisen toiminnan. Tämän säätelyn merkitys korostui erityisesti, kun syanobakteereja kasvatettiin glukoosin läsnäollessa. Osoitin, että pyridiininukleotiditranshydrogenaasi PntAB, joka samanaikaisesti hapettaa NADH:n ja pelkistää NADP$^+$:n, sijaitsee tylakoidikalvoilla. Reaktion vaatima energia saadaan protonien siirrosta kalvon puolelta toiselle. PntAB osoittautui välttämättömäksi *Synechocystis*-syanobakteerin kasvulle miksotrofisissa oloissa, kun valon määrä on pieni. Täten PntAB on solun pääasiallinen NADPH:n lähde näissä olosuhteissa, ja lisäksi entsyymin toiminnalla on epäsuora vaikutus fotosynteettisen koneiston toimintakuntoon.

NAD(P)H:ta hapettavat myös tyypin 2 NAD(P)H dehydrogenaasit (NDH-2), jotka katalysoivat elektronin siirtoa NAD(P)H:lta kinoneille. *Synechocystis*-syanobakteerilla on kolme NDH-2:ta: NdbA, NdbB ja NdbC, joiden osuus soluhengitykseen on kyseenalaistettu ja toiminta solussa on jäänyt epäselväksi. Työssäni osoitan, että fotoautotrofisissa olosuhteissa solukalvolla sijaitsevan NdbC:n puute johtaa glykolyyttisten entsyymien määrän vähenemiseen, joka todennäköisesti aiheutuu kohonneesta solunsisäisestä NADH/NAD$^+$ -suhteesta. Tämä taas saa aikaan muutoksia useissa metaboliareiteissä ja solun morfologiassa. NdbC-proteiini osoittautui välttämättömäksi *Synechocystis*-syanobakteerin kasvulle LAHG-olosuhteissa. Samoin NdbA, joka puolestaan sijaitsee tylakoidikalvolla, vaaditaan optimaaliseen kasvuun LAHG-olosuhteissa johtuen siitä, että NdbA osaltaan säätelee sekä fotosynteesin toimivuutta että epäorgaanisen hiilen kuljetusta solun sisälle näissä olosuhteissa.

Väitöskirjani tulokset tuovat lisää tietoa liittyen sekä elektronien maksimaalisen määrän ohjaamiseen haluttuihin lopputuotteisiin että NAD(P)H/NAD(P)$^+$ -suhteen optimaaliseen säätelyyn, jotka molemmat tulee ottaa huomioon tuotettaessa syanobakteereissa erilaisia hyödyllisiä kemikaaleja mahdollisimman tehokkaasti.

Giving up is the only sure way to fail.

- Gena Showalter -

1. INTRODUCTION

1.1. Cyanobacteria: prokaryotes with oxygenic photosynthesis

Cyanobacteria are an exceptional group among prokaryotes due to their ability to perform oxygenic photosynthesis. In this process, which was evolved in early cyanobacteria (for a review, see Holland, 2006), the physical energy from sunlight is converted to chemical energy to reduce atmospheric CO_2, using water as an electron source and releasing O_2 as a by-product. The exact timing of the birth of oxygenic photosynthesis is still under debate. The current view is that it may have evolved either shortly before the Great Oxygenation Event, about 2.4 billion years ago, or a few hundred million years prior to it (Brocks et al., 2003; Kopp et al., 2005; Rasmussen et al., 2008; Flannery and Walter, 2012; Lyons et al., 2014). On the other hand, fossil findings indicate that photosynthetic microbes in the form of stromatolites may have already existed 3.5 billion years ago (Schopf, 1993; Drews, 2011). As a result of oxygenic photosynthesis, the O_2 concentration of Earth's atmosphere began to increase gradually, which was a huge cataclysm for life on Earth. Organisms had to evolve mechanisms that helped them cope with the biotoxicity of O_2 and its derivatives (Rees and Howard, 2003). The accumulation of O_2 also made possible the evolution of aerobic respiration, where O_2 can be used as a strong terminal acceptor for electrons, leading to the evolution of more advanced life forms (Blankenship, 1992). In addition, the increased atmospheric O_2 concentration caused the formation of an ozone layer that protects Earth from UV radiation, which helped life spread to terrestrial habitats (Berkner and Marshall, 1965; reviewed in Cockell and Raven, 2007). Besides their role as pioneers of oxygenic photosynthesis, cyanobacteria are also considered as progenitors of chloroplasts (Wolfe et al., 1994). The primary endosymbiosis event, where a primal larger eukaryotic cell engulfed early cyanobacteria, has been dated to have occurred circa 1.5 billion years ago (Yoon et al., 2004). This eventually resulted in three lineages of organisms containing chloroplasts: chlorophyta, rhodophyta, and glaucophyta.

The cyanobacterial phylum is diverse, and it contains solitary and colony-forming unicellular and as filamentous species. Rippka et al. (1979) have classified cyanobacterial species in five main groups according to their morphology and their development. Sections I and II include unicellular cyanobacteria whereas sections III-V are composed of filamentous species. Nowadays cyanobacteria are more frequently classified based on the type of their ribulose bisphosphate carboxylase/oxygenase (Rubisco) and carboxysomes. The α-cyanobacteria, which are marine species, have

Form-1A Rubisco and α-carboxysomes whereas β-cyanobacteria, which inhabit a vast range of environmental niches, have Form-1B Rubisco and β-carboxysomes (for a review, see Badger et al., 2006). The α- and β-carboxysomes have different shell proteins (Badger and Price, 2003), but both carboxysome types share a common phylogenetic origin (Kerfeld et al., 2005). Even though α-carboxysomes are slightly smaller than β-carboxysomes, the higher intracellular copy number of α-carboxysomes compared to β-carboxysomes equalizes the concentration of Rubisco per unit volume (Whitehead et al., 2014). Despite significant amino acid sequence differences between Form-1A and Form-1B Rubisco, their reaction kinetics for CO_2 and ribulose 1,5-bisphosphate (RuBP) are similar (Whitehead et al., 2014).

One of the most common features of different cyanobacteria is their thick peptidoglycan layer consisting of sugars and amino acids that form a mesh-like layer which provides structural strength. It is situated in the periplasmic space between the outer (OM) and the plasma membranes (PM) (for a review, see Hoiczyk and Hansel, 2000). Thus, cyanobacteria belong to the group of Gram-negative bacteria. The OM is coated with a network of polysaccharides, called the glycocalyx, which protects cells from, for example, desiccation and also diminishes solute loss (Gantt, 1994). The PM houses several proteins involved in transportation, signal transduction and respiration (for a review, see Hahn and Schleiff, 2013). In cyanobacteria, the innermost membrane ensemble, the thylakoid membrane (TM), forms a sheet-like structure, as opposed to plants, where the TM is organized in grana stacks and non-appressed membranes (Nevo et al., 2007; Liberton et al., 2013). The TM forms the boundary for the lumenal compartment, separating it from other cellular components, which is essential for photosynthesis. Since TM accommodates both photosynthetic and respiratory electron transport (for a review, see Vermaas, 2001; Mullineaux, 2014a), it is a center of energy provision in cyanobacteria.

1.2. The ecological and economical significance of cyanobacteria

Cyanobacteria comprise one of the most abundant and widespread micro-organism groups on Earth. They can be found in terrestrial and aquatic habitats varying from hot springs to deserts. Some cyanobacterial species form symbiotic relationships with a variety of hosts including, plants, fungi, and animals, in which cyanobacteria supply the host with fixed carbon and nitrogen (for a review, see Bergman et al., 1993). Nowadays cyanobacteria account for circa 30% of O_2 production (DeRuyter and Fromme, 2008) and contribute about 30% of global CO_2 fixation (Bryant, 2003), which makes them one the most important groups of primary producers for all lifeforms on Earth. The

significance of cyanobacteria in primary production is highlighted in marine ecosystems. It is estimated that cyanobacteria contribute as much as one-half of oceanic primary production (Field et al., 1998). Some cyanobacteria are diazotrophic, fixing atmospheric nitrogen (N_2), which has a considerable influence on the nitrogen cycle. This is especially true in the oceans (Montoya et al., 2004) where, according to estimations, diazotrophic cyanobacteria produce almost half of the biologically available nitrogen (Stal, 2009).

Since cyanobacteria are the ancestors of chloroplasts, it is conceivable that their oxygen evolving photosynthetic machinery is principally similar to the one in plants. Therefore, cyanobacteria have been extensively utilized as model organisms in photosynthesis research as they offer several advantages compared to plants. First, cyanobacteria are prokaryotes containing small genome, which size varies from 1.4 Mbp to 9.1 Mbp depending on the species, being relatively little compared to eukaryotes. Currently, 376 completely sequenced cyanobaterial genomes, of which 86 are complete genomes and 290 are draft genomes, are available (Fujisawa et al., 2017). The second advantage is that several cyanobacteria are naturally competent for exogenous DNA-transformation, which is advantageous for targeted mutagenesis. Many important processes, including photosynthetic light reactions, carbon fixation, acclimation to environmental stress conditions, and cell differentiation, have been extensively studied with cyanobacteria. Widely used cyanobacterial model species include unicellular freshwater species *Synechocystis* sp. PCC 6803 (for details, see section 1.3.), *Synechococcus elongatus* PCC 7942, *Synechococcus elongatus* PCC 7002 and *Thermosynechococcus elongatus* BP-1, as well as nitrogen fixing filamentous freshwater *Anabaena* (*Nostoc*) sp. PCC 7120 and unicellular marine *Prochlorococcus marinus* MED4, but the list of model cyanobacteria expands continuously.

In addition to basic research, cyanobacteria have recently become one of the most intriguing options for practicing sustainable bioeconomy due to the several advantages they offer. Cyanobacteria have a high growth rate, which leads to fast biomass production, and their nutrient requirements are minimal. Furthermore, cyanobacteria do not compete for arable land, are capable of efficient CO_2 fixation and are relatively easy to manipulate genetically. Cyanobacteria have thus become an important source of proteins, lipids and other bioactive compounds, such as numerous high-value secondary metabolites that can be utilized either pharmacologically or in industrial biotechnology (for a review, see Singh et al., 2017). In addition, cyanobacteria produce several types of renewable biofuels, including carbohydrates, fatty acids, alcohols, and H_2 (for a review, see Sarsekeyeva et al., 2015). Even though biofuel production using

cyanobacteria is often considered as a non-profitable method, the development of emerging technologies that can overcome the bottlenecks of production systems, the application of genetic modifications and the adoption of synthetic biology approaches will lead to the generation of “designer cells” with strong production properties.

1.3. *Synechocystis* sp. PCC 6803

Synechocystis sp. PCC 6803 (hereafter *Synechocystis*) is a unicellular, nontoxic, non-diazotrophic freshwater β-cyanobacterium, which was collected from a Californian lake in 1968 (Stanier et al., 1971). *Synechocystis* became the first photosynthetic organism whose entire genome was sequenced (Kaneko et al., 1996). The genome (3.6 Mbp) exists in several copies depending on the growth phase (Zerulla et al., 2016) and includes around 3200 open reading frames (ORF) (Mitschke et al., 2011). In addition, *Synechocystis* has seven plasmids containing roughly 400 ORFs (Labarre et al., 1989). *Synechocystis* is naturally competent for exogenous DNA transformation, which simplifies targeted mutagenesis (Kufryk et al., 2002). The glucose-tolerant substrain is widely used in laboratories around the world due to its ability to grow without active photosynthesis (Williams, 1988). All this has made *Synechocystis* one of the most extensively studied photosynthetic model organisms.

1.4. Photosynthesis of cyanobacteria

Cyanobacteria perform oxygenic photosynthesis, where energy derived from sunlight is converted to chemical energy and oxygen is released as a by-product. The chemical energy is then utilized to produce energy-rich carbohydrates which are used for biosynthesis of other compounds and for sustaining growth. Photosynthetic reactions can be divided into light reactions and carbon fixation reactions. Light reactions are performed in the TM by four major protein complexes: the water splitting photosystem II (PSII), the cytochrome b_6f complex (Cyt b_6f), photosystem I (PSI) and ATP synthase (Figure 1A). Electrons derived from PSII are finally delivered to $NADP^+$ for NADPH-formation in the so-called linear electron transport (LET) process. Simultaneously, the proton motive force (pmf) is established across the TM and harnessed for ATP synthesis. The obtained NADPH and ATP are used as reducing power and energy for CO_2 fixation and the production of triosephosphates in the Calvin-Benson-Basham cycle (hereafter CBB cycle) in the cytosol. In addition to LET, cyanobacteria have several auxiliary electron transport routes which can be utilized for energy provision, as protective electron sinks, and for the regulation of the redox state of cells.

1.4.1. Light-harvesting in cyanobacteria

In cyanobacteria, the light-harvesting antennas are called phycobilisomes (PBS) (Figure 1A). These efficiently capture sun light for the excitation of photosystems (Grossman et al., 1993; for a review see MacColl, 1998). PBS form soluble assemblies, which can be up to 7000 kDa in size, on the cytosolic side of thylakoids. The light-capturing part of PBS consists of phycobiliproteins (PBP) which covalently bind the chromophores called phycobilins. PBPs can be divided into three groups: phycocyanins, allophycocyanins, and phycoerythrins. Together with chlorophyll *a* (Chl) and carotenoids, they ensure that cyanobacteria can utilize most of the visible light spectrum. PBPs are able to efficiently absorb wavelengths between 500–560 nm (Glazer, 1984; DeRuyter and Fromme, 2008), whereas the absorption maxima are at 430-440 nm/670 nm for Chl and at 420-480 nm for carotenoids (Mimuro and Katoh, 1991). Colorless linker polypeptides connect PBPs to the rods and core which form the basic structure of PBS. The strict arrangement of PBPs in a rod, due to their absorption and emission qualities, ensures unidirectional energy transport towards the core of PBS, and further to the photosystems. There are differences in the types of PBPs and the structure of PBS between cyanobacterial species. In *Synechocystis*, the rods are composed of phycocyanin (absorption peak at 620 nm). From the rods, energy is first transferred to a PBS core composed of allophycocyanin (absorption peak at 650 nm) and then, via linker proteins and terminal emitters, to the photosystems. A more detailed description about the structure of the *Synechocystis* PBS is provided by Arteni et al. (2009).

In cyanobacteria, the rearrangement of the PBS interaction either with PSII or with PSI is called a state transition (for a review, see Kirilovsky, 2015). This allows cells to control the energy distribution between photosystems during changes in illumination. If the PBSs are mainly energetically coupled to PSII and, PSII thus receives more light energy than PSI, cells are in state I (Campbell et al., 1998). Vice versa, when most of the PBSs are associated with PSI, cells are in state II. In cyanobacteria, state transitions are assumed to be triggered by the alterations in the redox state of the PQ pool (Mullineaux and Allen, 1990), but the mechanism mediating this signal still remains unknown. It has also been suggested that Cyt b_6f may be involved in the control of state transitions in cyanobacteria (Mao et al., 2002; Huang et al., 2003). In the dark, as opposed to green algae and higher plants, cyanobacteria are in state II caused by the reduced PQ pool as a result of respiration. Illumination of the cyanobacterial cells induces a shift towards state I. Several hypotheses have been presented regarding the mechanisms of state transitions. For example, PBS could move from one photosystem to the other (Joshua

and Mullineaux, 2004) or, otherwise, an energy "spillover" could happen from PSII to PSI mediated by Chl (McConnell et al., 2002). A functional megacomplex including a PBS antenna and both PSII and PSI was discovered in *Synechocystis*, supporting a model where PBSs transfer energy to both photosystems (Liu et al., 2013), and it has recently been shown that a portion of PBSs are reversibly decoupled from PSI in the light (Chukhutsina et al., 2015). In addition, a portion of PBS can be detached from photosystems during several stress conditions to regulate the amount of energy arriving at the photosystems (Stoitchkova et al., 2007; Richaud et al., 2001; Salomon and Keren, 2011; for a review, see Kirilovsky, 2015). The amount of energy reaching PSII is also regulated by non-photochemical quenching (NPQ), which converts excess excitation energy into heat. In most cyanobacterial species, NPQ is induced by the orange carotenoid protein (OCP), whose function is regulated by the fluorescence recovery protein (FRP) (Wilson et al., 2006; Wilson et al., 2007; Boulay et al., 2010; for a review, see Kirilovsky and Kerfeld, 2013).

1.4.2. Linear electron transport (LET)

In LET, three TM-embedded protein complexes – PSII, Cyt b_6f and PSI – transport electrons from water to $NADP^+$ (for a review, see Battchikova and Aro, 2013) (Figure 1A). To complete the electron transport, these protein complexes are connected to several mobile electron carriers. Plastoquinone (PQ) functions as an electron carrier in the TM between PSII and Cyt b_6f, forming a so called PQ pool. In addition, soluble plastocyanin (PC) and cytochrome c_6 (Cyt c_6) mediate electrons from Cyt b_6f to PSI in the TM lumen. Ferredoxin (Fd) and flavodoxin (Fdx) accept electrons from the cytosolic side of PSI and transport them to ferredoxin:$NADP^+$ oxidoreductase (FNR) which finally reduces $NADP^+$ to NADPH.

LET is based on the Z- scheme (Hill and Bendal 1980). The protein complexes involved in LET are arranged so that the absorbed light energy increases the energy of primary donors in both photosystems, while in other reactions the amount of free energy decreases, making these reactions spontaneous. The first protein complex in the Z-scheme is PSII. The crystal structure of PSII from *Thermosynechococcus vulcanus* was resolved at 1.9 Å (Umena et al., 2011). In the TM of cyanobacteria, PSII is organized as a dimer where both monomers are composed of 20 subunits, including core subunits (D1 and D2) as well as core antenna proteins (CP43 and CP47) that bind Chl and carotenoids (for a review, see Shen, 2015). Light energy (photons) captured by PBS (see section 1.2.2.) are conducted to the primary donor of PSII, P680, which comprises of two specialized Chl dimers. P680 gets excited, causing charge separation, which results

in the formation of $P680^+$, the strongest biological oxidizing agent. High energy electrons are transported further to PSII-bound cofactors, pheophytin, and to two plastoquinones, Q_A and Q_B. To reduce $P680^+$, the electron is eventually derived from H_20. This requires water splitting by the oxygen-evolving complex (OEC) residing on the lumenal side of PSII. The catalytically active center of OEC is composed of a Mn_4O_5Ca cluster where in a four-step reaction, called the Kok-cycle (Kok et al., 1970), two water molecules are split and four electrons deriving from them are transported one by one to $P680^+$ via Tyrosine Z, which is attached to the reaction center protein D1. In addition, four protons are released to the TM lumen and O_2 is evolved as a by-product. Due to a second charge separation, Q_B becomes doubly reduced after receiving the second electron and gets protonated by two protons derived from the cytosolic side of the TM forming plastoquinol, PQH_2. The PQH_2 is then released from the Q_B pocket of PSII into the PQ pool in the TM.

PQH_2 continues to the Cyt b_6f complex, which is a dimer consisting of 8 subunits per monomer. The crystal structure of Cyt b_6f from *Mastigocladus laminosus* was resolved at 3.0 Å (Kurisu et al., 2003). PQH_2 donates both of its electrons to the Cyt b_6f complex and deprotonates, releasing two protons to the lumen. The first electron accepted by Cyt b_6f from PQH_2 is transported via the Rieske-protein and Cyt *f* to soluble PC (or Cyt c_6) in the TM lumen, but the second electron continues to the Q-cycle. By reducing two haem groups in Cyt b_6, this electron ends up on PQ in the cytosolic side. After receiving the second electron, PQ protonates to PQH_2 by taking two protons from the cytosol, and it gets oxidized again by the Cyt b_6f complex, releasing two protons into the lumen. Thus, two protons are transported from the cytosol to the lumen per each electron arriving to the Cyt b_6f complex. The oxidized PQ is released back to the TM and eventually returns to the Q_B pocket of PSII to accept electrons again.

In cyanobacteria, another photosystem, PSI, is composed of 12 protein subunits. The crystal structure of PSI in *Synechococcus elongatus* was resolved at 2.5 Å (Jordan et al., 2001). PSI is commonly organized as a trimer in cyanobacteria (Jordan et al., 2001) but in some cyanobacterial species it may appear as a dimer or even as a tetramer (Li et al., 2014). The primary electron donor of PSI, a Chl dimer called P700, resides in the reaction center of PSI, which is comprised of PsaA and PsaB proteins (for a review see, Nelson and Yocum, 2006). When P700 gets excited during charge separation, it transports electrons to PSI-bound cofactors Chl A_0, phylloquinone A_1 and to three iron-sulfur clusters, F_X, F_A and F_B. Finally, electrons arrive to Fd or, under iron limitation, to Fdx, which are attached to PSI on the cytosolic side of the TM. FNR oxidizes Fd (or Fdx)

and transports electrons to $NADP^+$, forming NADPH, and the electron deficit in $P700^+$ is filled by an electron from PC (or Cyt c_6).

The proton gradient across the TM, which is obtained through water splitting and the oxidation of PQH_2, is utilized by ATP synthase to produce ATP in a process called photophosphorylation. ATP production occurs via H^+-dependent rotation of the ATP synthase. One rotation requires 12 protons and produces three ATP molecules.

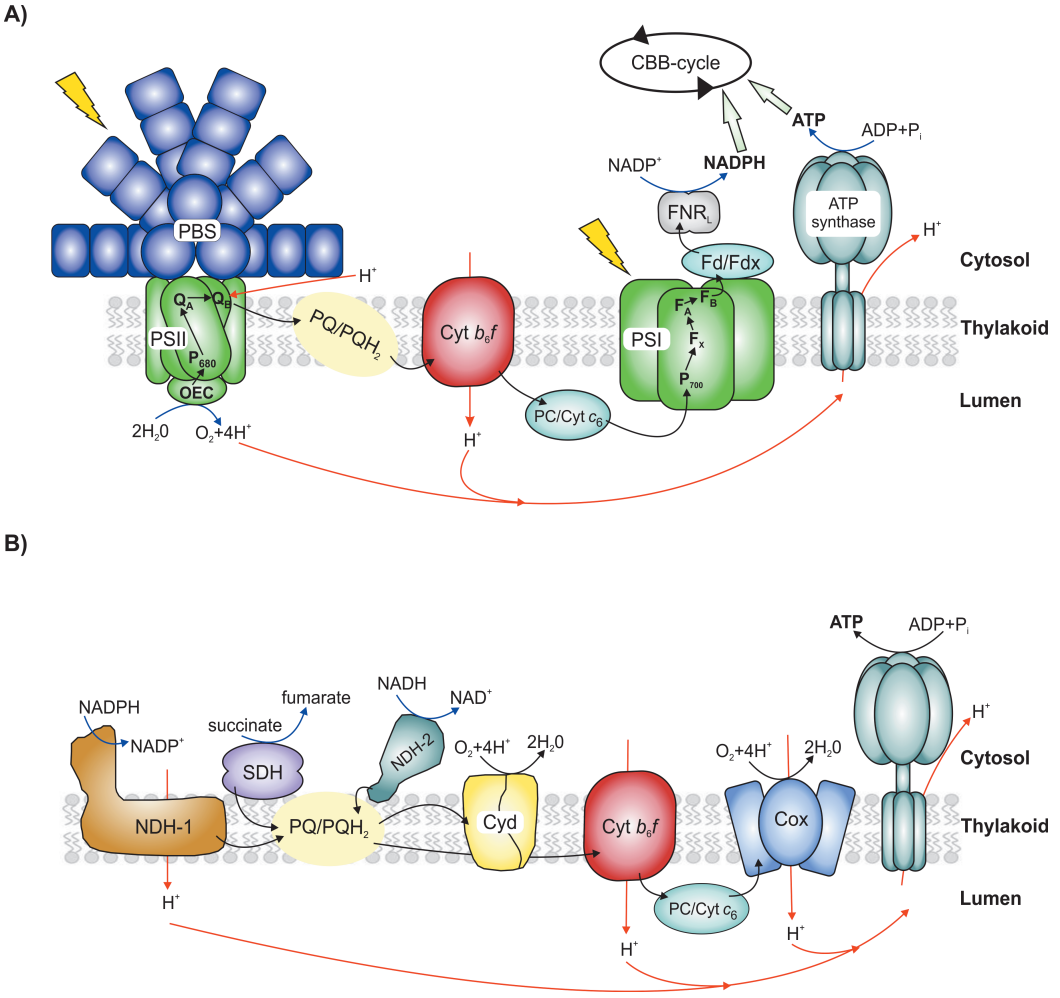

Figure 1. Simplified scheme of the A) photosynthetic and B) respiratory electron transport in *Synechocystis* thylakoid membrane. The H^+-pumping by Cox has been deduced based on its structure (Iwata et al., 1995; Brändén et al., 2006).

1.4.3. Auxiliary electron transport pathways and cyclic electron transport (CET)

Cyanobacteria have to maintain intracellular photosynthetic redox balance, with adequate reducing equivalent (NADPH) and energy (ATP) production needed for CO_2 fixation and the biosynthesis of other compounds, while simultaneously avoiding the over-reduction of the electron transport chain (ETC) (reviewed in Mullineaux, 2014b). The over-reduction of ETC causes the accumulation of reactive oxygen species (ROS), triggering oxidative damage to the photosynthetic apparatus, proteins and DNA and causing lipid peroxidation, which eventually leads to cell death (Latifi et al., 2009; Narainsamy et al., 2013). Cyanobacteria face rapidly changing environmental conditions and have evolved, in addition to LET, several auxiliary electron transport pathways that allow them to fine-tune the ATP/NADPH ratio and redistribute excess electrons in order to safeguard the photosynthetic apparatus under fluctuating and stressful environmental conditions.

The ATP/NADPH ratio produced by LET is 1.33-1.5 depending on organism (Bendall and Manasse, 1995; Behrenfeld et al., 2008). CO_2 fixation consumes 1.5 ATP per NADPH and thus, in principle, LET should cover this energy demand in ideal conditions. However, in nature the conditions are never optimal, and ATP is also used in several other biosynthesis routes in addition to CO_2 fixation. To increase the ATP/NADPH ratio, cells utilize light powered cyclic electron transport (CET) around PSI because it only produces ATP (for a review, see Yamori and Shikanai, 2016). During CET, electrons from the acceptor side of PSI are cycled to the PQ pool, or possibly straight to the Cyt b_6f complex, while simultaneously generating a proton gradient across the TM stimulating ATP production. The most established route is mediated by the proton pumping type 1 NAD(P)H dehydrogenase (NDH-1) complex, especially NDH-1_1 and NDH-1_2, donating electrons to the PQ pool (Mi et al., 1992b; for a review, see (Battchikova et al., 2011a; Peltier et al., 2016). The transfer of protons across the TM by NDH-1 was recently proven experimentally (Strand et al., 2017). The electron donor of NDH-1 has remained ambiguous for a long time, but recently it has become evident that Fd is at least one of the electron donors (Battchikova et al., 2011b; He et al., 2015). The other possible CET pathway involves the PGR5-like protein, which may be a putative Fd:PQ oxidoreductase (Yeremenko et al., 2005). In addition, *Synechocystis* has two forms of FNR, a longer form called FNR_L and a shorter form called FNR_S. They are encoded by the same gene, but the site for the initiation of translation is different (Thomas et al., 2006). FNR_L reduces $NADP^+$ to NADPH, whereas FNR_S works in the opposite direction, oxidizing NADPH. FNR_S accumulates under heterotrophic conditions and is possibly involved in enhancing CET

(Thomas et al., 2006; Korn, 2010). Interestingly, FNR_L has been shown to function independently in the salt stress induced CET (van Thor et al., 2000).

To prevent the over-reduction of ETC, especially under rapidly changing environmental conditions, cyanobacteria utilize several pathways that consume the excess electrons in a safe way. One important group of "safety valve" proteins is composed of flavodiiron proteins (FDPs) (for a review, see Allahverdiyeva et al., 2015). In cyanobacteria, their structure comprises (i) the N-terminal metallo-β-lactamase-like domain containing a non-heme diiron center where O_2 and/or NO reduction occurs, (ii) the flavodoxin-like domain including FMN and (iii) the C-terminal flavin reductase-like domain, which in this case enables the use of NAD(P)H as an electron donor. Flavodiiron proteins function as dimers or as tetramers arranged in a "head-to-tail" configuration that brings the diiron center and FMN close together, enabling electron transport between them (Frazão et al., 2000; Seedorf et al., 2007; Silaghi-Dumitrescu et al., 2005).

Synechocystis expresses four FDPs, Flv1-4. *In vitro* assays with recombinant Flv3 show that it is able to transport electrons from NAD(P)H to O_2, forming H_20 without the generation of ROS (Vicente et al., 2002). The amount of electrons transported via Flv1 and Flv3 to O_2 depends on light intensity and the availability of carbon (Helman et al., 2003; Helman et al., 2005). In *Synechocystis*, Flv1 and Flv3 are essential under fluctuating light conditions, since they protect PSI by alleviating acceptor side limitation (Allahverdiyeva et al., 2013). Flv1 and Flv3 have been suggested to work as a Flv1/3 dimer, but it has been shown recently that homo-oligomers of Flv3 are also formed (Mustila et al., 2016). It seems that Flv3 homo-oligomers are involved in yet unidentified auxiliary electron transport routes where the terminal acceptor is not O_2. Unlike Flv 1/3, the Flv2/4 heterodimer formation has been confirmed biochemically (Zhang et al., 2012). The Flv2/4 dimer together with the small Sll0218 protein encoded by the *flv4-sll0218-flv2* operon is involved in photoprotection of PSII, especially under high light conditions and carbon deprivation (Zhang et al., 2009b; Zhang et al., 2012, Bersanini et al., 2014). In addition to FDPs, bidirectional hydrogenase is able to transiently consume electrons derived from PSI, thus preventing slowdown of photosynthetic electron transport during dark to light transition under anoxic conditions (Appel et al., 2000).

1.4.4. CO_2 fixation in cyanobacteria

The end products of photosynthesis are organic carbon compounds produced from inorganic carbon in the cytosol during a reaction series in the CBB cycle, powered by the end products of photosynthetic light reactions - NADPH as a reducing power and

ATP as an energy carrier that facilitates metabolic reactions. The CBB cycle begins with the incorporation of CO_2 into RuBP by Rubisco and the formation of 3-phosphoglycerate (3-PGA). Rubisco consists of large (RbcL) and small (RbcS) subunits arranged into a L_8S_8 molecule (Whitney et al., 2011). In the following reactions, glyceraldehyde 3-phosphate (GA3P) is generated. This triosephosphate is a precursor for the synthesis of several biomolecules. The efficient functioning of cyanobacterial Rubisco requires a high CO_2 concentration in its surroundings because it has significantly lower affinity for CO_2 compared to the Rubisco of higher plants (Mueller-Cajar and Whitney, 2008; Whitney et al., 2011). In addition, uncharged CO_2 diffuses out of the cell easily, whereas lipid membranes are much less permeable to charged HCO_3^- (Badger and Price, 2003). Cyanobacteria have evolved carbon concentrating mechanisms (CCM), which (i) isolate Rubisco from the cytosol into carboxysomes and (ii) increase the intracellular C_i-concentration by pumping HCO_3^- into the cells as well as by converting CO_2 to HCO_3^- (for a review see Badger and Price, 2003; Price, 2011; Kaplan, 2017).

To increase the CO_2 concentration in the vicinity of Rubisco, cyanobacteria encapsulate their Rubisco into protein micro bodies called carboxysomes (Badger and Price, 2003; Price, 2011; Kaplan, 2017). Cyanobacteria have two types of carboxysomes, called α- and β- carboxysomes, which differ in their shell proteins but essentially their function is similar to the description provided in section 1.1. HCO_3^- penetrates the carboxysome shell, and the carbonic anhydrase inside catalyzes the conversion of HCO_3^- to CO_2, thus elevating the CO_2 concentration to the level required for the efficient functioning of Rubisco in cyanobacteria.

Different cyanobacterial species use various methods to actively pump C_i into the cell (for a review see Badger and Price, 2003; Price, 2011; Kaplan, 2017). *Synechocystis* possesses two major transporters for HCO_3^- residing in the PM. BCT1, encoded by the Cmp-operon, is an inducible, high affinity ATP-binding cassette (ABC)-type HCO_3^- transporter and it is expressed especially under C_i limitation (Omata et al., 1999). The Na^+ -dependent symporter SbtA is the other inducible, high affinity HCO_3^- transporter in *Synechocystis* (Shibata et al., 2002b). CO_2 uptake in *Synechocystis* is maintained by two different NDH-1 complexes, NDH-1_3 and NDH-1_4 (for a review, see Battchikova et al., 2011a; Peltier et al., 2016). $NDH1_3$ is a high-affinity CO_2 uptake complex whose expression is induced under carbon deprivation, while the NDH-1_4 complex is a constitutively expressed, low-affinity CO_2 uptake system (Ohkawa et al., 2000; Shibata et al., 2002a; Battchikova et al., 2011a). NDH-1 complexes are not transporters per se, but they hydrate CO_2 to HCO_3^-, reducing CO_2 diffusion out of the cell.

Despite CCM, RuBP occasionally undergoes oxygenation instead of carboxylation because Rubisco is not able to accurately distinguish between its two substrates, CO_2 and O_2. This process that uses oxygen as a substrate is called photorespiration. In addition to 3-PGA, it also produces toxic 2-phosphoglycolate (2-PG), which must be converted back to 3-PGA and CO_2, which requires ATP (for a review, see Moroney et al., 2013). Photorespiration does, however, seem to be a crucial process for all photosynthetic organisms, including cyanobacteria (Eisenhut et al., 2008a). Photorespiratory gas exchange has been observed in mutant cells lacking Flv1 and Flv3 proteins under severe C_i-starvation (Allahverdiyeva et al., 2011).

1.5. Respiratory electron transport and respiratory terminal oxidases (RTOs)

The primary role of respiration in cyanobacteria is to provide metabolic energy during darkness, using carbohydrates synthesized through photosynthesis (Matthijs and Lubberding, 1988). In respiration, electrons derived from the catabolism of organic compounds are transported into the PQ pool, which promotes the proton gradient for ATP production (for a review, see Vermaas, 2001; Mullineaux, 2014a). The vast majority of the respiration in cyanobacteria takes place in the TM, and several redox-active components, such as the PQ pool, the Cyt b_6f complex and PC/(Cyt c_6), are shared between photosynthetic and respiratory ETCs (Scherer, 1990; Peschek et al., 2004) (Fig. 1B). During respiration, two major dehydrogenases, the NDH-1 complex (Mi et al., 1992a; Ohkawa et al., 2000) and succinate dehydrogenase (SDH) (Cooley and Vermaas, 2001), donate electrons across the TM to the PQ pool. From there, electrons are transported either to Cyt b_6f or to membrane-bound respiratory terminal oxidases (RTOs). RTOs reduce molecular oxygen to water and simultaneously contribute to the generation of a proton gradient for ATP production. There are two RTOs that reside in the TM of *Synechocystis*: the cytochrome *bd* quinol oxidase (Cyd) and the aa_3-type cytochrome *c* oxidase (Cox) (Howitt and Vermaas, 1998; Lea-Smith et al., 2013; for a review, see Hart et al., 2005; Schmetter, 2016).

Cyd consists of two subunits, CydA and CydB, and contains two haems in its active center (Howitt and Vermaas, 1998). Even though Cyd is not able to pump protons across the membrane, it contributes to the proton gradient across the TM by consuming H^+ during the reduction of O_2 to water on the cytosolic side (Hart et al., 2005). In addition to Cyd, another quinol oxidase resembling plastid terminal oxidase (PTOX) of plants (Krieger-Liszkay and Feilke, 2015) has been found in several cyanobacterial species, though not in *Synechocystis* (McDonald et al., 2011).

The second TM-localized RTO, Cox, is composed of three subunits: (i) subunit I, which ligates haem *a* and haem a_3-Cu_B in the binuclear center, (ii) subunit II, which binds CuA and forms the docking site for soluble donors and (iii) subunit III, which completes the structure (Hart et al., 2005). Cox is able to accept electrons from both PC and Cyt c_6 (Navarro et al., 2005; Paumann et al., 2004). Based on its structure, Cox is likely to translocate protons across the TM (Iwata et al., 199; Brändén et al., 2006). Cox is the main RTO contributing to dark respiration (Pils et al., 1997; Howitt and Vermaas, 1998; Pils and Schmetterer, 2001), and its expression peaks at the end of the day (Kucho et al., 2005). The importance of Cox is emphasized by the fact that all sequenced cyanobacterial genomes have genes encoding Cox (Pils and Schmetterer, 2001; Lea-Smith et al., 2013), and the function of Cox is necessary under heterotrophy (Pils et al., 1997).

Some respiratory processes occur in the PM, in addition to the TM. In *Synechocystis*, the PM-localized respiratory chain lacks Cyt $b_6 f$ (Schultze et al., 2009) and Cox (Huang et al., 2002), but is likely to contain Cyd (Howitt and Vermaas, 1998; Lea-Smith et al., 2013) and, in particular, it includes the third RTO of *Synechocystis*, the alternative oxidase complex (ARTO) (Huang et al., 2002; Pisareva et al., 2011). ARTO is a member of a haem-copper protein superfamily similar to Cox (Pils and Schmetterer, 2001). Even though ARTO does not significantly contribute to photosynthetic electron transport (Abramson et al., 2000; Lea-Smith et al., 2013), it might have a more specific role in reductive iron uptake (Kranzler et al., 2014). The input of electrons to the PQ pool in the PM is most probably provided by SDH or type 2 NAD(P)H dehydrogenases (see section 1.7.2), because NDH-1 has been detected to reside exclusively in the TM (Ohkawa et al., 2000; Zhang et al., 2004; Pisareva et al., 2011; Liberton et al., 2016). Electrons are transported to ARTO or Cyd from the PQ pool, and the presence of ATP synthase in the PM (Huang et al., 2002) suggests the formation of a proton gradient in order to energize several transporter complexes (Zhang et al., 2009a). The importance of this is demonstrated e.g. by the increase in respiration under salt stress, since additional energy is needed for the extrusion of Na^+ (Jeanjean et al., 1993; Pils and Schmetterer, 2001).

It is evident that the main role of RTOs is to function in dark respiration and that the presence of RTOs is not crucial for *Synechocystis* when cells are not facing severe stress conditions (Howitt and Vermaas, 1998; Pils and Schmetterer, 2001; Lea-Smith et al., 2013). However, because both photosynthetic and respiratory electron transport occur in the TM, there is an intriguing possibility: RTOs could be participating in the redox poising of ETC during illumination. It has been recently demonstrated that the presence

of at least one TM- localized RTO, either Cox or Cyd, is essential under 12-h-high light/12-h-dark square-wave cycles (Lea-Smith et al., 2013). In addition, earlier studies based on indirect fluorescence methods suggested that Cyd might contribute to the oxidation of the PQ pool during illumination (Schneider et al., 2001; Berry et al., 2002).

1.6. Central carbon metabolism of cyanobacteria

Cyanobacteria accumulate carbon and other energy reserves as polymers to survive during starvation periods, which frequently occur in nature (Allen, 1984). To store carbon, GA3P generated in the CBB cycle is first metabolized to hexose-phosphates via gluconeogenesis and then stored in the form of glycogen. The plasticity in the sugar catabolism of cyanobacteria allows the adjustment of the intracellular redox balance and energy level to meet the demands of cellular metabolism under changing growth conditions. When the stored carbon is needed, glycogen is first degraded to glucose or glucose 6-phosphate, which can be catabolized via various glycolytic pathways (Fig 2.). One of them is glycolysis, where glucose 6-phosphate is catabolized to pyruvate, with concomitant production of ATP and NAD(P)H. Glycolysis has two variants in cyanobacteria: the Embden–Meyerhof–Parnas (EMP) pathway and the Entner–Doudoroff (ED) pathway. The second option for carbohydrate catabolism is the oxidative pentose phosphate (OPP) pathway, which produces reducing power in the form of NADPH. All of these pathways lead to the tricarboxylic acid (TCA) cycle, which provides reducing power and energy in the form of NAD(P)H, $FADH_2$, and ATP and produces precursor metabolites utilized in the biosynthesis of amino and fatty acids, oxaloacetate, 2-oxoglutarate (2-OG) and succinate, and the latter can also be used in respiration. The majority of cyanobacteria possess a complete TCA cycle (Zhang and Bryant, 2011), though there are some variations depending on species (Steinhauser et al., 2012). However, the metabolic flux rate through the TCA cycle is low in cyanobacteria (Wan et al., 2017). Thus, its main role is likely to produce carbon skeletons and other precursors rather than supply energy and reducing equivalents.

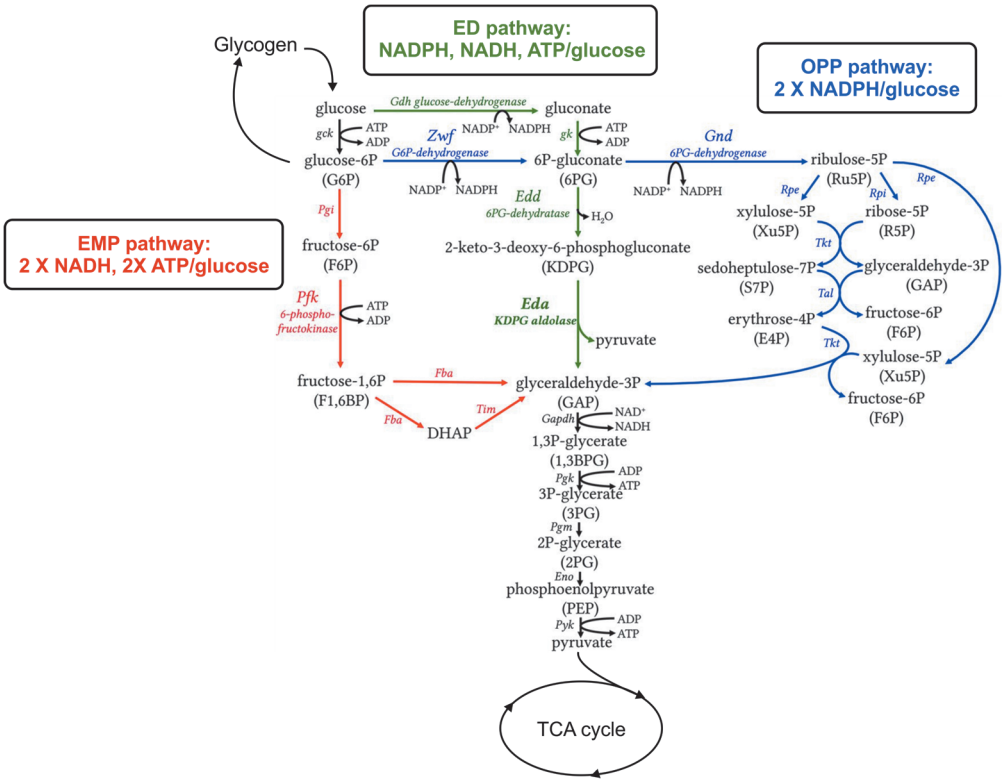

Figure 2. Glycolytic routes and their yields in cyanobacteria. Modified from Chen et al. 2016.

1.6.1. Glycogen: more than just a storage molecule

Glycogen is required by *Synechocystis* for biomass formation (Knoop et al., 2010) and it is the main oxidizable reserve during darkness for energy production in cyanobacteria (Gründel et al., 2012). Glycogen is a water-soluble polyglucan and it consists of interlinked linear chains of α-D-glucose forming visible granules inside the cell (Allen, 1984). Glycogen synthesis starts in the cytosol with the formation of ADP-glucose from glucose 1-phosphate and ATP, catalyzed by the ADP-glucose pyrophosphorylase (GlgC) (for a review, see Zilliges, 2014). In the next phase, glycogen synthase (GlgA) elongates a pre-existing α-(1-4)-glucan chain using the ADP-glucose as a sugar donor. The genome of *Synechocystis* encodes two isoforms of this enzyme (Beck et al., 2012), and both are able to synthesize α-polyglucan (Gründel et al., 2012). The branching enzyme (GlgB) forms linkages between glucan chains in the growing polymer, finalizing the structure. Glycogen degradation provides phosphorylated sugar intermediates which can be utilized as an energy source. Degradation is initiated by glycogen phosphorylase (GlgP), which releases glucose-1-phosphates until only the last four glucose residues are left in the branch. *Synechocystis* has two GlgP homologs, and their expression varies

depending on growth conditions, indicating possible functional divergence (Fu and Xu, 2006). The remaining four glucoses in the branch act as a recognition site for the debranching enzyme (GlgX) that cleaves the outer branches, releasing maltotetraose. The gene sets for glycogen synthesis (*glg*A,B,C) and degradation (*glg*P,X) are conserved in the majority of cyanobacterial species (Beck et al., 2012).

In cyanobacteria, as well as in plants and algae, polyglucan biosynthesis is closely linked to photosynthetic reactions (reviewed in Zilliges, 2014). It follows the diurnal cycle in most cyanobacteria (Schneegurt et al., 1994): glycogen is synthesized only during the light period and degraded during the dark period for respiratory needs. The availability of carbon is one of the main factors controlling the accumulation of glycogen in cyanobacteria. Cells grown under carbon-replete conditions accumulate significantly higher amounts of glycogen compared to carbon-deprived cells (Eisenhut et al., 2007), and a transient shortage of carbohydrates synthesized by the CBB cycle can be compensated for by degrading glycogen (Eisenhut et al., 2008b). In addition, nitrogen shortage increases the intracellular glycogen amount in cyanobacteria (Wilson et al., 2010). Thus, both photosynthetic reactions and the intracellular C/N balance affect glycogen biosynthesis in cyanobacteria.

The pathways for glycogen synthesis and degradation are regulated at different levels in cyanobacteria (reviewed in Zilliges, 2014). Synthesis is mainly regulated at the enzymatic level, and it responds to the amount of light available. All the enzymes involved in glycogen synthesis – GlgA,B,C – are under thioredoxin mediated regulation in cyanobacteria, which explains their activation strictly under illumination (Lindahl and Florencio, 2003; Lindahl and Kieselbach, 2009). In addition, GlgC is activated by 3-PGA, which is a signal for intracellular high carbon and energy status but is inhibited by inorganic phosphate P_i (Levi and Preiss, 1976; Iglesias et al., 1991). In contrast, the degradation of glycogen is regulated at the transcriptional level, in response to the C/N status of the cell as well as its energy requirements. The expression of *glgX* and *glgP* is induced during the dark period by the group 2 σ-factor SigE, which is a positive regulator of several sugar enzymes functioning in sugar catabolism (Osanai et al., 2005; Osanai et al., 2007). Furthermore, histidine kinase Hik8 (Singh and Sherman, 2005), and likely also nitrogen metabolism regulators NtcA and PII (Forchhammer, 2004), activate the expression of *glgX* and *glgP* (Osanai et al., 2007).

Glycogen, however, is not required only for storing carbon and energy. Mutants deficient in glycogen synthesis in several cyanobacterial species, including *Synechocystis*, *Synechococcus* sp. PCC 7002 and *Synechococcus elongatus* PCC 7942, show reduced photosynthetic and respiratory capacity, sensitivity against several stress

conditions (high light, high salt, heat, and oxidative stress), growth defects during dark to light transitions as well as under low carbon conditions and mixotrophy, in addition to the non-bleaching phenotype under nitrogen starvation (Carrieri et al., 2012; Gründel et al., 2012; Hickman et al., 2013; Miao et al., 2003; Suzuki et al., 2010; Xu et al., 2013b). Interestingly, *Synechocystis* mutants incapable of glycogen synthesis demonstrate an overflow metabolism causing "energy spilling": instead of being routed to glycogen synthesis, excess energy and carbon are consumed in the production of pyruvate and 2-OG, which are released into the medium (Gründel et al., 2012). This demonstrates that glycogen is a dynamic depositary for carbon and electrons, utilized as a reserve and as a redox buffer, as was proposed by Smith (1982).

1.6.2. Sugar catabolism and carbon flow in cells cultivated under various growth modes

Under ***photoautotrophy***, when light as an energy source and CO_2 as a carbon source are available, the CBB cycle is the main metabolic route for carbon utilization. The carbon flux from GA3P can be directed to either biosynthesis or the regeneration of CBB cycle intermediates, and it occurs with a ratio of around 1:8 in *Synechocystis* (Knoop et al., 2010). Under ***photoautotrophy,*** only a minor flux is routed through the OPP pathway that produces 2 NADPH-molecules per glucose (Young et al., 2011), albeit substantial amount of NADPH are produced by photosynthetic light reactions.

In the absence of light, cyanobacteria exhibit ***heterotrophic*** metabolism, where electrons are derived from the oxidation of reduced substrates, mainly carbohydrates, to provide energy and reducing power. When the growth medium is supplemented with glucose and cells are illuminated daily with a short pulse of light, that is insufficient for photosynthetic growth, the growth mode is called ***light-activated heterotrophic growth*** (LAHG) (Anderson and McIntosh, 1991). These conditions are often applied instead of genuine heterotrophy, because the presence of a daily short blue light pulse is required for the growth of *Synechocystis*. However, the blue light pulse does not support growth by inducing photosynthesis – instead, the effect probably occurs through the regulation of heterotrophic metabolism and cell division (Anderson and McIntosh, 1991). Indeed, light is required for the maintenance of cell shape dimensions in cyanobacteria, yet factors regulating this remain elusive (reviewed in Montgomery, 2015). Under heterotrophy, at least 90% of the carbon flow from sugar catabolism is directed to the OPP pathway (Yang et al., 2002; Wan et al., 2017), because this pathway is the only source providing required intermediates for nucleotide biosynthesis in the dark (Kruger and von Schaewen, 2003). In fact, the mutant deficient of *gnd*, one of the

key enzymes producing NADPH in the OPP pathway, could not grow under heterotrophic conditions (Wan et al., 2017). In addition, some carbon flux under heterotrophy is directed to the EMP-pathway producing two NADH- and ATP-molecules per glucose (Yang et al., 2002), and only minor flux through the TCA cycle was observed (Wan et al., 2017). However, cyanobacteria are not able to grow heterotrophically under anaerobic conditions, because oxygen is needed for oxidative phosphorylation.

Under ***photomixotrophic*** conditions, carbon for metabolic needs derives from a combination of photosynthetically fixed CO_2 and an external carbon source, e.g. glucose, which is imported to the cell. Under photomixotrophy, the growth of cyanobacteria is significantly enhanced compared to that under photoautotrophy, due to the increased availability of carbon (Summerfield et al., 2013; Chen et al., 2016). During photomixotrophy, the CBB cycle is highly active (You et al., 2014). From glycolytic routes, the ED pathway producing one NADH, NADPH and ATP molecule per glucose, is crucial in *Synechocystis* under photomixotrophy (Chen et al., 2016), whereas the carbon flow through the EMP pathway, the OPP pathway, and the TCA cycle is marginal under these conditions (You et al., 2014). The choice of the ED pathway over the EMP pathway under photomixotrophy is most probably caused by almost 3.5 times lower protein cost and diminished ATP production of the ED pathway compared to the EMP pathway (Flamholz et al., 2013). This is beneficial because photosynthesizing organisms are usually limited by nutrients rather than by ATP (Chen et al., 2016). The simultaneous operation of the ED pathway and the CBB cycle does not cause futile cycles that slow down CO_2 fixation, which could happen if the OPP or the EMP pathways were induced (Narainsamy et al., 2013). The ED pathway is also highly advantageous to cyanobacteria under autotrophic conditions during the dark/night-cycle, which may be the reason why it is so widespread, not only among cyanobacteria but also in plants (Chen et al., 2016).

1.6.3. Regulation of sugar catabolism

Studies indicate that sugar catabolism is indispensable for cyanobacteria in the absence of illumination (for a review, see Osanai et al., 2007). There are several proteins regulating sugar catabolism in *Synechocystis*. The group 2 σ-factor SigE generally induces the expression of genes participating in sugar catabolism (Osanai et al., 2005). The expression of *sigE* follows the circadian rhythm, peaking at the end of the light period together with the sugar catabolism genes (Kucho et al., 2005). Another activator of sugar catabolism is Hik8 (Singh and Sherman, 2005), which is a homolog of the

circadian clock protein SasA in *Synechococcus* (Iwasaki et al., 2000). It is plausible to suggest that in *Synechocystis*, SigE is under the control of Hik8, which would explain the circadian expression of SigE, though this has not been verified experimentally (Osanai et al., 2007). In *Synechococcus elongatus* PCC 7942, the global regulator of circadian output, RpaA, induces the expression of genes that function in glycolysis, the OPP pathway and glycogen biosynthesis (Markson et al., 2013), and the gene encoding RpaA can also be found in *Synechocystis*.

Nitrogen status has also been proposed to have an influence on sugar catabolism in cyanobacteria (for a review, see Osanai et al., 2007). In *Synechocystis*, the expression of genes encoding enzymes that function in glycolysis and the OPP pathway as well as in glycogen catabolism are downregulated under nitrogen depletion (Osanai et al., 2006). During N depletion, the cells accumulate glycogen granules and when nitrogen source is available again, the cells switch to heterotrophic metabolism (respiration) and utilize glycogen for recovery (Klotz et al., 2016). The expression of a cyanobacterial global nitrogen regulator, *ntcA*, is upregulated under nitrogen deprivation (Forchhammer, 2004), and NtcA is known to induce the expression of *sigE* in *Synechocystis* (Muro-Pastor et al., 2001). Additionally, intracellular C/N status may be one factor that regulates sugar catabolism via PII. Furthermore, PBS are degraded during nitrogen depletion (Richaud et al., 2001), resulting in the decreased provision of reducing power (NADPH) and energy (ATP) which is, at least partially, compensated by sugar catabolism (Osanai et al., 2007).

1.7. Redox regulation of NAD(P)H/NAD(P)$^+$ homeostasis in photosynthetic organisms

NADH and NADPH are universal soluble reducing equivalents that provide electrons and protons to enzyme-catalyzed redox reactions in all cells. They differ from each other by the presence of a 2´phosphate group in the adenine ribose ring, which causes different substrate specificities in the corresponding enzymes. In addition, NAD(H) and NADP(H) have different metabolic roles in photosynthetic organisms. NADPH is mainly produced by photosynthesis. The amount of NADPH is kept higher than NADP$^+$ to maintain reductive reactions, such as CO_2 fixation as well as fatty and amino acid biosynthesis. In contrast, NADH is mainly produced in catabolic reactions, like glycolysis and the TCA cycle, and the NADH/NAD$^+$ ratio is kept low to maintain oxidative reactions.

1.7.1. Pyridine nucleotide transhydrogenase PntAB

Pyridine nucleotide transhydrogenase PntAB, also known as energy-dependent transhydrogenase, is an integral membrane protein complex coupling the oxidation of NADH and concurrent reduction of $NADP^+$ to proton translocation along the proton gradient (Sauer et al., 2004; for a review, see Jackson, 2012; Jackson et al., 2015). The structure of the enzyme is composed of three different domains: the dI domain binds NAD(H), the dII domain forms a proton channel, consisting of several transmembrane helices, across the membrane, and the dIII domain binds NADP(H). These are then arranged into two protomers. The catalytic reaction performed by PntAB couples the proton translocation to the allosteric conformational changes. During the reaction cycle, the enzyme can be in two different forms known as the open and occluded conformations. In the open conformation, the dI and dII domains bind and release their respective substrates, NAD(H) and NADP(H). The proton translocation through dII causes a conformational change from the open to the occluded form, placing reacting species to the right orientation, which enables hydride transfer from NADH to $NADP^+$. One proton is translocated across the membrane per hydride transfer (Bizouarn et al., 1996). By utilizing PntAB, the intracellular NADPH/NAD^+ ratio can be elevated to level that is over 400 times higher than the $NADP^+$/NADH ratio (Jackson, 2012). The function of PntAB has been studied in heterotrophic organisms, but its biological function in oxygenic photosynthetic organisms, including cyanobacteria, has remained largely indefinable. *Synechocystis* has two putative genes encoding transhydrogenase, *pntA* (*slr1239*) and *pntB* (*slr1434*).

1.7.2. Type 2 NAD(P)H dehydrogenases (NDH-2s)

Cyanobacterial pyridine nucleotide dehydrogenases are classified into two groups (for a review, see Melo et al., 2004; Peltier et al., 2016). The first group is the NDH-1 complex, which functions in CET (see section 1.4.3.), respiration (see section 1.5) and C_i-uptake (see section 1.4.4). The second group is formed by type 2 NAD(P)H dehydrogenases (NDH-2s), which consist of a single polypeptide, have molecular masses close to 50 kDa and catalyze electron transport from NAD(P)H to quinones without simultaneous proton translocation (Yagi, 1991). The NDH-2 primary structure typically features two GXGXXG motifs within the β-sheet-α-helix-β-sheet domains (Rossman fold), where the first motif binds FAD or FMN, and the second one binds NAD(P)H (Wierenga et al., 1986). The model for NAD(P)H:quinone oxidoreduction by NDH-2s has been proposed recently (Marreiros et al., 2017) based on the available crystal structures (Feng et al., 2012; Heikal et al., 2014; Sena et al., 2015), but the

precise mechanism for this reaction still remains elusive. However, NDH-2s have to be strongly attached to the membrane to be able to transport electrons to the quinone, which is indicated by substantial increase in the activity of NDH-2s in the presence of lipids (Björklöf et al., 2000; Gomes et al., 2001; Bandeiras et al., 2003). It seems that the majority of NDH-2s do not contain transmembrane helices, but instead, have amphipathic α-helices, which attach the enzyme in a position parallel to the plane of the membrane, addressing the need for a hydrophobic environment (Melo et al., 2004).

NDH-2s are found in several heterotrophic as wells as autotrophic organisms. The photosynthesizing eukaryotes expressing NDH-2s, like *Arabidopsis thaliana* (Michalecka et al., 2003; Carrie et al., 2008), *Chlamydomonas reinhardtii* (Desplats et al., 2009; Terashima et al., 2010) and *Physcomitrella patens* (Xu et al., 2013a), typically have several copies of NDH2s but the majority of these are targeted at mitochondria or peroxisomes instead of chloroplasts. NDH-2s may have a special importance in cyanobacteria because the genomes of all sequenced cyanobacteria contain at least one copy of NDH-2 (Marreiros et al., 2016). In *Synechocystis*, three genes encode NDH-2s; *ndbA* (*slr0851*), *ndbB* (*slr1743*), and *ndbC* (*sll1484*) (Kaneko et al., 1996; Howitt et al., 1999). They all contain conserved motifs for binding a FAD as a cofactor and NAD(P)H as a substrate, but the sequence of the latter binding motif indicates that NADH is highly favored in comparison with NADPH (Howitt et al., 1999). Only the product of *ndbC* contains a membrane spanning region. NdbB was recently demonstrated to be involved in vitamin K1 biosynthesis in *Synechocystis* (Fatihi et al., 2015). However, the precise functions of different NDH-2s, especially concerning possible role in redox regulation of pyridine nucleotides in cyanobacteria, remain still poorly understood.

2. AIMS OF THE STUDY

In cyanobacteria, photosynthetic linear and auxiliary electron transport pathways, together with respiratory pathways, are located in the TM. They provide balanced energy (ATP) and reducing equivalent (NADPH) to the cell. They create a complicated but well-orchestrated intracellular network of electron transport reactions. Linear electron transport has been studied extensively during the last decades, yet our understanding of its interactions with auxiliary and, in particular, respiratory electron transport pathways remains far from complete. The aim of my thesis was to study the crosstalk between these major bioenergetics networks in the TM. In parallel with these thylakoid oxidation-reduction pathways, I searched for novel proteins located in the TM and the PM that could potentially function in the redox regulation of cellular metabolism in *Synechocystis*. I investigated how the oxidized and reduced pyridine nucleotides, $NADPH/NADP^+$ and $NADH/NAD^+$ produced by photosynthetic light reactions and the sugar catabolism are inter-regulated. These interactions are expected to be vital for the maintenance of cellular redox homeostasis, especially when the primary carbon source changes from CO_2 to carbohydrates.

The primary aims of my thesis were

(i) to reveal the precise location of the thylakoid membrane localized respiratory terminal oxidases and their possible function in *Synechocystis* also during illumination;

(ii) to elucidate the role of pyridine nucleotide transhydrogenase PntAB in *Synechocystis;*

(iii) to investigate the roles of type 2 pyridine nucleotide dehydrogenases NdbA and NdbC in the regulation of the different growth modes of *Synechocystis*.

3. METHODOLOGY

3.1. Cyanobacterial strains and growth conditions

Table 1. Cyanobacterial strains used in this work. The detailed construction of each mutant is described in the given reference. All strains are constructed based on a glucose tolerant WT-strain. (1) Integration site in *psbAI,* the integrated gene under the *psbAII*-promoter.

Strain	Deleted genes	Reintroduced genes	Paper	Reference
Δ*cox*	*slr1136-slr1138*		I	Lea-Smith et al. 2013
Δ*cyd*	*slr1379-slr1380*		I	Lea-Smith et al. 2013
Δ*cox/cyd*	*slr1136-slr1138* *slr1379-slr1380*		I	Lea-Smith et al. 2013
Δ*flv1/3*	*sll1521*::Cm^R *sll0550*::Sp^R		I	Allahverdiyeva et al. 2011
PSI-less	*slr1834*::Cm^R, *slr1835*::Cm^R		I	Shen et al. 1993
Δ*pntA*	*slr1239*::Km^R		II	Paper II
Δ*ndbC*	*sll1484*::Zeo^R		III	Paper III
Δ*ndbA*	*slr0851*::Em^R		IV	Paper VI
Δ*ndbA*::*ndbA*	*slr0851*::Em^R	*slr0851*:: $Km^{(1)}$	IV	Paper VI

A glucose-tolerant *Synechocystis* sp. PCC 6803 (WT) and the mutant strains (Table 1) were grown at 30 °C in the BG-11 medium (Ripka et al. 1979) supplemented with 20 mM HEPES-NaOH (pH 7.5) or 10 mM TES-KOH (pH 8.0 or 8.2). Pre-experimental cultures were grown in flasks under continuous white fluorescent light (L30W/865 Osram) of 50 µmol photons m^{-2} s^{-1}, under air enriched with 3% CO_2 (HC) and with agitation at 150 rpm. Prior to the experiments, cells were harvested at the midlogarithmic phase from pre-experimental cultures and inoculated to fresh BG-11 medium. Experimental cultures were grown in fresh BG-11 medium under continuous illumination (5, 50 or 500 µmol photons m^{-2} s^{-1}), under different dark-light cycles (illumination 50 or 200 µmol photons m^{-2} s^{-1} during the light period), under fluctuating light using the 20/500 regime (20 µmol photons m^{-2} s^{-1} background light interrupted every 5 min with 30 second high light pulses of 500 µmol photons m^{-2} s^{-1}) in flasks in growth chambers with cool-white light-emitting diodes (LED) (AlgaeTron AG130 by PSI Instruments) with agitation at 150 rpm. The other applied growth system was a multi-cultivator (Multi-Cultivator MC 1000, PSI Instruments) with aeration, temperature control and white LED-lights as a light source. In the cultivator, cells were grown under continuous light (5, 20 and 50 µmol photons m^{-2} s^{-1}) or under diurnal sinusoidal 12 h

light rhythm with maximum 20, 50 and 200 µmol photons m^{-2} s^{-1} followed by a 12 h dark period. Experiments were conducted under ambient CO_2 conditions (LC) and under HC conditions. The experimental cultures were grown without antibiotics, and glucose was provided when mentioned. OD_{750} was measured using the Lambda 25 UV/VIS spectrometer (PerkinElmer) or the Multi-Cultivator MC 1000.

For physiological experiments, cells were harvested at the logarithmic phase (OD_{750} between 0.6 and 1.3). For activity measurements, cells were harvested and resuspended in fresh BG-11 medium at the desired Chl concentration and acclimated under the respective growth conditions 1 h before the measurements. Chl was extracted using 90% methanol and an extinction coefficient of 78.74 L g^{-1} cm^{-1} was applied to determine and adjust the Chl concentration (Meeks and Castenholz, 1971).

3.2. Biophysical methods

3.2.1. Oxygen evolution measurements with a Clark-type oxygen electrode

The net O_2 production was measured in the presence of several DBMIB concentrations (0, 1, 10 and 25 µM) with a Clark-type oxygen electrode (Hansatech Ltd, Norfolk, England) at 30 °C under 400 µmol photons m^{-2} s^{-1} actinic light applied using a 150-Watt, 21 V, EKE quartz halogen-powered fiber optic illuminator (Fiber-Lite DC-950, Dolan-Jenner, MA, USA). Before measurements, the Chl concentration of the samples was adjusted to 15 µg ml^{-1} and samples were supplied with 1 mM $NaHCO_3$ during measurements.

3.2.2. Membrane inlet mass spectrometry (MIMS)

The production of $^{16}O_2$ (mass 32) and the consumption of $^{18}O_2$ (mass 36) as well as the CO_2 consumption (mass 44) were monitored online with mass spectrometry (Prima PRO, Thermo Fisher Scientific) which was connected to a thermo-regulated DW1 oxygen electrode chamber sealed with a gas-permeable thin Teflon membrane (1 mm stretch membrane; YSI). Before the measurement, $^{18}O_2$ (isotope purity > 98%; CK Gas Products) was injected into the cell suspension and the concentrations of $^{16}O_2$ and $^{18}O_2$ in the solution were left to equalize. During measurement, samples were under continuous stirring. First, samples with Chl concentration of 15 µg ml^{-1} were monitored in the dark to record respiratory oxygen consumption and after this, actinic light (400 or 150 µmol photons m^{-2} s^{-1}) was applied using a 150-W, 21-V EKE quartz halogen powered fiber optic illuminator (Fiber-Lite DC-950; Dolan-Jenner) to record gross O_2 production, total O_2 uptake under illumination and CO_2 exchange. Gas-exchange

kinetics and rates were determined according to Beckmann et al. (2009): O_2 uptake=$\Delta^{18}O_2$ x (1+[$^{16}O_2$]/[$^{18}O_2$]) and O_2 evolution=$\Delta^{16}O_2$- $\Delta^{18}O_2$ x ([$^{16}O_2$]/[$^{18}O_2$]). All the measurements were performed in the presence of 1 mM $NaHCO_3$. Several inhibitors and artificial acceptor were used during experiments at the following final concentrations; 25 µM DBMIB, 50 µM HQNO, 0.5 µM DCBQ, and 1 mM KCN.

3.2.3. Fluorescence measurements

The Chl fluorescence from intact cells was recorded with a pulse amplitude-modulated fluorometer (Dual-PAM-100; Walz). Before measurements, the Chl concentrations of cell suspensions were adjusted to 15 µg mL^{-1} and dark adapted for 10 min. Saturating pulses of 5,000 µmol photons m^{-2} s^{-1} (300 ms) and strong far-red (FR) light (720 nm, 75 W m^{-2}) were applied during analysis to obtain the photosynthetic parameters. The F_m^D was obtained by applying a saturating pulse to dark adapted cells, the F_m^{FR} was recorded by applying a saturating pulse onto the FR background (after 8 s illumination), and the F_m', was recorded upon firing a saturating pulse during illumination. The effective yield of PSII, Y(II), was calculated as $(F_m' - F_s)/F_m'$. The maximum quantum yield of PSII was measured in the presence of 20 µM DCMU from dark-adapted cells upon illumination with actinic light (200 µmol photons m^{-2} s^{-1}) for 1 min and calculated as $F_v/F_m = (F_m - F_0)/F_m$. F_0= the mimimal fluorescence from dark-dapted samples, F_s= the steady state fluorescence, F_m'= the maximal fluorescence under the light.

The photosynthetic response to changing light intensities was monitored by measuring rapid light response curves with a Dual-PAM-100, applying a standard protocol of 60 s illumination periods of gradually increasing light intensity without dark-adapting the samples. To obtain the photosynthetic parameters, the saturating pulse was applied at the end of every light period.

The F_0 rise was monitored for 40 s after the termination of actinic light (1 min illumination with 50 µmol photons m^{-2} s^{-1} actinic light) with a Dual-PAM-100. Cell suspensions at a Chl concentration of 15 µg mL^{-1} were dark adapted for 10 min before the measurements.

State transitions were monitored with a Dual-PAM-100 by illuminating dark acclimated cells (Chl concentration 15 µg mL^{-1}) first with blue light (460 nm, 44 µmol photons m^{-2} s^{-1}) to induce transition from State II to State I. Light quality was changed to red light (620 nm, 50 µmol photons m^{-2} s^{-1}) to induce transition to State II. Light quality was changed once more to blue light to induce transition to State I. During illumination, saturating pulses were applied to monitor F_m'.

The kinetics of the Chl fluorescence decay after a single-turnover saturating flash were monitored with a FL 3500 fluorometer (PSI Instruments) according to Vass et al. (1999). Measurements were also performed in the presence of a 20 µM DCMU and with 30 s pre-illumination with FR light. Before all measurements, the Chl concentration of the samples was adjusted to 7.5 µg ml $^{-1}$ and they were dark adapted for 5 min.

The fluorescence emission spectra at 77K were measured from intact cells using a QE Pro-FL spectrofluorometer (Ocean Optics). Before measurements samples adjusted to a Chl concentration of 7.5 µg ml $^{-1}$ were rapidly frozen in liquid nitrogen. Cells were then excited with the 440 nm or the 580 nm light, generated using a monochromator (Applied Photophysics Ltd; f/3.4 grating).

3.2.4. P700 measurements

The P700 signal was recorded simultaneously with fluorescence using a Dual-PAM-100. Samples at a Chl concentration of 15 µg mL^{-1} were dark adapted for 10 min prior to the measurement process. The maximal change of P700 upon transformation of P700 from the fully reduced to the fully oxidized state, P_m, was achieved by applying a saturation pulse onto the FR background. The effective yield of PSI, Y(I), was calculated as (P_m' – P)/P_m. The donor side limitation of PSI, Y(ND), was calculated as P/P_m. The acceptor side limitation of PS I, Y(NA), was calculated as (P_m -P_m')/ P_m. P represents $P700^+$ signal under steady-state actinic light. P_m' is obtained by application of saturating pulse to the illuminated cells and represents maximum oxidizable P700 under actinic light illumination.

The oxidation and rereduction of P700 were monitored using a Dual-PAM-100. Cell suspensions at a Chl concentration of 20 µg mL^{-1} were dark adapted for 2 min before measurements. For the oxidation of P700, samples were illuminated with FR light (720 nm, 75 W m^{-2}) for 5 s, and the following rereduction was recorded in darkness.

3.3. Microscopy

3.3.1. Light microscopy and cell counting

Cells suspended in BG-11 were inspected with an Orthoplan Large Field Research Microscope (Leitz) and photographs of them were taken with a digital microscope camera (Leica DFC420C). The digital slide photograph brightness and contrast were optimized with Leica Application Suite version 4.1. (Leica). The number of cells in a culture (normalized to OD_{750} = 1) was calculated with a Bürker chamber (Marienfeld-Superior).

3.3.2. Transmission electron microscopy (TEM)

TEM-analysis was performed in the Laboratory of Electron Microscopy (University of Turku). Samples were prefixed with 5% glutaraldehyde in a 0.16 M s-collidin buffer (pH 7.4) and postfixed with 2% OsO_4 + 3% K-ferrocyanide. After this samples were dehydrated, embedded and cut to thin sections (70 nm). These were stained with 1% uranyl acetate and 0.3% lead citrate. A JEM-1400 Plus Transmission Electron Microscope (JEOL) was used in the analysis.

3.4. Glycogen determination

Cells in the logarithmic growth phase were collected and resuspended in OD_{750} =1, and 10 ml of the cell suspension was lysed by sonication (BIORUPTOR; CosmoBio). To determine the glycogen concentration in the lysates, a Total Starch Assay Kit (Megazyme) was applied according to the manufacturer's instructions.

3.5. Dry weight determination

Cells were grown to the logarithmic growth phase and 20 ml of the cell culture was passed through a preweighed and prewashed glass-fiber filter (pore size 1.0 µm, Millipore). Filters were then dried at 60°C for 24 h, kept in a desiccator for another 24 h and weighed.

3.6. Room temperature whole cell absorption spectra

The room temperature whole cell absorption spectra were measured using an Olis 17 UV/VIS/NIR Spectrophotometer (On-Line Instrument Systems, Inc.). Fry's correction was applied to correct the raw spectra. The OD_{750} of cells was adjusted to 0.3 before measurement.

3.7. Transcript analysis

3.7.1. Isolation of total RNA

Total RNA was extracted using the hot-phenol method as described in Tyystjärvi et al. (2001). A TURBO DNA-free kit (Invitrogen) was applied according to the manufacturer's instructions to degrade genomic DNA. The integrity of isolated RNA was verified with agarose gel electrophoresis.

3.7.2. Real-time quantitative PCR (RT-qPCR)

For the first strand cDNA synthesis from the isolated RNA, an iScript cDNA synthesis kit (Biorad) was applied according to the manufacturer's instructions. The generated cDNA was then used as a template for RT-qPCR, which was performed with the IQ5 system (Bio-Rad) using iQ SYBR Green Supermix (BioRad) as described in Mustila et al. (2014). Two reference genes with constitutive expression, *rimM* and *cysK* (Mustila et al., 2016), were used in the analysis. The primer sequences for the reference and the monitored genes are described in Paper III.

3.8. Protein analysis

3.8.1. Western blotting: protein isolation, electrophoresis and immuno-detection

Total protein extracts were isolated as described by Zhang et al. (2009) and the membrane fractions from them were prepared as described by Zhang et al. (2004). Proteins were separated using 12% (w/v) SDS-PAGE including 6 M urea, transferred to a polyvinylidene difluoride membrane (Immobilon-P; Millipore), and immunoblotted with protein-specific antibodies.

3.8.2. MS-analysis and proteomics

3.8.2.1. Sample Preparation

For liquid chromatography-tandem mass spectrometry (LC-MS/MS) analysis, *Synechocystis* cells were grown in triplicates. Total proteins were isolated as described above and further digested with trypsin according to two protocols. For the Δ*ndbC* mutant, 30 µg of proteins were denatured with 2× Laemmli buffer containing 8 M urea, and run subjected to electrophoresis in 12 % stacking PAGE (50% acrylamide/1.3% bis-acrylamide, 0.5 M Tris-HCl (pH 6.8), 6 M urea) until proteins entered the gel. Gel bands containing proteins were reduced, alkylated, and digested as described by Shevchenko et al. (1996, 2006). For the Δ*ndbA* mutant in solution digestion was applied according to Vuorijoki et al. (2016) with small differences. In the resuspension buffer ammonium bicarbonate was replaced by TRIS of equal molarity. 100 µg of proteins were reduced, alkylated and precipitated from solution with cold acetone. On-pellet trypsin digestion was performed overnight. The peptide mixture was further desalted on Sep-Pak 100 mg C18 columns. Extracted peptides were dried in a SpeedVac (Savant SPD1010,

SpeedVac Concentrator, Thermo Fisher Scientific) and further solubilized in 2% acetonitrile (ACN) and 0.1% formic acid (FA) prior MS analysis.

3.8.2.2. Data-dependent acquisition (DDA) for protein identification and quantification

The peptide mixtures were analyzed by LC-MS/MS using a QExactive or QExactive HF mass spectrometer (Thermo Fisher Scientific) connected in-line with a nano-liquid chromatography system EasyNanoLC 1000 or Easy NanoLC 1200 (Thermo Fisher Scientific) in Paper III and IV, respectively. In Paper III peptides (200 ng) were injected onto a 15-cm C18 nano-column (Michrom BioResources) and eluted into mass spectrometer with 110 min gradient of ACN. In Paper IV peptides (200 ng) were injected onto 40-cm C18 1.9 μm column and eluted with two-step 110 min gradient. MS data acquisition on QExactive (Paper III) or QExactive HF (Paper IV) was performed in a positive ionization mode, with 2.3-kV ionization potential. The DDA method comprised MS survey scans (mass-to-charge range of 300-2000) followed by MS/MS scans of 10 (Paper III) or 12 (Paper IV) most intensive 2+ and more -charged precursor ions. For protein identification, raw files were searched against the *Synechocystis* protein database retrieved from Cyanobase (Kaneko et al., 1996) using an in-house Mascot (version 2.4 in Paper III or 2.6.1 in Paper IV) server (Perkins et al., 1999) and further analyzed using Proteome Discoverer (version 1.4 in Paper III or version 2.2 in Paper IV) software (Thermo Fisher Scientific). The Mascot search parameters are reported in details in Paper III. For validation of the spectrum identifications, the Percolator algorithm (Käll et al., 2007) was used, with a relaxed false discovery rate of 0.05.

For quantification DDA data were analyzed using Progenesis QI for proteomics, LC-MS 4.0 (Nonlinear Dynamics). For protein identification and quantitation, detection of at least 2 unique peptides was required. The quantitation was based on areas of peaks representing peptides from a fragmented protein. Statistical analysis was performed with data obtained for three biological replicates; the statistical significance threshold in ANOVA was set to $P < 0.05$, and the practical significance threshold for fold change (FC) was set to $-1.3 \leq FC \geq 1.3$.

3.8.2.3. Selected reaction monitoring (SRM) for targeted quantification

Based on the DDA results, a spectral library was created in Skyline (MacLean et al., 2010) for selected reaction monitoring (SRM). The SRM analysis was performed on a TSQ Vantage (Thermo Fisher Scientific), with four biological replicates, as described by Vuorijoki et al. (2016) with some modifications; for details see Paper III. The SRM results

were loaded to the Panorama Public (Dharma et al., 2014). For the protein targets missing in Vuorijoki et al. (2016), the SRM assays were developed according to the published protocol. Data were analyzed using RStudio with MSstats algorithm version 3.5.1 (Choi et al., 2014) and normalized to three housekeeping peptides; *sll1818*, FSLEPLDR and SYTDQPQIGR; *slr0638*, GVIAVTER; and *sll0145*, AISLSDLGLTPNNDGK.

3.9. Bioinformatics

3.9.1. Homology modeling of PntAB quaternary structure

The amino acid sequences for *Synechocystis* PntA and PntB were retrieved from the Protein Data Bank (PDB) using BLAST, and where the identity was above 40% for PntA (<39% for the transmembrane structure) and above 50% for PntB (<42% for the transmembrane structure) the sequence were selected for further analyses. 13 templates were used for the modeling of the hydrophilic α dI domain, 3 templates for the hydrophobic α dII, and 10 templates for the dIII/dII β domain (for details see Paper II). The number of transmembrane helices and the amino acids forming them in the α and β subunits were predicted using TMHMM server 2.0 (Krogh et al., 2001) and modeled based on the crystal structure of *T. thermophilus*. Homology models for PntA and PntB were assembled with MODELLER (Sali and Blundell, 1993), evaluated with MOLPROBITY (Chen et al., 2010) and visualized and analyzed with UCSF CHIMERA (Pettersen et al., 2004).

3.9.2. Phylogenetic analysis

The amino acid sequences from PDB and the UniProt Knowledgebase were compared by applying BLAST. Rooted phylogenetic trees were aligned in CLUSTAL OMEGA (Sievers et al., 2011) and generated with iTOL (Letunic and Bork, 2007).

4. MAIN RESULTS

4.1. Application of MIMS for monitoring of thylakoid located respiratory electron transport under illumination

The location of Cox and Cyd in the TM of *Synechocystis* leads to an intriguing possibility that, in addition to their traditional role in respiration, they may also function as regulatory components of electron transport and/or as an electron valve during illumination. However, it is challenging to monitor RTO based O_2 consumption during illumination since (i) PSII simultaneously evolves O_2 and (ii) several other enzymes are also using O_2 as an electron acceptor, thus increasing the complexity of the network around photosynthetic electron transport. To this end, I made use of membrane inlet mass spectrometry (MIMS), a modern technique that allows real-time monitoring of O_2 isotopes and allows differentiation between gross photosynthetic O_2 evolution and O_2 consumption during illumination, which is not possible when using a traditional Clark-type oxygen electrode. The application of specific inhibitors of electron transport and RTOs makes it possible to further differentiate the location and roles of RTOs in *Synechocystis*. In addition to MIMS, distinguishing the different functions of RTOs required the application of several biophysical methods in combination with inhibitor treatments.

4.1.1. Cyd accepts electrons from the PQ pool under illumination when LET is disrupted

The gas exchange experiments with the Δ*cyd* mutant lacking functional Cyd demonstrated only slightly decreased dark respiration (Paper I, Table 1, Fig. 2). In line with this, the redox state of the PQ pool in Δ*cyd* was not affected in darkness (Paper I, Figs. 7–9). However, the deletion of Cyd caused a significant decrease in the effective PSII yield, Y(II), when the cells were exposed to short (1 min) high-light pulses and the intensity was increased stepwise (Paper I, Fig. 6A). To discover the exact localization of RTOs in the TM, DBMIB was applied as an inhibitor of LET functioning at the Cyt b_6f site (Draber et al., 1970; Yan et al., 2006). Use of DBMIB allows the study of electron flow from PSII and the PQ pool and also eliminates contribution of Flv1/3 to light-induced O_2 uptake occurring down-stream of PSI. In the presence of DBMIB, WT was still able to maintain the light-induced O_2 uptake which demonstrates that electrons are routed from the PQ pool to O_2 during illumination (Paper I, Fig. 2, Table 1). In contrast, the simultaneous addition of DBMIB and HQNO, the latter being the specific inhibitor of Cyd (Pils et al., 1997), abolished the light induced O_2 uptake in WT as well as in the Δ*cox*

mutant. In the Δ*cyd* mutant and the Δ*cox/cyd* mutant, the addition of DBMIB was, by itself, enough to prevent light-induced O_2 uptake. Importantly, the addition of DCBQ, the artificial electron acceptor acting at the Q_B site of PSII (Graan and Ort, 1986), also completely inhibited light-induced O_2 uptake by Cyd (Paper I, Supplemental Fig. S2A). Together, these results demonstrated that, of the RTOs residing in the TM, Cyd was the one that was able to perform light-induced O_2 uptake accepting electrons directly from the PQ pool when LET was disrupted.

4.1.2. Cox accepts electrons under illumination in the absence of Cyd or functional PSI

The deletion of Cox significantly decreased dark respiration (Paper I, Table 1), in line with previous studies (Pils et al., 1997; Howitt and Vermaas, 1998; Pils and Schmetterer, 2001), and caused slightly higher reduction of the PQ pool in the dark but not during mild or high intensity illumination (Paper I, Figs. 7–9). These results demonstrate that Cox is the main RTO involved in dark respiration in *Synechocystis*. However, a clear difference in the Q_A^- reoxidation kinetics in darkness and in the P700 oxidoreduction kinetics between Δ*cox* and Δ*cox/cyd* cells (Paper I, Figs. 7-9) indicate that Cyd can, at least partially, substitute for Cox in *Synechocystis*.

Even though it is evident that Cyd is the main RTO performing O_2 photoreduction, Cox can also act as an electron sink during illumination in certain occasions. The higher donor side limitation of PSI, Y(ND), in Δ*cyd* compared to Δ*cox*/*cyd* under strong illumination (Paper I, Fig. 6B) indicated that the capacity of Cox to regulate the quantity of electrons arriving to PSI during high-light illumination increases when Cyd is absent. In addition, experiments with the PSI-less mutant (Shen et al., 1993) showed that Cox is the major RTO mediating electrons to O_2 in light if PSI is absent (Paper I, Fig. 5).

4.1.3. Interplay between RTOs and Flv 1/3

Despite the ability of RTOs to perform O_2 uptake at the same rate during illumination and darkness, Flv1/3 seems to perform the majority of O_2 uptake during illumination in *Synechocystis* when cells are shifted from darkness to high light (Paper I, Supplemental Fig. 1; Helman et al., 2003; Allahverdiyeva et al., 2011). Furthermore, Flv1/3 are essential under fluctuating light (FL)-conditions (when background low light is regularly interrupted with high light pulses) protecting the cells, and particularly PSI, from photodamage (Allahverdiyeva et al., 2013). Surprisingly, the Δ*flv1/3* cells incubated for 3 days in FL (20 µmol photons m^{-2} s^{-1} background light that was interrupted with 30-s high light pulses of 500 µmol photons m^{-2} s^{-1} every 5 min) demonstrated a low but

significant level of O_2 photoreduction that did not respond to the changes in light intensity and was KCN sensitive (Allahverdiyeva et al., 2013; Paper I, Fig. 3). The addition of HQNO to the cells grown under FL caused a significant decrease in the light-induced O_2 uptake in the Δ*flv1/3* mutant but not in the WT (Paper I, Fig. 3), indicating the involvement of Cyd in O_2 photoreduction under suboptimal conditions in the Δ*flv1/3* mutant.

4.1.4. The duration of alternating dark and high-light phases is crucial for the viability of Δ*cyd*/*cox*

Importantly, the Δ*cyd*, Δ*cox*, and Δ*cyd*/*cox* mutant strains did not show any growth phenotype under high light (500 µmol photons m^{-2} s^{-1}) (Paper I, Supplemental Fig. 3) or FL conditions (Paper I, Fig. 4). It was recently demonstrated that the presence of either Cox or Cyd is essential for the growth of *Synechocystis* under 12-h-high light/12-h-dark square-wave cycles unless the transitions are sinusoidal (Lea-Smith et al., 2013). When the cells were subjected to a 5 min high light / 5 min dark square-wave cycles (Paper I, Fig. 4), all the RTO mutants were viable, although the growth of the Δ*cox* and Δ*cox/cyd* mutants started to slow down after 7 days in comparison with the WT. The importance of RTOs during light-dark interfaces depends on the lengths of both the dark and high-light periods. In the absence of thylakoid localized RTOs, the PQ pool becomes highly over-reduced in the dark (Paper I, Figs. 7-9). This causes the production of ROS but also prevents the generation of a proton gradient across the TM for ATP synthesis, which is needed to repair damaged proteins accumulated during the high light period. If the lengths of the dark and high light periods are shorter and, thus, alternate more frequently, cells missing both Cox and Cyd can also oxidize the PQ pool and produce ATP for the purpose of repairing photodamaged proteins.

4.2. Characterizing the role of energy dependent pyridine transhydrogenase PntAB in *Synechocystis*

The regulation of the NAD(P)H/$NAD(P)^+$ ratio is among the most essential functions of cellular metabolism in all living organisms. One of the enzymes involved in this regulation process is PntAB. Its structure and physiological role have already been broadly characterized in several heterotrophic organisms (Sauer et al., 2004; for a review, see Jackson, 2012; Jackson et al., 2015). However, the biological importance of PntAB in photosynthetic organisms, including cyanobacteria, has not been determined in detail. Thus, the knock-out mutant (Δ*pntA*), missing the α-subunit of heteromultimeric PntAB, was constructed, which resulted in nonfunctional

transhydrogenase. This mutant was subjected to phenotypical and biophysical characterization under photoautotrophic and photomixotrophic growth conditions.

4.2.1. Peptides encoded by *pntA* and *pntB* are both needed to form functional PntAB

To model the 3D-structure of PntAB from *Synechocystis*, the amino acid sequences of PntA (which forms the α-subunit) and PntB (which forms the β-subunit) were used to search for suitable templates among several resolved crystal structures of transhydrogenases from both eukaryotes and prokaryotes (Paper II, Fig. 1). Outside of the cyanobacterial phylum, *E. coli* transhydrogenase showed the highest similarity with 61% and 68% sequence identity to the α and β subunits, respectively, whereas for other organisms the similarity was lower (39–54% for the α-subunit and 42–54% for the β-subunit). These sequences were then applied to construct a model describing how polypeptides are assembled in *Synechocystis* to the native quaternary structure forming the functional PntAB dimer (Paper II, Fig. 2) (Fig.3). The constructed model indicated that both the α and β subunits in *Synechocystis* are needed for the binding of NADH and $NADP^+$ substrates and for the formation of the proton channel across the membrane. Therefore, the deletion of PntA was enough to eliminate the transhydrogenase activity in *Synechocystis*. The constructed model demonstrated that the N-terminal region of PntA contains a NADH/NAD^+ binding domain (domain I) while the C-terminus forms a part of the integral transmembrane domain constituting the proton channel (domain II, 4 transmembrane helixes formed by PntA). In PntB, the functional regions are in reverse order: the N-terminal part completes the transmembrane domain (domain II, 9 transmembrane helixes formed by PntB) and the C-terminal region forms the NADPH/$NADP^+$ binding part (domain III). Modelling results also indicated that in the native quaternary structure two of these heterodimers are required to form a biologically active conformation (α2β2) (Paper II, Fig. 2) (Fig.3).

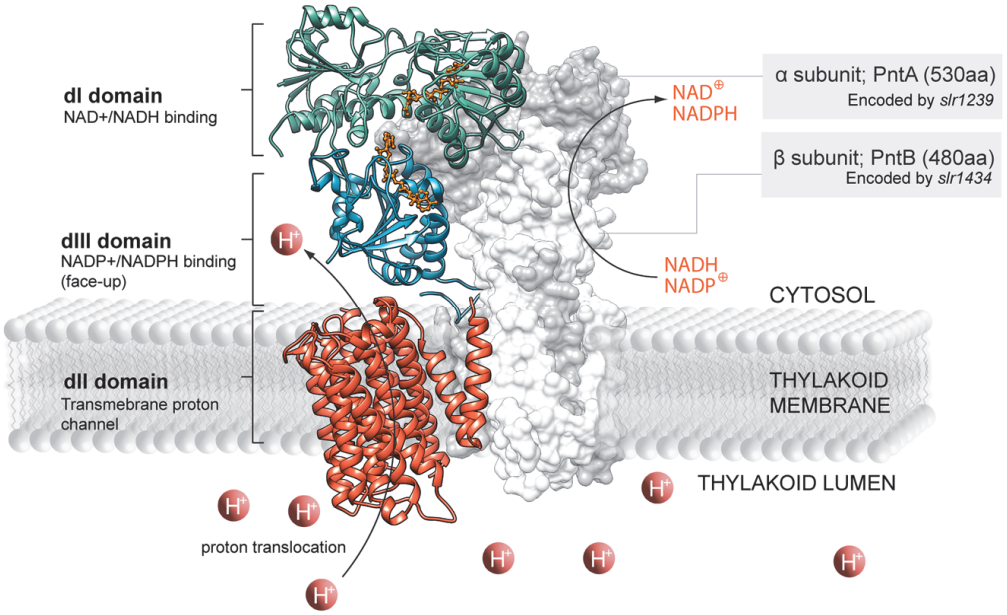

Figure 3. The quaternary structure model of *Synechocystis* pyridine nucleotide transhydrogenase PntAB.

4.2.2. PntAB is located in the thylakoid membrane of *Synechocystis* and utilizes the proton gradient to energize the conversion of NADH to NADPH

To discover the location of PntAB in *Synechocystis*, the cells were fractionated to the TM, the PM, and the soluble compartment. The preparations were subjected to immunoblotting with a specific antibody raised against PntA (Paper II). A strong signal was detected from the thylakoid fraction and only a minor signal from the plasma membrane (Paper II, Fig. 3). The latter was most probably due to contamination as a result of fractionation. The location of PntAB in the same compartment with the photosynthetic machinery allows the enzyme to use the proton gradient established during photosynthesis. Protons are transported from the thylakoid lumen into the cytosol via the proton channel in the PntAB transmembrane domain, thus providing energy for catalytic hydride transport between NAD(H) and NADP(H).

4.2.3. PntAB enables cell growth at the interphase of photomixotrophy and heterotrophy

The deletion of PntAB did not affect growth under photoautotrophic conditions or under photomixotrophic conditions when there was enough light for photosynthesis (Paper II, Figs. 4-5). However, under photomixotrophic conditions when light intensity

was too low for cells to efficiently perform photosynthesis, the growth of Δ*pntA* was drastically compromised compared to the WT and the difference in the growth rate between the WT and Δ*pntA* increased in accordance with decreasing light intensity. These results indicate that the function of transhydrogenase is crucial when photosynthesis is not able to produce enough energy and reducing power for growth, causing cells to use carbohydrates as an energy source. There was, however, no difference in growth between the WT and Δ*pntA* cells during the dark periods with or without glucose, which is likely due to the adequate NADPH production by the OPP pathway for metabolic needs under these conditions.

4.2.4. The presence of PntAB is needed for the protection of photosynthetic machinery under low-light mixotrophy

To find out the reason behind the compromised growth of Δ*pntA* under low-light mixotrophic conditions, a Δ*pntA* mutant grown under these conditions was subjected to extensive biophysical characterization. First, fluorescence analysis was performed with a Dual-PAM fluorometer. The Δ*pntA* mutant exhibited significantly lower effective yield of PS II, Y(II), and higher donor side limitation of PS I, Y(ND), compared to the WT (Paper II, Fig. 6). In line with these, the maximum quantum yield of PS II (F_v/F_m) in Δ*pntA* was only half of that measured in the WT (Paper II, Table 2). The observed decrease in the capacity of PSII was primarily caused by a diminished PSII/PSI ratio, which was indicated by lower emission from PS II (685 and 695 nm) in the 77K fluorescence emission spectra (440 nm excitation) (Paper II, Fig. 7) in Δ*pntA* compared to the WT. The decrease of the PSII yield in the Δ*pntA* mutant was confirmed by western blotting with the D1-specific antibody (Paper II, Fig. 8). Differences in Y(II) and in Y(ND) between the WT and Δ*pntA* became less evident when light intensity was increased, in line with the importance of PntAB under low-light mixotrophy (Paper II, Fig. 9).

In addition to PSII, the function of PSI was also compromised in Δ*pntA* under low-light mixotrophy, indicated by a decreased maximal amount of oxidizable P700 (P_m) (Paper II, Table 2) as well as by a lower amount of the PsaB protein (Paper II, Fig. 8) in Δ*pntA* compared to the WT. However, this was most probably a secondary effect due to the damage to PSII. The concept of impaired photosynthetic energy transport in Δ*pntA* was further supported by the significant amount of detached PBS during the light period, indicated by a higher F_0 value (Paper II, Fig. 6) as well as by significantly higher emission peaks originating from PBS (650 nm-670 nm) and from the terminal emitter (685 nm) in the 77K fluorescence emission spectra when samples were excited with 580 nm light (Paper II, Fig. 7). Moreover, the analysis of state transition kinetics demonstrated that

Δ*pntA* is almost locked in State II (Paper II, Fig. 6), which might be caused by the detachment of PBS (Stoitchkova et al., 2007; for a review, see van Thor et al., 1998; Mullineaux and Emlyn-Jones, 2005).

4.3. Investigating the roles of NDH-2s NdbC and NdbA in *Synechocystis*

In *Synechocystis*, the NDH-2s have been suggested to have a regulatory role as redox sensors that respond to the redox state of the PQ pool (Howitt et al., 1999). To study this hypothesis further, mutants lacking NdbA and NdbC were constructed and characterized using modern quantitative proteomic methods as well as various biophysical and biochemical methods. Because NDH-2s oxidize pyridine nucleotides, special attention was paid to their function under different growth modes.

4.3.1. NdbC is located in the plasma membrane and its deletion causes changes in cell morphology, growth rate and intracellular glycogen content in *Synechocystis*

To determine the subcellular location of NdbC in *Synechocystis*, the cells were fractionated to the TM, the PM, and the soluble compartment, followed by immunoblotting with the NdbC-specific antibody. An intense NdbC protein band was detected only in the fraction representing the PM (Paper III, Fig. 5). The mutant deficient in the NdbC protein, Δ*ndbC*, demonstrated a larger cell size than the WT both when cells were grown both under ambient CO_2 conditions (LC) and when they were grown in the presence of 3% CO_2 (HC) (Paper III, Fig 3B).

The number of the cells corresponding to the same OD value was almost halved in the Δ*ndbC* mutant compared to the WT in both studied conditions (Paper III, Table 1). Due to the bigger cell size, the growth was monitored based on a cell number. The WT grew almost twice as fast as the Δ*ndbC* mutant under LC as well as under HC conditions (Paper III, Fig. 2C-D). The bigger cell size of the mutant was in line with the increased dry weight, Chl concentration, and total protein amount per cell compared to the WT under both studied conditions (Paper III, Table 1). In addition to bigger cell size, transmission electron microscopy (TEM) figures revealed the accumulation of putative glycogen granules inside the Δ*ndbC* cells (Paper III, Fig. 3B). In line with this result, the intracellular glycogen content per cell in the Δ*ndbC* mutant was almost three times as high as in the WT under both LC and HC conditions (Paper III, Fig. 3D).

4.3.2. The deletion of NdbC affects photosynthetic electron transport

Despite of observed defects related to growth and morphology in Δ*ndbC* under photoautotrophy, the deletion of NdbC did not have a drastic influence on the capacity of photosystems under these conditions because no significant differences were detected in F_v/F_m and P_m values (Paper III, Supplemental Table S1) under LC or HC conditions. Furthermore, no considerable change in respiration was detected between the WT and Δ*ndbC* (Paper III, Table 2). However, the Δ*ndbC* mutant demonstrated a slightly lower effective yield of PSII, Y(II), (Paper III, Fig. 4A) as well as decreased gross and net oxygen evolution rates (Paper III, Table 2) compared to the WT. Moreover, CET around PSI was increased in the Δ*ndbC*, which was demonstrated by the higher F_0 rise when cells were transferred to darkness (Paper III, Fig. 4D) as well as by the slower oxidation and faster re-reduction of P700 (Paper III, Fig. 4C). The increase in CET was further supported by the upregulation of Cyt b_6f, PSI and the small form of FNR, FNR_S, (Paper III, Table 3) which was proposed to participate in CET by oxidizing NADPH (Korn, 2010).

4.3.3. Global proteome analysis reveals modifications in several metabolic pathways and in the expression of multiple transporters due to the deletion of NdbC

To get a more comprehensive picture of the metabolic changes induced by the deletion of NdbC in *Synechocystis* cells, an extensive proteomic analysis was conducted from the cells grown under autotrophic conditions. In the Δ*ndbC* mutant, a diminished sugar catabolism compared to the WT was deduced from the downregulation of several glycolysis specific enzymes, including phosphofructokinase (PfkA), pyruvate kinase (Pyk1), and glyceraldehyde-3-phosphate dehydrogenase (Gap1), together with Glc-6-P dehydrogenase (Zwf) and 6-phosphogluconolactonase (Pgl), belonging to the OPP pathway (Paper III, Table 3). Furthermore, SigE, which upregulates the expression of genes involved in sugar catabolism (Osanai et al., 2005), as well as its anti-σ factor ChlH (Osanai et al., 2009) were downregulated in Δ*ndbC* compared to the WT (Paper III, Table 3). Nonetheless, the amounts of proteins performing glycogen synthesis or degradation were not altered in Δ*ndbC* compared to the WT (Paper III, Supplemental Tables 4-5). Several proteins directly involved in cell division, like FtsZ, ZipN, MinC, MinD and MinE (Mazouni et al., 2004), were downregulated in Δ*ndbC* compared to the WT (Paper III, Table 3), which may explain the bigger size of Δ*ndbC* cells (Paper III, Fig. 2). In addition, some global regulators that influence cell division, including SigE (Osanai et al., 2013), the AbrB-like transcription factor Sll0822 (Yamauchi et al., 2011) and

circadian clock proteins KaiB and KaiC (Cohen and Golden, 2015), were downregulated in the Δ*ndbC* mutant under LC conditions (Paper IIII, Table 3).

The deletion of NdbC affected the expression of a higher number of proteins under LC conditions than under HC conditions. In particular, many transporters and binding proteins located in the PM were downregulated in LC (Paper III, Table 3). Phosphate transporters Pst1 and Pst2 (Pitt et al., 2010) were severely downregulated in Δ*ndbC* (Paper III, Table 3). In addition, NRT transporters that perform nitrate and nitrite uptake, as well as ammonium and urea transporters, were downregulated in Δ*ndbC*, together with regulatory proteins PII and PipX (Llácer et al., 2010; Espinosa et al., 2014; for a review, see Forchhammer, 2004). Furthermore, multiple transporters functioning in the uptake of other nutrients, including metal ions, potassium, polysaccharides and amino acids, were downregulated in Δ*ndbC* (Paper III, Table 3). In contrast, all the subunits of the high affinity HCO_3^- transporter BCT1 (Omata et al., 1999) were upregulated, while no upregulation of known BCT-1 inducers CmpR (Nishimura et al., 2008; Daley et al., 2012) or Sll0822 (Orf et al., 2016) was detected (Paper III, Table 3).

4.3.4. NdbC is in crosstalk with NDH-1

The deletion of NdbC altered the expression of NDH-1 complexes under LC conditions. First, NdhF4 and CupB, specific subunits for the low-affinity CO_2 uptake complex NDH-1_4 (Ohkawa et al., 2000), were downregulated in the mutant compared to the WT (Paper III, Table 3). Meanwhile, the expression of the low-CO_2-inducible high-affinity complex NDH-1_3 was not altered (Paper III, Table 3). In line with these results, MIMS measurements demonstrated the decline in the fast phase of CO_2 uptake in Δ*ndbC* compared to the WT (Paper III, Table 2), which probably occurs due to the decreased levels of the NDH-1_4 complex (Paper III, Table 3). In addition, the deletion of NdbC affected the expression of NDH-1 complexes that take part in respiration and CET (for a review, see Peltier et al., 2016). NDH-1_2 was upregulated in the Δ*ndbC* mutant, which was indicated by a prominent increase in the amount of NDH-1_2 specific NdhD2, but NDH-1_1 was expressed similarly in Δ*ndbC* and the WT (Paper III, Table 3). To investigate a possible interplay between NDH-1 and NdbC more extensively, total proteins from several NDH-1 mutants lacking specific subunits of the different complexes were analyzed with western blotting using α-NdbC. Interestingly, the M55-mutant that was unable to form any functional NDH-1 complexes (Ogawa, 1991) did not express NdbC in detectable amounts (Paper III, Fig. 5B). In addition, the mutants missing NdhD2 expressed considerably less NdbC compared to the WT, but in the mutants missing NdhD4, the NdbC levels were similar to those in the WT (Paper III, Fig. 5B).

4.3.5. NdbC is essential under LAHG conditions

Proteomic analysis of the Δ*ndbC* mutant showed that sugar catabolism in general was downregulated in this mutant under autotrophic conditions (Paper III, Table 3). To investigate this effect further, the Δ*ndbC* cells were grown under LAHG conditions, where cells were illuminated for only 10 min every 24 h and glucose was added to the growth medium. Such conditions should stimulate the utilization of metabolic pathways involved in the degradation of sugars. Indeed, the Δ*ndbC* mutant was not able to grow under LAHG conditions (Paper III, Fig. 6A). However, the defect in the growth of Δ*ndbC* was not caused by the inability to utilize external glucose, because no difference in growth was observed between the WT and Δ*ndbC* under photomixotrophic conditions (Paper III, Fig. 6C). Fluorescence analysis demonstrated that the ETC of Δ*ndbC* only became considerably over-reduced in darkness and during the dark-light transition when glucose was supplemented (Paper III, Fig. 7). Despite this, Δ*ndbC* managed to grow in the presence of glucose during the dark-light rhythm if the light period was provided frequently enough (Paper III, Fig 6B). This is due to the efficient oxidation of ETC under illumination (Paper III, Fig. 7).

4.3.6. NdbA is located in the thylakoid membrane and is required for optimal growth under LAHG conditions

The protein fractions from the isolated TM, PM and soluble compartment were analyzed using immunoblotting with α-NdbA. The results clearly demonstrated that in *Synechocystis*, NdbA is located in the TM (Paper IV, Fig. 1C). The deletion of NdbA did not have a substantial effect on growth (Paper IV, Fig. 2A), the protein expression (Paper IV, Supplemental Tables 1-3) or the photosynthetic capacity (Paper IV, Fig. 5A-B, Table 2) under photoautotrophic conditions. In addition, the NdbA-protein amount in WT remained below the clear detection level in the DDA analysis under these conditions (Paper IV, Fig. 4). NdbA was produced in considerably higher amounts in the Δ*ndbA*::*ndbA* strain (with the functional *ndbA* gene reintroduced to Δ*ndbA*) than in the WT (Paper IV, Fig. 1; Fig. 4). Under LAHG conditions, the NdbA amount increased past the DDA analysis detection level in the WT, yet NdbA was still expressed in a higher quantity in the Δ*ndbA*::*ndbA* strain than in WT (Paper IV, Fig. 4). The deletion of NdbA caused a growth retardation under LAHG conditions which was not detected in the Δ*ndbA*::*ndbA* strain (Paper IV, Fig. 2C). However, the changes in the amount of NdbA did not affect growth under photomixotrophy (Paper IV, Fig. 2B).

4.3.7. Alterations in the amount of NdbA cause changes in the expression of photosynthetic components and C_i assimilation proteins under LAHG conditions

Several subunits of PSII (PsbE, D2, PsbV, D1 and PsbB) were upregulated in Δ*ndbA* compared to the WT under LAHG conditions (Paper IV, Table 1). PSII (indicated by PsbE, D2, PsbV, D1, CP43, PsbP, PsbU and PsbZ) was also upregulated in the Δ*ndbA*::*ndbA* strain compared to the WT under LAHG conditions, being more prominent than in Δ*ndbA*. Additionally, the expression of PSI (indicated by PsaK, PsaB, and Ycf4) and Cyt b_6f (indicated by PetA,B,C,D) was upregulated in the Δ*ndbA*::*ndbA* strain compared to the WT under these conditions, while Flv2/4 and OCP were downregulated (Paper IV, Table 1). Moreover, the Δ*ndbA*::*ndbA* strain demonstrated elevated Chl and phycobilin content compared to the WT (Paper IV, Fig. 3), accompanied by the increased expression of proteins participating in the biosynthesis of Chl (indicated by ChlB,N,L,H,G) and the formation of PBS (indicated by CpcD, CpcA, ApcF, CpcC1, ApcE, ApcD, and CpcG2) (Paper IV, Table 1).

Despite the increased amount of PSII in Δ*ndbA* under LAHG conditions (Paper IV, Table 1), the effective yield of PSII during illumination, Y(II), was practically not detected in this strain, similarly to the WT (Paper IV, Fig. 5C). On the contrary, a clear, yet small, induction in Y(II) was observed in the Δ*ndbA*::*ndbA* strain under these conditions (Paper IV, Fig. 5C), while no significant difference was detected in the effective yield of PSI, Y(I), between the studied strains (Paper IV, Fig. 5D). However, in Δ*ndbA*::*ndbA* the P_m value, indicating the maximal amount of oxidizable P700, was almost twice as high as in the WT and Δ*ndbA* mutant under LAHG conditions (Paper IV, Table 2).

Furthermore, several components involved in inducible C_i uptake (for a review, see Kaplan, 2017), including BCT1 (indicated by CmpB and CmpC), SbtA and NDH-1_3 (indicated by CupA and CupS) had upregulated protein levels in Δ*ndbA* compared to the WT under LAHG conditions (Paper IV, Table 1). On the contrary, in the Δ*ndbA*::*ndbA* strain overexpressing NdbA, BCT1 (indicated by CmpA, CmpB and CmpC), SbtA and NDH-1_3 (indicated by NdhF3, CupA and CupS) together with the large subunit of Rubisco, RbcL, were downregulated compared to the WT (Paper IV, Table 1).

5. DISCUSSION

In this doctoral thesis work, I have studied the redox reactions occurring in the TM, focusing on the interplay between photosynthetic and respiratory electron transfer during illumination. In addition, I have investigated how the redox states of pyridine nucleotides, NADPH/$NADP^+$ and NADH/NAD^+, produced by photosynthetic light reactions and glycolytic pathways are inter-regulated by the proteins residing in both the TM and the PM, especially when the primary carbon source changes from CO_2 to carbohydrates.

5.1. *Synechocystis* RTOs contribute to the alleviation of redox pressure under suboptimal light conditions

RTOs have an important role in completing the respiratory electron transport and creating the proton gradient needed for ATP production in the dark. However, the two RTOs in *Synechocystis*, Cox and Cyd, reside in the TM, and my experiments clearly demonstrate that respiratory reactions of *Synechocystis* also continue during illumination (Paper I). This indicates that RTOs must make a significant contribution to the regulation of the ETC and to the photoprotection of the photosynthetic apparatus. However, it is challenging to accurately determine the contribution of each individual RTO regulation process. Furthermore, many other enzymes besides RTOs also use O_2 as an electron acceptor in *Synechocystis*. It was demonstrated in Paper I that Cyd oxidizes the PQ pool when there is a blockage of electron transport, or under FL conditions if Flv1/3 are missing and thus preventing the efficient oxidation of the ETC. The role of Cyd in the oxidation of the PQ pool was suggested earlier based on fluorescence measurements (Schneider et al., 2001; Berry et al., 2002). The fluorescence signal could, however, be affected by various factors. The gas exchange measurements described in Paper I provided, for the first time, direct experimental evidence that the photoreduction of O_2 by Cyd alleviates the redox pressure of the PQ pool. This alternative pathway for PQ pool oxidization seems to be especially important, since all cyanobacteria, which may be exposed to strong illumination in their natural growth environments, encode at least one PQH_2 oxidizing RTO (Cyd or PTOX) in their genomes (Lea-Smith et al., 2013).

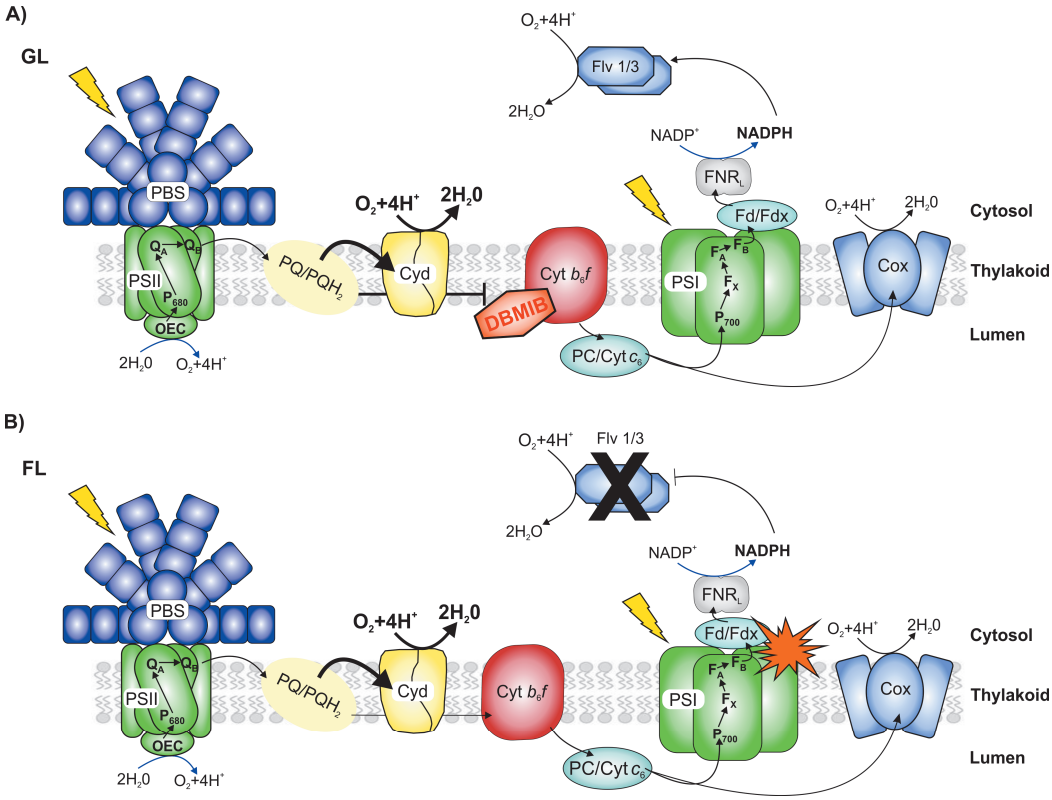

Figure 4. Schematic representation of O_2 photoreduction by Cyd as evidenced A) by inhibition of the linear electron transport chain by DBMIB under growth light and B) under fluctuating light conditions in the absence of Flv 1/3. GL=growth light, FL=fluctuating light.

Despite elevated Cyd activity (Paper I; Berry et al., 2002), there was no increase in the transcript levels of genes encoding *Synechocystis* Cyd under high light (Gendrullis et al., 2008) or FL conditions (Mustila et al., 2016). Surprisingly, the transcription of genes encoding subunits of Cyd was not elevated even in the presence of DBMIB (Hihara et al., 2003). This suggests that the activity of Cyd is controlled at the later steps of gene expression, most probably at the post-transcriptional level, when the ETC becomes over-reduced.

In addition to its significant role under illumination, Cyd also plays a minor role in dark respiration. This was indicated by only slightly lower O_2 uptake in the dark in Δ*cyd* compared to the WT (Paper I, Table 1) and by a similar-to-WT redox state of the PQ pool in the dark (Paper I, Figs. 7-9). Contrary to Cyd, Cox is the major RTO performing dark respiration in *Synechocystis*. This was indicated by a significant decrease in the respiration rate in the absence of Cox (Paper I, Table 1), which is in agreement with earlier studies (Howitt and Vermaas, 1998; Pils and Schmetterer, 2001). Moreover, the

ETC was clearly over-reduced in the Δ*cox* mutant in darkness (Paper I, Figs. 7-9). However, Cox can also regulate the amount of electron flow to PSI under high light, albeit the activity of Cox increases only in the absence of Cyd (Paper I, Fig. 6) or PSI (Paper I, Fig. 5).

Earlier studies focusing on Flv 1/3 (Helman et al., 2003; Allahverdiyeva et al., 2011) and the results presented in Paper I indicate that Flv1/3 and RTOs perform O_2 photoreduction in a different manner. Flv1/3 reduces O_2 rapidly and with greater capacity, while RTOs function on slower time ranges and on a more limited scale. The reported maximum O_2 photoreduction rate by Flv1/Flv3 at high light intensities was 26 µmol O_2 mg^{-1} Chl h^{-1} (Paper I, Fig. 3) but under severe C_i limitation this value can be much higher (Allahverdiyeva et al., 2011). In contrast, the RTO-based O_2 uptake in the Δ*flv1/3* mutant treated with FL was only 6 µmol O_2 mg^{-1} Chl h^{-1} (Paper I, Fig. 3). The maximum capacity of Cyd mediated O_2 uptake, measured in the presence of DBMIB in the WT, was around 11 µmol O_2 mg^{-1} Chl h^{-1} (Paper I, Table 1). The location of these enzymes in *Synechocystis* may partially contribute to their functional differences: Flv1/3 are soluble cytosolic proteins, which allows them to quickly associate with NADPH, whereas RTOs are located in the highly crowded TM. In addition, Flv1/3 are probably much more abundant proteins compared to RTOs in *Synechocystis*, but this remains obscure due to the difficulty of detecting RTOs in proteomic studies. Furthermore, the results presented in Paper I clearly indicate a separation of the main roles between TM-localized RTOs in *Synechocystis*: Cyd is accountable for the light induced O_2 uptake, and Cox is the main RTO under dark respiration, even though they can at least partially substitute each other. This is in line with the hypothesis suggested by *Schmetterer* (2016) that several cyanobacterial species encode in their genomes multiple RTOs, which must have specific functions. Otherwise, the synthesis of several multisubunit enzymes for the same purpose during every cell division would be a waste of resources.

5.2. Redox regulation optimizes *Synechocystis* metabolism under different growth modes

Pyridine nucleotides NADPH and NADH are essential molecules which provide reducing power to various metabolic reactions in all living organisms. In photosynthetic organisms, NADPH is abundant under photoautotrophic conditions and in *Synechocystis,* the intracellular NADP(H) pool is an order of magnitude larger compared to the NAD(H) pool (Cooley and Vermaas, 2001). This is due to their different roles in cellular metabolism in photosynthetic organisms: NAD(P)H is utilized in reductive

reactions such as CO_2 fixation and the biosynthesis of fatty and amino acids, whereas NAD(H) is mainly associated with oxidative catabolic reactions. However, the other possible roles of the NAD(P)H/NAD(P)$^+$ ratio, in addition to the provision of reducing power, have not been thoroughly studied in cyanobacteria. In higher plants, this ratio may have an important role during different developmental stages, responding to environmental stresses and forming a component of defense-related signaling, yet the exact mechanism remains largely unknown (for a review, see Noctor et al., 2006; Hashida et al., 2009; Pétriacq et al., 2013). In addition, NADH/NAD$^+$ status has been shown to regulate the interplay between nitrogen metabolism and carbon assimilation in higher plants (Dutilleul et al., 2005; Pétriacq et al., 2017).

Optimal ratios of NADPH/NADP$^+$ and NADH/NAD$^+$ are most likely controlled independently since these molecules are used in different types of metabolic reactions in the cell. This becomes important for the maintenance of cellular redox homeostasis when the growth mode of cyanobacteria changes and alters the activities of various metabolic pathways, especially those related to carbon utilization. However, much work remains to be done in understanding the mechanisms through which the intracellular NAD(H)/NADP(H) balance is maintained in cyanobacteria. To gain insights into two groups of enzymes oxidizing NADH, transhydrogenase PntAB (Paper II) and NDH-2s (Papers III and IV) were studied in this thesis work.

5.2.1 PntAB adjusts NADH/NADPH ratio during transition from heterotrophy to low-light mixotrophy

The results in Paper II indicate that the function of PntAB becomes extremely important for the growth of *Synechocystis* under low-light mixotrophic conditions when photosynthesis is not able to produce enough energy (ATP) and reducing power (NADPH) and the energy demand of the cells is fulfilled by the utilization of external carbohydrates. Under these conditions, the deletion of PntAB seems to cause both direct and indirect consequences in *Synechocystis* (Fig. 5). First, the intracellular NADPH/NADP$^+$ ratio is likely to decrease considerably, which results in the shortage of reducing power which is essential in, for example, CO_2 fixation as well as amino and fatty acid biosynthesis. Importantly, under these conditions the amount of NADPH derived from photosynthesis or the OPP pathway is apparently not sufficient to compensate for the absence of PntAB. Simultaneously, the NADH/NAD$^+$ ratio is expected to increase and accumulated NADH prevents glycolytic reactions. The imbalanced NAD(P)/NAD(P)H ratio would have a secondary effect on the intracellular ATP/ADP balance, shifting it towards of ADP. The decreased sugar catabolism will

obviously slow down ATP synthesis, but the amount of ATP produced by respiration will also be lower, because respiratory electron and proton transport via the NDH-1 complex in cyanobacteria is, at least indirectly, dependent on NADPH (Peltier et al., 2016). In terms of photosynthesis, one of the most important targets of ATP consumption is the maintenance of the PSII repair cycle, which is required even under low-light conditions (Tyystjärvi and Aro, 1996). Possible problems in the PSII repair cycle caused by the energy shortage would explain the described defects in the integrity of the photosynthetic apparatus. These defects originate from the malfunction of PSII and eventually lead to the impaired growth of the Δ*pntA* mutant under low-light mixotrophy. However, it is important to note that PntAB is dispensable in *Synechocystis* when the light intensity is high enough for photosynthesis to maintain the NADPH and ATP production.

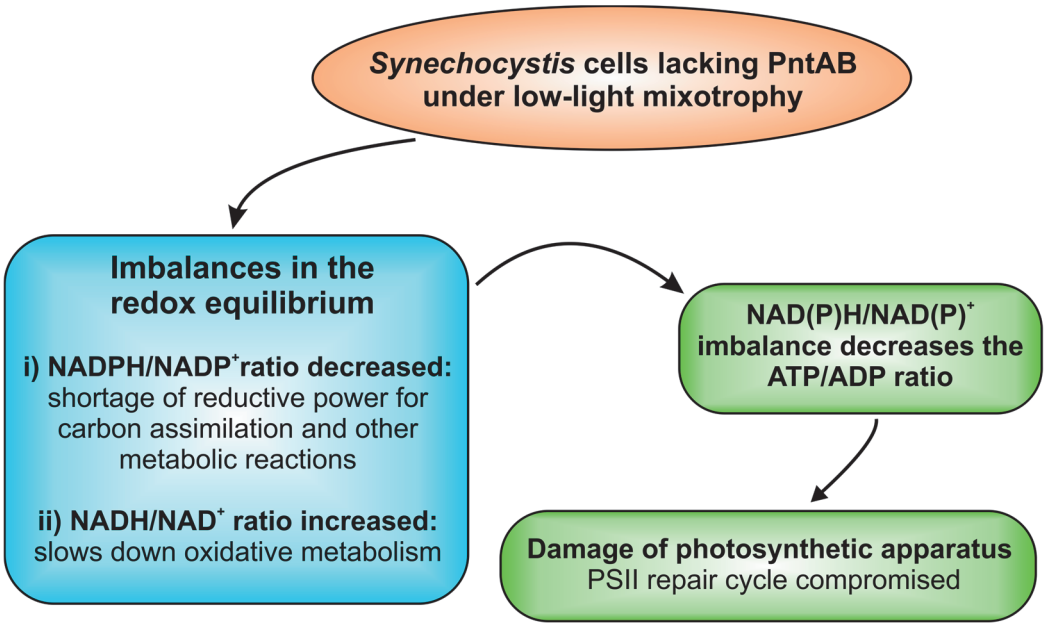

Figure 5. The consequences of PntAB deletion in *Synechocystis* under low-light mixotrophy.

Thus, the main physiological role of PntAB in *Synechocystis* is to ensure that the NADPH/NADH ratio stays high enough for cellular needs even when photosynthesis is not the main source for NADPH production. The direction of electron transport from NADH to $NADP^+$ is in agreement with the reported function of PntAB in *E. coli* (Sauer et al., 2004). At the same time, the PntAB activity keeps the NADH/NAD^+ ratio low enough to sustain oxidative metabolism and especially sugar catabolism. The importance of PntAB in maintaining glycolytic reactions is supported by the accumulation of *pntA* and

pntB transcripts when the rate of carbohydrate breakdown is increased in *Synechocystis* (Osanai et al., 2005). It is also important to notice that under low-light mixotrophic growth conditions, PntAB is the main source of NADPH in *Synechocystis* because its absence cannot be compensated for by the OPP or ED pathways, which also produce NADPH.

5.2.2. What is the purpose of NDH-2s in *Synechocystis*?

In addition to PntAB, NDH-2s oxidize pyridine nucleotides in *Synechocystis*, and they prefer NADH as a substrate over NADPH due to their amino acid sequences (Howitt et al., 1999). *Synechocystis* has three NDH-2s: NdbA, NdbB and NdbC. The role of NdbB in vitamin K_1 biosynthesis has been demonstrated recently (Fatihi et al., 2015), but the functions of the other two NDH-2s in *Synechocystis* have remained somewhat unclear. If the organism does not have any other enzyme that could perform NAD(P)H oxidation, the main role of NDH-2 is to function in respiratory NAD(P)H turnover (Melo et al., 2004). In this case, the proton gradient driving ATP synthesis is generated by the other respiratory complexes that accept electrons, directly or indirectly, from NDH-2. However, this is not the situation in *Synechocystis*, and the deletion of NDH-2s in *Synechocystis* did not result in decreased respiration (Paper III; Howitt et al., 1999). Thus, it was proposed by Howitt and co-workers (1999) that in *Synechocystis*, NDH-2s may rather have a regulatory function, possibly monitoring the redox state of the PQ pool. The other possibility for the function of NDH-2s in *Synechocystis* could be related to maintaining the redox balance of $NADH/NAD^+$, and it was demonstrated that the simultaneous deletion of all three *Synechocystis* NDH-2s substantially increased the $NADH/NAD^+$ ratio (Cooley and Vermaas, 2001). The specific targets of the possible NDH-2 mediated regulation, however, have remained elusive so far.

5.2.3. NdbC functions in the redox regulation of carbon allocation and is indispensable under LAHG conditions in *Synechocystis*

My thesis provides evidence that in cells grown under photoautotrophic conditions, NdbC plays a significant role in carbon allocation, balancing the storage and utilization (Paper III) (Fig. 6). The intracellular glycogen amount was at a significantly elevated level in the absence of NdbC (Paper III, Fig. 3), and it was accompanied by the general downregulation of sugar catabolic enzymes that play a role in glycolysis and the OPP pathway (Paper III, Table 3). Interestingly, the enzymes of the ED pathway were upregulated, possibly partially compensating for the downregulation of other glycolytic pathways. However, the exact mechanism for how the deletion of NdbC causes the

downregulation of sugar catabolism remains uncertain. The simplest explanation points to the elevated intracellular NADH/NAD^+ ratio: e.g. Gap1, which is a common enzyme to all glycolytic pathways (Chen et al., 2016), requires NAD^+ as a substrate. On the other hand, the observed effect on sugar catabolism in the absence of NdbC might be more indirect. SigE, which activates the expression of sugar catabolic genes (Osanai et al., 2005), was downregulated together with the increased amount of SigE anti-σ factor ClhH (Osanai et al., 2009) in the absence of NdbC (Paper III, Table 3). Despite glycogen accumulation, the expression of proteins involved in glycogen synthesis or degradation was not altered in the Δ*ndbC* mutant (Paper III, Supplemental Tables S4-S5). The glycogen accumulation could be explained by decelerated carbohydrate catabolism, which would result in the accumulation of glucose 6-phosphate. This, in turn, would increase the amount of substrate available to the enzymes involved in glycogen synthesis, causing glycogen accumulation without changes in the amounts of enzymes. Even though the deletion of NdbC led to bigger cell size (Paper III, Fig. 3), evidently due to defects in cell division, the increase in the intracellular glycogen amount was relatively more conspicuous compared to the Chl amount or to the total protein amount per cell (Paper III, Fig. 3, Table 1).

Under photoautotrophy, in addition to the effect on sugar catabolism, the deletion of NdbC disrupted the normal expression pattern of several transport systems (Paper III) located in the PM (Pisareva et al., 2011). The majority of these transporters, involved in the uptake of CO_2 as well as N, P and several other nutrients and metal ions, were downregulated (Paper III, Table 3). Particularly the downregulation of N and P uptake might be caused by the decreased sugar catabolism, due to the necessity of maintaining the intracellular C/N/P ratio. In addition to N-transporters, regulatory proteins PII and PipX, which activate N-metabolism (Llácer et al., 2010; Espinosa et al., 2014), were downregulated (Paper III, Table 3). The deviation of Δ*ndbC* in the expression of transport and binding proteins from WT expression was clearly more profound under LC conditions than under HC conditions, which is most probably due to the shortage of terminal electron acceptors under C-limiting conditions.

Even though the deletion of NdbC caused the retardation of growth under photoautotrophy (Paper III, Fig. 2), photosynthesis was not drastically compromised in these conditions (Paper III, Fig. 4, Supplemental Table 1). Intriguingly, the rate of CET was significantly elevated (Paper III, Fig. 4), which may compensate the lower ATP yield derived from sugar catabolism. Elevated CET in Δ*ndbC* was accompanied by the upregulation of the NDH-1_2 complex (Paper III, Table 3), which in *Synechocystis* is generally expressed considerably less than the NDH-1_1 complex (Herranen et al., 2004).

Furthermore, the proteomic results in Paper III suggested that the expressions of NdbC and NDH-1_2 are mutually affected by each other. The upregulation of Flv1/3 in Δ*ndbC* (Paper III, Table 3) could further contribute to the production of ATP via a functional water-water cycle (Allahverdiyeva et al., 2015).

In contrast to photoautotrophy, NdbC was essential for the survival of *Synechocystis* under LAHG conditions (Paper III, Fig. 6). Under these conditions, sugar catabolic pathways are stimulated because the breaking down of the added glucose provides the main source of energy. Thus, the most probable cause for the incapability of Δ*ndbC* to grow under these conditions is the general downregulation of glycolytic pathways, and particularly the downregulation of the OPP pathway, which was detected also under photoautotrophic conditions (Paper III, Table 3). Of the glycolytic pathways, the OPP pathway is especially important under heterotrophic conditions because it is the only metabolic route providing intermediates for nucleotide biosynthesis in darkness (Kruger and von Schaewen, 2003), and thus under heterotrophy 90% of glucose is directed to this pathway (Yang et al., 2002). Osanai et al. (2005) also demonstrated the retarded growth of the mutant deficient of sugar catabolism inducing SigE under LAHG conditions, and this result supports the hypothesis presented above.

In the absence of NdbC, the ETC became highly reduced under LAHG conditions (Paper III, Fig. 7), which may be caused by the reprogramming of carbon metabolism. The long-term severe over-reduction of the ETC induces the accumulation of ROS and oxidative stress, which, in the worst case, leads to cell death (Latifi et al., 2009; Narainsamy et al., 2013). Without added glucose, the over-reduction of the ETC under darkness in Δ*ndbC* was not significant (Paper III, Fig. 7), which further supports the hypothesis that defects in sugar catabolism are the reason for the growth retardation observed under LAHG conditions.

The results presented in Paper III demonstrated that NdbC is an important element in the regulation of the cytosolic NADH/NAD^+ balance. Under photoautotrophy, when the redox balance of the cytosol is mainly affected by photosynthetic light reactions occurring in the TM, NdbC is dispensable, although its absence causes slower growth and changes in the morphology of *Synechocystis* cells. Notably, the deletion of NdbC causes several distinct changes in the global protein expression pattern with apparent consequences on the metabolic balance under these conditions (Figure 6). Thus, the main function of NdbC under photoautotrophy is to fine-tune the balance between various metabolic pathways. However, under heterotrophy, where glycolysis is the only metabolic route to assimilate carbon for metabolic purposes, the role of NdbC in maintaining a low cytosolic NADH/NAD^+ ratio becomes crucial for cell viability.

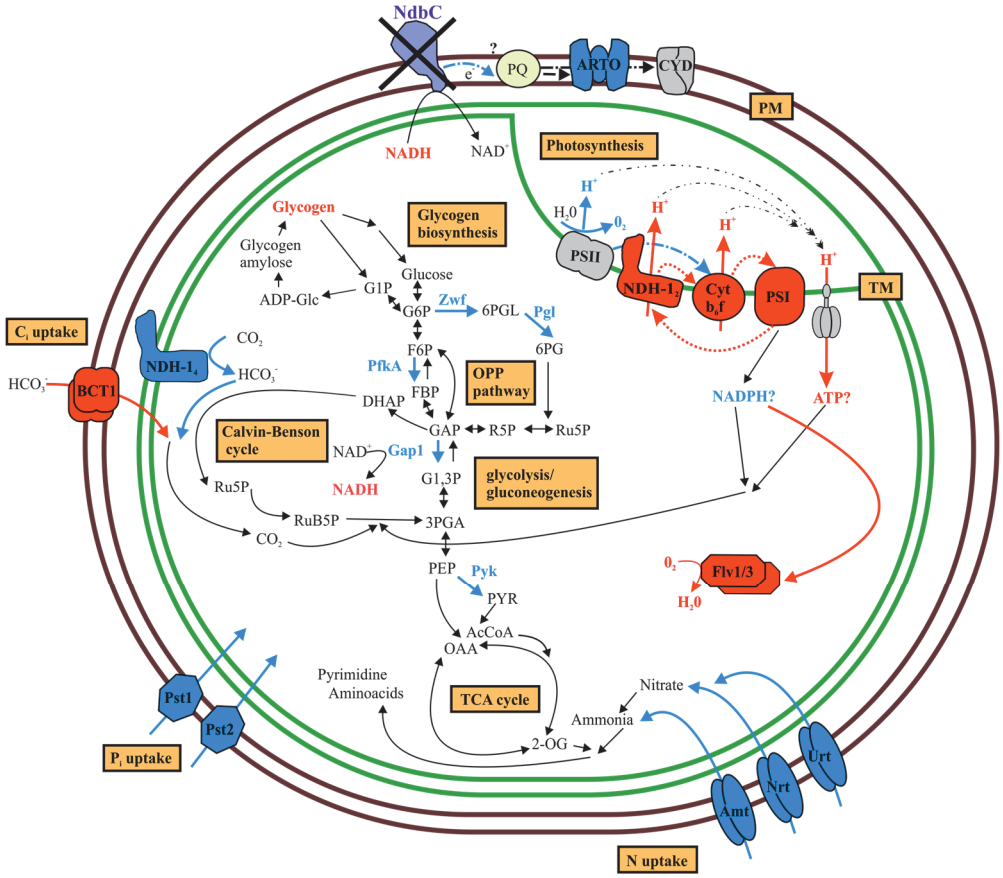

Figure 6. Representation of effects due to the NdbC deletion in *Synechocystis* under photoautotrophy. The upregulated or elevated protein complexes, metabolic routes, or compounds are marked in red, and the downregulated ones are marked in blue.

5.2.4. NdbA optimizes the growth of *Synechocystis* under LAHG conditions by regulating thylakoid functionality and C_i uptake

The results in Paper IV clearly demonstrate that NdbA offers no benefits to the growth of *Synechocystis* under photoautotrophic conditions. In contrast, the optimal growth of *Synechocystis* under LAHG conditions requires the expression of NdbA, as demonstrated by the growth retardation of the NdbA deletion mutant under these conditions (Paper IV, Fig. 2). The deletion of another NDH-2, NdbC, caused a general downregulation of sugar catabolism, which was postulated to lead to the observed incapability of Δ*ndbC* to grow under LAHG conditions (Paper III). Global proteome studies with both the Δ*ndbA* deletion and overproduction mutants, however, did not reveal any major changes in the expression of sugar catabolic proteins, either under LAHG conditions or photoautotrophy, as compared to the WT (Paper IV, Table 1; Supplemental Tables 1-5). These results demonstrate that NdbA and NdbC are clearly

associated with different metabolic pathways in *Synechocystis*, even though they both function in the oxidation of NADH and donate electrons to quinone. Their distinct roles might be due to their location in different cellular compartments in *Synechocystis*: NdbC resides in the PM (Paper III) whereas NdbA is found in the TM (Paper IV, Fig.1).

In *Synechocystis*, the internal TM system is almost completely lost under LAHG conditions (Plohnke et al., 2015), and the amounts of Chl (Barthel et al., 2013) and pigment-binding proteins (Plohnke et al., 2015) are significantly reduced in comparison to the situation under photoautotrophic growth conditions. However, the overexpression of NdbA maintained high phycobilisome and Chl content in *Synechocystis* under LAHG conditions (Paper IV, Fig. 5, Table 1). The increased Chl content in the Δ*ndbA*::*ndbA* strain was apparently caused by the upregulation of the protein subunits of the light-independent protochlorophyllide reductase (DPOR), which catalyzes the limiting step in the light-independent chlorophyll synthesis (LICS) pathway (Paper IV, Table 1; Fujita, 1996; Kada et al., 2003). LICS is necessary for adequate Chl accumulation when *Synechocystis* cells are grown under a light/dark rhythm in the presence of glucose (Fang et al., 2017). These results demonstrate that the excess NdbA prevents *Synechocystis* cells from downregulating the amount of pigments under LAHG conditions.

It has been shown previously that PSI remains to partially functional under darkness in *Synechocystis* (Barthel et al., 2013), and the data presented in Paper IV strongly suggest that NdbA has an important function in the preservation of PSI functionality. When NdbA was produced in excess under LAHG conditions, the P_m value, which represents the maximum oxidized P700 content, was substantially higher than in the WT (Paper IV, Table 2), together with proteins encoding PSI subunits (Paper IV, Table 1). In contrast, the deletion of NdbA resulted in significantly lower P_m values than in the WT under LAHG conditions (Paper IV, Table 2) without changes in the amounts of PSI-proteins (Paper IV, Table 1).

In contrast to PSI, PSII is inactive in the dark-grown *Synechocystis* cells (Barthel et al., 2013). Nevertheless, the overexpression of NdbA retained a low, yet significant, level of activity of PSII under LAHG conditions (Paper IV, Fig. 5). In both the NdbA deletion and overexpression mutants, the PSII proteins were at an elevated level as compared to the WT (Paper IV, Table 1) but it is difficult to judge the ultimate reasons for increased PSII-protein amounts in these mutants, as they can be caused by either elevated protein synthesis or decreased protein degradation. However, the excess of NdbA led to decreased amounts of OCP and Flv2/4 under LAHG conditions (Paper IV, Table 1), which can increase the effective yield of PSII, Y(II). OCP decreases the amount

of excitation energy arriving to PSII (for a review, see Kirilovsky and Kerfeld, 2013), whereas Flv2/4 probably accepts electrons in the vicinity of the Q_B site of PSII (Zhang et al., 2009b; Zhang et al., 2012; Bersanini et al., 2014), so both of them decrease the amount of electrons ending up to the PQ pool. In addition to photosystems, high NdbA content under LAHG conditions also keeps the Cyt b_6f complex at an elevated level (Paper IV, Table 1).

The mechanism through which NdbA regulates the photosynthetic machinery remains elusive. Yet, the location of NdbA in the TM (Paper IV, Fig. 1) suggests that the electron acceptor is PQ. Growth under LAHG conditions is maintained by sugar catabolism (Plohnke et al., 2015) that produces NADH in high amounts as a substrate for NdbA. Thus, under LAHG conditions, the deletion of NdbA is expected to cause an oxidation of the PQ pool while NdbA overexpression likely reduces the PQ pool. It has been demonstrated that the redox status of the PQ pool has a partial control over the transcription of photosynthetic genes during illumination in cyanobacteria: the oxidized PQ pool induces the expression of genes encoding PSII-proteins, while the reduced PQ pool provokes the expression of PSI-genes (Li and Sherman, 2000). Thus, the oxidized PQ pool in the Δ*ndbA* strain under LAHG conditions could, even in darkness, provoke the expression of only the PSII-proteins whilst in the Δ*ndbA*::*ndbA* strain the increased reduction of the PQ pool by excess of NdbA is expected to elevate the PSI amount in comparison to WT.

Another possible reason behind the observed elevated PSI amount and functionality, when NdbA is overexpressed under LAHG conditions, is the elevated content of DPOR and, consequently, enhanced Chl biosynthesis via LICS. Indeed, it has been demonstrated that under high-light conditions, most of the newly synthesized Chl is incorporated into PSI instead of PSII (Kopecná et al., 2012). However, the possibility that NdbA directly regulates LICS under LAHG conditions requires experimental evidence.

In addition to the photosynthetic components, NdbA also exerts an effect on the expression of proteins involved in C_i uptake under LAHG conditions (Paper IV, Table 1). The deletion of NdbA resulted in the upregulated expression of inducible HCO_3^- transporters BCT1 (Omata et al., 1999) and SbtA (Shibata et al., 2002b) together with the inducible CO_2 uptake complex NDH-1_3 (for a review, see Battchikova et al., 2011a). On the contrary, overexpression of NdbA had an opposite effect under LAHG conditions, resulting in lower amounts of proteins involved in C_i uptake than in the WT (Paper IV, Table 1). It is known that the expression of BCT1 is induced at the transcript level by CmpR (Omata et al., 2001), whereas the transcription of genes encoding SbtA

and NDH-1_3 are repressed by CcmR (Wang et al., 2004). In addition, the cyAbrB2 protein Sll0822 functions in co-inducing the expression of both BCT1 and SbtA related genes (Orf et al., 2016). However, the amount of the NdbA protein in the TM did not alter the amounts of these regulatory proteins involved in the expression of C_i uptake proteins (Paper IV; Supplemental Tables S4-S5). C_i uptake is not beneficial for *Synechocystis* under LAHG conditions due to the extensive utilization of glucose as a carbon source (Plohnke et al., 2015). Although the primary reason behind the growth retardation in the absence of NdbA under LAHG conditions remains elusive, it is conceivable that the energy required to maintain the C_i uptake systems at a high level would wastefully consume energy in a form of ATP, and result in an energy shortage that apparently compromises the growth of Δ*ndbA* under LAHG conditions.

6. CONCLUSIONS AND FUTURE PERSPECTIVES

The data presented in this doctoral thesis significantly expands the knowledge of light-dependent crosstalk between the various photosynthetic and respiratory electron transfer components residing in the thylakoid membrane of cyanobacteria. In addition, my results provide new information on the regulation of the NADP(H)/NAD(H) ratio, which becomes extremely important for the viability of cyanobacteria when their carbon source changes as the result of different growth modes. In this doctoral thesis work, I have demonstrated that in the cyanobacterium *Synechocystis* sp. PCC 6803:

1) RTOs continue to function under strong illumination at a similar rate as in darkness, thus contributing to the withdrawal of electrons from LET to O_2. In contrast to Flv1/3, RTOs do not have a high capacity and are therefore unable to adjust their activity under high light. Cyd resides just next to PSII and accepts electrons directly from the PQ pool. However, the activity of Cyd in O_2 photoreduction is not easy to demonstrate, only becoming obvious when LET was blocked at the Cyt b_6f level and when the Flv1/3 proteins were missing in the respective mutant grown in FL. Cox is the most important RTO in dark respiration, but was shown to still compete with PSI for electrons under high light in the absence of Cyd. (Paper I)

2) PntAB is essential for the growth of cells under low-light mixotrophic conditions because it is the source for the majority of NADPH under these conditions. Furthermore, PntAB affects the intracellular NADP(H)/NAD(H) ratio but has also an indirect effect on the maintenance of the photosynthetic machinery under low-light mixotrophy. (Paper II)

3) In the absence of NdbC, the glycolytic enzymes are downregulated, most probably due to the elevated NADH/NAD^+ ratio, which causes modulations in several metabolic pathways and changes in cell morphology under photoautotrophic conditions. Yet, the presence of NdbC becomes essential for cell viability under LAHG conditions when sugar catabolism is the sole carbon source. (Paper III)

4) NdbA optimizes the growth of *Synechocystis* under LAHG conditions by regulating photosynthetic functionality as well as C_i uptake. (Paper IV)

The characterization and optimization of the electron transfer routes in photosynthetic membranes are very important subjects to research if we are to meet the present-day challenges posed by the need to enhance the photon capture process in order to work towards the production of sustainable energy and high-value compounds in

cyanobacteria. The main goal is to re-direct the majority of electrons derived from solar energy stimulated water-splitting to desired end products, while at the same time preventing damage to the photosystems. To achieve this, extensive knowledge is required, not only about the roles of the components involved in the photosynthetic electron transport, but also about the pathways protecting the photosynthetic machinery. Together, they form an extremely complicated and well-regulated energy and electron transfer network, and it is crucial to find out which components of these electron transfer routes are, directly or indirectly, in interaction with each other.

The majority of my thesis focuses on studying the cellular redox balance, another important aspect for applied bioproduction in cyanobacteria. Because both NADH and NADPH are fundamental reducing equivalents used for the maintenance of cellular metabolism, their regulation must always be taken into consideration when harnessing cyanobacteria for the production of desired compounds. The addition of an external carbon source, along with CO_2, significantly boosts the production of cyanobacterial biomass as well as high-value compounds. This provides interesting future avenues of research, since various waste-streams (e.g. the sugars from lignocellulose produced by the pulp and paper industry) have a capacity to boost biomass yield and serve the circular economy when used as a substrate. However, any change in the growth mode of cyanobacteria, e.g. from photoautotrophy to photomixotrophy or heterotrophy, concomitantly alters the means through which the NADP(H)/NAD(H) ratio is regulated, which highlights the need to understand how the intracellular NADH/NAD^+ status is maintained in cyanobacteria to make the best possible use of sugar catabolism.

7. ACKNOWLEDGEMENTS

I want to thank everybody at the Laboratory of Molecular Plant Biology for creating an environment where high-quality research and spirit to help each others meet in a very pleasant way. For financial support, the Academy of Finland, DPLMS doctoral program and Alfred Kordelin foundation are gratefully acknowledged.

I am deeply grateful to Academician Eva-Mari Aro for providing this exhilarating scientifical environment and for her support, trust and especially encouragement when times were tough. I am truly grateful to Associate Professor Yagut Allahverdiyeva-Rinne for introducing me to the world of biophysics, her endless support and teaching to believe in me. I am very thankful to Dr. Natalia Battchikova for teaching me tricks of molecular biology, showing the importance of precision in science and giving me several scientific writing lectures. I thank Professor Eevi Rintamäki for guidance through my studies and especially for help with the bureaucracy related to approaching disputation.

I want to acknowledge all my co-authors and collaborators for their valuable input to the research presented in this thesis. Special thanks to Dr. Dorota Muth-Pawlak for demonstrating me the efectivity of proteomics and to Assistant Professor Pauli Kallio for his inspiring way to do research. For technical support and keeping laboratories up and running Anniina, Eveliina, Kurt, Maija, Mika, Tapio and Vipu are acknowledged.

Dr. Taina Tyystjärvi is one of the biggest reasons why I got interested about photosynthesis and cyanobacteria in the first place and for that I am deeply grateful. Special thanks to Professor emerita Marjatta Raudaskoski for fruitful and cheerful discussions.

I am thankful to Prof. Nir Keren for agreeing to be my learned Opponent. I am also grateful to Professor Julian Eaton-Rye and Dr. Kirstin Gutekunst for critical reviewing the thesis. Henna Raudaskoski is thanked for revising the language.

I want to thank my fellow PhD students, past and present, who I was privileged to meet during these years. Especially I want to thank Lauri, Juha, Pasi, Vesa, Markus and former "laboratory master" Janne for several laughs and bad jokes. I am thankful to Masha, Henna and Luca for helping me to solve number of cyanobacteria-related problems and to Martina J. for advising me on practical things related to finishing thesis.

From all my heart, I want to thank my dear friends and family for all the love and support. Olette mittaamattoman tärkeitä. Erityiskiitos kuuluu kuitenkin rakkaimmalleni, Monicalle.

Cuomas

8. REFERENCES

Abramson, J., Riistama, S., Larsson, G., Jasaitis, A., Svensson-Ek, M., Laakkonen, L., Puustinen, A., Iwata, S., and Wikström, M. (2000). The structure of the ubiquinol oxidase from Escherichia coli and its ubiquinone binding site. Nat Struct Biol 7, 910-917.

Allahverdiyeva, Y., Isojärvi, J., Zhang, P., and Aro, E.M. (2015). Cyanobacterial Oxygenic Photosynthesis is Protected by Flavodiiron Proteins. Life (Basel) **5,** 716-743.

Allahverdiyeva, Y., Ermakova, M., Eisenhut, M., Zhang, P., Richaud, P., Hagemann, M., Cournac, L., and Aro, E.M. (2011). Interplay between flavodiiron proteins and photorespiration in *Synechocystis* sp. PCC 6803. J Biol Chem **286,** 24007-24014.

Allahverdiyeva, Y., Mustila, H., Ermakova, M., Bersanini, L., Richaud, P., Ajlani, G., Battchikova, N., Cournac, L., and Aro, E.M. (2013). Flavodiiron proteins Flv1 and Flv3 enable cyanobacterial growth and photosynthesis under fluctuating light. Proc Natl Acad Sci U S A **110,** 4111-4116.

Allen, M.M. (1984). Cyanobacterial cell inclusions. Annu Rev Microbiol **38,** 1-25.

Anderson, S.L., and McIntosh, L. (1991). Light-activated heterotrophic growth of the cyanobacterium *Synechocystis* sp. strain PCC 6803: a blue-light-requiring process. J Bacteriol **173,** 2761-2767.

Appel, J., Phunpruch, S., Steinmüller, K., and Schulz, R. (2000). The bidirectional hydrogenase of *Synechocystis* sp. PCC 6803 works as an electron valve during photosynthesis. Arch Microbiol **173,** 333-338.

Arteni, A.A., Ajlani, G., and Boekema, E.J. (2009). Structural organisation of phycobilisomes from *Synechocystis* sp. strain PCC6803 and their interaction with the membrane. Biochim Biophys Acta **1787,** 272-279.

Badger, M.R., and Price, G.D. (2003). CO2 concentrating mechanisms in cyanobacteria: molecular components, their diversity and evolution. J Exp Bot **54,** 609-622.

Badger, M.R., Price, G.D., Long, B.M., and Woodger, F.J. (2006). The environmental plasticity and ecological genomics of the cyanobacterial CO2 concentrating mechanism. J Exp Bot **57,** 249-265.

Bandeiras, T.M., Salgueiro, C.A., Huber, H., Gomes, C.M., and Teixeira, M. (2003). The respiratory chain of the thermophilic archaeon Sulfolobus metallicus: studies on the type-II NADH dehydrogenase. Biochim Biophys Acta **1557,** 13-19.

Barthel, S., Bernát, G., Seidel, T., Rupprecht, E., Kahmann, U., and Schneider, D. (2013). Thylakoid membrane maturation and PSII activation are linked in greening *Synechocystis* sp. PCC 6803 cells. Plant Physiol **163,** 1037-1046.

Battchikova, N., and Aro, EM. (2013) Proteomics in revealing the composition, acclimation and biogenesis of thylakoid membranes. In Herrero, A., and Flores, E. (eds.) The Cell Biology of Cyanobacteria. Caister Academic Press, UK, pp. 89-120.

Battchikova, N., Eisenhut, M., and Aro, E.M. (2011a). Cyanobacterial NDH-1 complexes: novel insights and remaining puzzles. Biochim Biophys Acta **1807,** 935-944.

Battchikova, N., Wei, L., Du, L., Bersanini, L., Aro, E.M., and Ma, W. (2011b). Identification of novel Ssl0352 protein (NdhS), essential for efficient operation of cyclic electron transport around photosystem I, in NADPH:plastoquinone oxidoreductase (NDH-1) complexes of *Synechocystis* sp. PCC 6803. J Biol Chem **286,** 36992-37001.

Beck, C., Knoop, H., Axmann, I.M., and Steuer, R. (2012). The diversity of cyanobacterial metabolism: genome analysis of multiple phototrophic microorganisms. BMC Genomics **13,** 56.

Beckmann, K., Messinger, J., Badger, M.R., Wydrzynski, T., and Hillier, W. (2009). On-line mass spectrometry: membrane inlet sampling. Photosynth Res **102,** 511-522.

Behrenfeld, M.J., Halsey, K.H., and Milligan, A.J. (2008). Evolved physiological responses of phytoplankton to their integrated growth environment. Philos Trans R Soc Lond B Biol Sci **363,** 2687-2703.

Bendall, D., and Manasse, R. (1995). Cyclic photophosphorylation and electron transport. Biochimica Et Biophysica Acta-Bioenergetics **1229,** 23-38.

Bergman, B., Rai, A., Johansson, C., and Soderback, E. (1993). Cyanobacterial-planst symbioses. Symbiosis **14,** 61-81.

Berkner, L., and Marshall, L. (1965). History of major athmospheric components. Proc Natl Acad Sci U S A **53,** 1215-1226.

Berry, S., Schneider, D., Vermaas, W.F., and Rögner, M. (2002). Electron transport routes in whole cells of *Synechocystis* sp. strain PCC 6803: the role of the cytochrome bd-type oxidase. Biochemistry **41,** 3422-3429.

Bersanini, L., Battchikova, N., Jokel, M., Rehman, A., Vass, I., Allahverdiyeva, Y., and Aro, E.M. (2014). Flavodiiron protein Flv2/Flv4-related photoprotective mechanism dissipates excitation pressure of PSII in cooperation with phycobilisomes in Cyanobacteria. Plant Physiol **164,** 805-818.

Bizouarn, T., Sazanov, L.A., Aubourg, S., and Jackson, J.B. (1996). Estimation of the H+/H- ratio of the reaction catalysed by the nicotinamide nucleotide transhydrogenase in chromatophores from over-

expressing strains of Rhodospirillum rubrum and in liposomes inlaid with the purified bovine enzyme. Biochim Biophys Acta **1273,** 4-12.

Björklöf, K., Zickermann, V., and Finel, M. (2000). Purification of the 45 kDa, membrane bound NADH dehydrogenase of Escherichia coli (NDH-2) and analysis of its interaction with ubiquinone analogues. FEBS Lett **467,** 105-110.

Blankenship, R.E. (1992). Origin and early evolution of photosynthesis. Photosynth Res **33,** 91-111.

Boulay, C., Wilson, A., D'Haene, S., and Kirilovsky, D. (2010). Identification of a protein required for recovery of full antenna capacity in OCP-related photoprotective mechanism in cyanobacteria. Proc Natl Acad Sci U S A **107,** 11620-11625.

Brocks, J., Buick, R., Summons, R., and Logan, G. (2003). A reconstruction of Archean biological diversity based on molecular fossils from the 2.78 to 2.45 billion-year-old Mount Bruce Supergroup, Hamersley Basin, Western Australia. Geochimica Et Cosmochimica Acta **67,** 4321-4335.

Bryant, D.A. (2003). The beauty in small things revealed. Proc Natl Acad Sci U S A **100,** 9647-9649.

Brändén, G., Gennis, R.B., and Brzezinski, P. (2006). Transmembrane proton translocation by cytochrome c oxidase. Biochim Biophys Acta **1757,** 1052-1063.

Campbell, D., Hurry, V., Clarke, A.K., Gustafsson, P., and Oquist, G. (1998). Chlorophyll fluorescence analysis of cyanobacterial photosynthesis and acclimation. Microbiol Mol Biol Rev **62,** 667-683.

Carrie, C., Murcha, M.W., Kuehn, K., Duncan, O., Barthet, M., Smith, P.M., Eubel, H., Meyer, E., Day, D.A., Millar, A.H., and Whelan, J. (2008). Type II NAD(P)H dehydrogenases are targeted to mitochondria and chloroplasts or peroxisomes in Arabidopsis thaliana. FEBS Lett **582,** 3073-3079.

Carrieri, D., Paddock, T., Maness, P., Seibert, M., and Yu, J. (2012). Photo-catalytic conversion of carbon dioxide to organic acids by a recombinant cyanobacterium incapable of glycogen storage. Energy & Environmental Science **5,** 9457-9461.

Chen, V.B., Arendall, W.B., Headd, J.J., Keedy, D.A., Immormino, R.M., Kapral, G.J., Murray, L.W., Richardson, J.S., and Richardson, D.C. (2010). MolProbity: all-atom structure validation for macromolecular crystallography. Acta Crystallogr D Biol Crystallogr **66,** 12-21.

Chen, X., Schreiber, K., Appel, J., Makowka, A., Fähnrich, B., Roettger, M., Hajirezaei, M.R., Sönnichsen, F.D., Schönheit, P., Martin, W.F., and Gutekunst, K. (2016). The Entner-Doudoroff pathway is an overlooked glycolytic route in cyanobacteria and plants. Proc Natl Acad Sci U S A **113,** 5441-5446.

Choi, M., Chang, C.Y., Clough, T., Broudy, D., Killeen, T., MacLean, B., and Vitek, O. (2014). MSstats: an R package for statistical analysis of quantitative mass spectrometry-based proteomic experiments. Bioinformatics **30,** 2524-2526.

Chukhutsina, V., Bersanini, L., Aro, E.M., and van Amerongen, H. (2015). Cyanobacterial Light-Harvesting Phycobilisomes Uncouple From Photosystem I During Dark-To-Light Transitions. Sci Rep **5,** 14193.

Cockell, C.S., and Raven, J.A. (2007). Ozone and life on the Archaean Earth. Philos Trans A Math Phys Eng Sci **365,** 1889-1901.

Cohen, S.E., and Golden, S.S. (2015). Circadian Rhythms in Cyanobacteria. Microbiol Mol Biol Rev **79,** 373-385.

Cooley, J.W., and Vermaas, W.F. (2001). Succinate dehydrogenase and other respiratory pathways in thylakoid membranes of *Synechocystis* sp. strain PCC 6803: capacity comparisons and physiological function. J Bacteriol **183,** 4251-4258.

Daley, S.M., Kappell, A.D., Carrick, M.J., and Burnap, R.L. (2012). Regulation of the cyanobacterial CO_2-concentrating mechanism involves internal sensing of NADP+ and α-ketogutarate levels by transcription factor CcmR. PLoS One **7,** e41286.

DeRuyter, Y., and Fromme, P. (2008) Molecular structure of the photosynthetic apparatus. In Herrero, A., and Flores, E. (eds) The cyanobacteria: Molecular biology, genomics and evolution. Caister Academic Press, Norfolk, UK, pp. 217-268.

Desplats, C., Mus, F., Cuiné, S., Billon, E., Cournac, L., and Peltier, G. (2009). Characterization of Nda2, a plastoquinone-reducing type II NAD(P)H dehydrogenase in chlamydomonas chloroplasts. J Biol Chem **284,** 4148-4157.

Draber, W., Trebst, A., and Harth, E. (1970). On a new inhibitor of photosynthetic electron-transport in isolated chloroplasts. Z Naturforsch B **25,** 1157-1159.

Drews, G. (2011) The evolution of cyanobacteria and photosynthesis. In Peschek, G.A., Obinger C., and Renger, G. (eds) Bioenergetic processes of cyanobacteria - From evolutionary singularity to ecological diversity. Springer, The Netherlands, pp. 265-284.

Dutilleul, C., Lelarge, C., Prioul, J.L., De Paepe, R., Foyer, C.H., and Noctor, G. (2005). Mitochondria-driven changes in leaf NAD status exert a crucial influence on the control of nitrate assimilation and the integration of carbon and nitrogen metabolism. Plant Physiol **139,** 64-78.

Eisenhut, M., Ruth, W., Haimovich, M., Bauwe, H., Kaplan, A., and Hagemann, M. (2008a). The photorespiratory glycolate metabolism is essential for cyanobacteria and might have been conveyed endosymbiontically to plants. Proc Natl Acad Sci U S A **105,** 17199-17204.

Eisenhut, M., Huege, J., Schwarz, D., Bauwe, H., Kopka, J., and Hagemann, M. (2008b). Metabolome phenotyping of inorganic carbon limitation in cells of the wild type and photorespiratory mutants of the cyanobacterium *Synechocystis* sp. strain PCC 6803. Plant Physiol **148,** 2109-2120.

Eisenhut, M., Aguirre von Wobeser, E., Jonas, L., Schubert, H., Ibelings, B.W., Bauwe, H., Matthijs, H.C., and Hagemann, M. (2007). Long-term response toward inorganic carbon limitation in wild type and glycolate turnover mutants of the cyanobacterium *Synechocystis* sp. strain PCC 6803. Plant Physiol **144,** 1946-1959.

Espinosa, J., Rodríguez-Mateos, F., Salinas, P., Lanza, V.F., Dixon, R., de la Cruz, F., and Contreras, A. (2014). PipX, the coactivator of NtcA, is a global regulator in cyanobacteria. Proc Natl Acad Sci U S A **111,** 2423-2430.

Fang, L., Ge, H., Huang, X., Liu, Y., Lu, M., Wang, J., Chen, W., Xu, W., and Wang, Y. (2017). Trophic Mode-Dependent Proteomic Analysis Reveals Functional Significance of Light-Independent Chlorophyll Synthesis in *Synechocystis* sp. PCC 6803. Mol Plant **10,** 73-85.

Fatihi, A., Latimer, S., Schmollinger, S., Block, A., Dussault, P.H., Vermaas, W.F., Merchant, S.S., and Basset, G.J. (2015). A Dedicated Type II NADPH Dehydrogenase Performs the Penultimate Step in the Biosynthesis of Vitamin K1 in *Synechocystis* and Arabidopsis. Plant Cell **27,** 1730-1741.

Feng, Y., Li, W., Li, J., Wang, J., Ge, J., Xu, D., Liu, Y., Wu, K., Zeng, Q., Wu, J.W., Tian, C., Zhou, B., and Yang, M. (2012). Structural insight into the type-II mitochondrial NADH dehydrogenases. Nature **491,** 478-482.

Field, C.B., Behrenfeld, M.J., Randerson, J.T., and Falkowski, P. (1998). Primary production of the biosphere: integrating terrestrial and oceanic components. Science **281,** 237-240.

Flamholz, A., Noor, E., Bar-Even, A., Liebermeister, W., and Milo, R. (2013). Glycolytic strategy as a tradeoff between energy yield and protein cost. Proc Natl Acad Sci U S A **110,** 10039-10044.

Flannery, D., and Walter, M. (2012). Archean tufted microbial mats and the Great Oxidation Event: new insights into an ancient problem. Australian Journal of Earth Sciences **59,** 1-11.

Forchhammer, K. (2004). Global carbon/nitrogen control by PII signal transduction in cyanobacteria: from signals to targets. FEMS Microbiol Rev **28,** 319-333.

Frazão, C., Silva, G., Gomes, C.M., Matias, P., Coelho, R., Sieker, L., Macedo, S., Liu, M.Y., Oliveira, S., Teixeira, M., Xavier, A.V., Rodrigues-Pousada, C., Carrondo, M.A., and Le Gall, J. (2000). Structure of a dioxygen reduction enzyme from Desulfovibrio gigas. Nat Struct Biol **7,** 1041-1045.

Fu, J., and Xu, X. (2006). The functional divergence of two glgP homologues in *Synechocystis* sp. PCC 6803. FEMS Microbiol Lett **260,** 201-209.

Fujisawa, T., Narikawa, R., Maeda, S., Watanabe, S., Kanesaki, Y., Kobayashi, K., Nomata J., Hanaoka, M., Watanabe, M., Ehira, S., Suzuki, E., Awai, K., and Nakamura, Y. (2017) CyanoBase: a large-scale update on its 20th anniversary. Nucleic Acids Res **45:** 551–554.

Fujita, Y. (1996). Protochlorophyllide reduction: a key step in the greening of plants. Plant Cell Physiol **37,** 411-421.

Gantt, E. (1994) Supramolecular membrane organization. In Bryant, D.A. (ed) The Molecular Biology of Cyanobacteria. Kluwer Academic Publishers, Dordrecht, pp. 119–138.

Gendrullis, M., Dyczmons, N., Gomolla, D., Gathmann, S., Bernát, G., Schneider, D., and Rögner, M. (2008) PetP, a new cytochrome b_6f subunit, and cytochrome bd oxidase – two potential regulatory players of cyanobacterial electron transport. In Allen, J.F., Gantt, E., Golbeck, J.H., and Osmond, B. (eds) Photosynthesis, Energy from the Sun. Springer, Dordrecht, pp. 585–589.

Glazer, A. (1984). Phycobilisome-a macromolecular complex optimized for light energy transfer. Biochim Biophys Acta **768,** 29-51.

Gomes, C.M., Bandeiras, T.M., and Teixeira, M. (2001). A new type-II NADH dehydrogenase from the archaeon Acidianus ambivalens: characterization and in vitro reconstitution of the respiratory chain. J Bioenerg Biomembr **33,** 1-8.

Grossmann, A., Schaefer, M., Chiang , G., and Collier, J. (1993). The phycobilisome, a light-harvesting complex responsive to environmantal conditions. Microbiol Rev **57,** 725-749.

Graan, T., and Ort, D.J. (1986) Detection of oxygen-evolving photosystem II centers inactive in plastoquinone reduction. Biochim Biophys Acta **852,** 320–330.

Gründel, M., Scheunemann, R., Lockau, W., and Zilliges, Y. (2012). Impaired glycogen synthesis causes metabolic overflow reactions and affects stress responses in the cyanobacterium *Synechocystis* sp. PCC 6803. Microbiology **158,** 3032-3043.

Hahn, A., and Schleiff, E. (2013) The Cell Envelope. In Herrero, A., and Flores, E. (eds.) The Cell Biology of Cyanobacteria. Caister Academic Press, UK, pp. 29 – 87.

Hart, S.E., Schlarb-Ridley, B.G., Bendall, D.S., and Howe, C.J. (2005). Terminal oxidases of cyanobacteria. Biochem Soc Trans **33,** 832-835.

Hashida, S.N., Takahashi, H., and Uchimiya, H. (2009). The role of NAD biosynthesis in plant development and stress responses. Ann Bot **103,** 819-824.

He, Z., Zheng, F., Wu, Y., Li, Q., Lv, J., Fu, P., and Mi, H. (2015) NDH-1L interacts with ferredoxin via the subunit NdhS in *Thermosynechococcus elongatus*. Photosynth Res **126,** 341–349.

Heikal, A., Nakatani, Y., Dunn, E., Weimar, M.R., Day, C.L., Baker, E.N., Lott, J.S., Sazanov, L.A., and Cook, G.M. (2014). Structure of the bacterial type II NADH dehydrogenase: a monotopic membrane protein with an essential role in energy generation. Mol Microbiol **91,** 950-964.

Helman, Y., Barkan, E., Eisenstadt, D., Luz, B., and Kaplan, A. (2005). Fractionation of the three stable oxygen isotopes by oxygen-producing and oxygen-consuming reactions in photosynthetic organisms. Plant Physiol **138,** 2292-2298.

Helman, Y., Tchernov, D., Reinhold, L., Shibata, M., Ogawa, T., Schwarz, R., Ohad, I., and Kaplan, A. (2003). Genes encoding A-type flavoproteins are essential for photoreduction of O_2 in cyanobacteria. Curr Biol **13,** 230-235.

Herranen, M., Battchikova, N., Zhang, P., Graf, A., Sirpiö, S., Paakkarinen, V., and Aro, E.M. (2004). Towards functional proteomics of membrane protein complexes in *Synechocystis* sp. PCC 6803. Plant Physiol **134,** 470-481.

Hickman, J., Kotovic, K., Miller, C., Warrener, P., Kaiser, B., Jurista, T., Budde, M., Cross, F., Roberts, J., and Carleton, M. (2013). Glycogen synthesis is a required component of the nitrogen stress response in Synechococcus elongatus PCC 7942. Algal Res **2,** 98-106.

Hihara, Y., Sonoike, K., Kanehisa, M., and Ikeuchi, M. (2003). DNA microarray analysis of redox-responsive genes in the genome of the cyanobacterium Synechocys*tis* sp. strain PCC 6803. J Bacteriol **185,** 1719-1725.

Hill, R., and Bendall, F. (1960) Function of two cytochrome components in chloroplasts: a working hypothesis. Nature **186,** 136-137.

Hoiczyk, E., and Hansel, A. (2000). Cyanobacterial cell walls: news from an unusual prokaryotic envelope. J Bacteriol **182,** 1191-1199.

Holland, H.D. (2006). The oxygenation of the atmosphere and oceans. Philos Trans R Soc Lond B Biol Sci **361,** 903-915.

Howitt, C.A., and Vermaas, W.F. (1998). Quinol and cytochrome oxidases in the cyanobacterium *Synechocystis* sp. PCC 6803. Biochemistry **37,** 17944-17951.

Howitt, C.A., Udall, P.K., and Vermaas, W.F. (1999). Type 2 NADH dehydrogenases in the cyanobacterium *Synechocystis* sp. strain PCC 6803 are involved in regulation rather than respiration. J Bacteriol **181,** 3994-4003.

Huang, C., Yuan, X., Zhao, J., and Bryant, D.A. (2003). Kinetic analyses of state transitions of the cyanobacterium Synechococcus sp. PCC 7002 and its mutant strains impaired in electron transport. Biochim Biophys Acta **1607,** 121-130.

Huang, F., Parmryd, I., Nilsson, F., Persson, A., Pakrasi, H., Andersson, B., and Norling, B. (2002). Proteomics of *Synechocystis* sp strain PCC 6803 - Identification of plasma membrane proteins. Molecular & Cellular Proteomics **1,** 956-966.

Iglesias, A.A., Kakefuda, G., and Preiss, J. (1991). Regulatory and Structural Properties of the Cyanobacterial ADPglucose Pyrophosphorylases. Plant Physiol **97,** 1187-1195.

Iwasaki, H., Williams, S.B., Kitayama, Y., Ishiura, M., Golden, S.S., and Kondo, T. (2000). A kaiC-interacting sensory histidine kinase, SasA, necessary to sustain robust circadian oscillation in cyanobacteria. Cell **101,** 223-233.

Iwata, S., Ostermeier, C., Ludwig, B., and Michel, H. (1995). Structure at 2.8 A resolution of cytochrome c oxidase from *Paracoccus denitrificans*. Nature **376,** 660-669.

Jackson, J.B. (2012). A review of the binding-change mechanism for proton-translocating transhydrogenase. Biochim Biophys Acta **1817,** 1839-1846.

Jackson, J.B., Leung, J.H., Stout, C.D., Schurig-Briccio, L.A., and Gennis, R.B. (2015). Review and Hypothesis. New insights into the reaction mechanism of transhydrogenase: Swivelling the dIII component may gate the proton channel. FEBS Lett **589,** 2027-2033.

Jeanjean, R., Matthijs , H., Onana, B., Havaux, M., and Joset, F. (1993). Exposure of the cyanobacterium *Synechocystis* PCC6803 to salt stress induces concerted changes in respiration and photosynthesis. Plant and Cell Physiology **34,** 1073-1079.

Jordan, P., Fromme, P., Witt, H.T., Klukas, O., Saenger, W., and Krauss, N. (2001). Three-dimensional structure of cyanobacterial photosystem I at 2.5 A resolution. Nature **411,** 909-917.

Joshua, S., and Mullineaux, C.W. (2004). Phycobilisome diffusion is required for light-state transitions in cyanobacteria. Plant Physiol **135,** 2112-2119.

Kada, S., Koike, H., Satoh, K., Hase, T., and Fujita, Y. (2003). Arrest of chlorophyll synthesis and differential decrease of Photosystems I and II in a cyanobacterial mutant lacking light-independent protochlorophyllide reductase. Plant Mol Biol **51,** 225-235.

Kaneko, T., Sato, S., Kotani, H., Tanaka, A., Asamizu, E., Nakamura, Y., Miyajima, N., Hirosawa, M., Sugiura, M., Sasamoto, S., Kimura, T., Hosouchi, T., Matsuno, A., Muraki, A., Nakazaki, N., Naruo, K., Okumura, S., Shimpo, S., Takeuchi, C., Wada, T., Watanabe, A., Yamada, M., Yasuda, M., and Tabata, S. (1996). Sequence analysis of the genome of the unicellular

cyanobacterium *Synechocystis* sp. strain PCC6803. II. Sequence determination of the entire genome and assignment of potential protein-coding regions (supplement). DNA Res **3,** 185-209.

Kaplan, A. (2017). On the cradle of CCM research: discovery, development, and challenges ahead. J Exp Bot. **68**, 3785-3796

Kerfeld, C.A., Sawaya, M.R., Tanaka, S., Nguyen, C.V., Phillips, M., Beeby, M., and Yeates, T.O. (2005). Protein structures forming the shell of primitive bacterial organelles. Science **309,** 936-938.

Kirilovsky, D. (2015). Modulating energy arriving at photochemical reaction centers: orange carotenoid protein-related photoprotection and state transitions. Photosynth Res **126,** 3-17.

Kirilovsky, D., and Kerfeld, C.A. (2013). The Orange Carotenoid Protein: a blue-green light photoactive protein. Photochem Photobiol Sci **12,** 1135-1143.

Klotz, A., Georg, J., Bučinská, L., Watanabe, S., Reimann, V., Januszewski, W., Sobotka, R., Jendrossek, D., Hess, W.R., and Forchhammer, K. (2016). Awakening of a Dormant Cyanobacterium from Nitrogen Chlorosis Reveals a Genetically Determined Program. Curr Biol **26,** 2862-2872.

Knoop, H., Zilliges, Y., Lockau, W., and Steuer, R. (2010). The metabolic network of *Synechocystis* sp. PCC 6803: systemic properties of autotrophic growth. Plant Physiol **154,** 410-422.

Kok, B., Forbush, B., and McGloin, M. (1970). Cooperation of charges in photosynthetic O2 evolution-I. A linear four step mechanism. Photochem Photobiol **11,** 457-475.

Kopecná, J., Komenda, J., Bucinská, L., and Sobotka, R. (2012). Long-term acclimation of the cyanobacterium *Synechocystis* sp. PCC 6803 to high light is accompanied by an enhanced production of chlorophyll that is preferentially channeled to trimeric photosystem I. Plant Physiol **160,** 2239-2250.

Kopp, R.E., Kirschvink, J.L., Hilburn, I.A., and Nash, C.Z. (2005). The Paleoproterozoic snowball Earth: a climate disaster triggered by the evolution of oxygenic photosynthesis. Proc Natl Acad Sci U S A **102,** 11131-11136.

Korn, A. (2010). Respective roles of the ferredoxin :NADP-oxidoreductase isoforms in the cyanobacterium *Synechocystis* sp. PCC 6803. In Biological Physics [physics.bio-ph] (Universitte Paris Sud- Paris XI).

Kranzler, C., Lis, H., Finkel, O.M., Schmetterer, G., Shaked, Y., and Keren, N. (2014). Coordinated transporter activity shapes high-affinity iron acquisition in cyanobacteria. ISME J **8,** 409-417.

Krieger-Liszkay, A., and Feilke, K. (2015). The Dual Role of the Plastid Terminal Oxidase PTOX: Between a Protective and a Pro-oxidant Function. Front Plant Sci **6,** 1147.

Krogh, A., Larsson, B., von Heijne, G., and Sonnhammer, E.L. (2001). Predicting transmembrane protein topology with a hidden Markov model: application to complete genomes. J Mol Biol **305,** 567-580.

Kruger, N.J., and von Schaewen, A. (2003). The oxidative pentose phosphate pathway: structure and organisation. Curr Opin Plant Biol **6,** 236-246.

Kucho, K., Okamoto, K., Tsuchiya, Y., Nomura, S., Nango, M., Kanehisa, M., and Ishiura, M. (2005). Global analysis of circadian expression in the cyanobacterium *Synechocystis* sp. strain PCC 6803. J Bacteriol **187,** 2190-2199.

Kufryk, G.I., Sachet, M., Schmetterer, G., and Vermaas, W.F. (2002). Transformation of the cyanobacterium *Synechocystis* sp. PCC 6803 as a tool for genetic mapping: optimization of efficiency. FEMS Microbiol Lett **206,** 215-219.

Kurisu, G., Zhang, H., Smith, J.L., and Cramer, W.A. (2003). Structure of the cytochrome b6f complex of oxygenic photosynthesis: tuning the cavity. Science **302,** 1009-1014.

Käll, L., Canterbury, J.D., Weston, J., Noble, W.S., and MacCoss, M.J. (2007). Semi-supervised learning for peptide identification from shotgun proteomics datasets. Nat Methods **4,** 923-925.

Labarre, J., Chauvat, F., and Thuriaux, P. (1989). Insertional mutagenesis by random cloning of antibiotic resistance genes into the genome of the cyanobacterium *Synechocystis* strain PCC 6803. J Bacteriol **171,** 3449-3457.

Latifi, A., Ruiz, M., and Zhang, C.C. (2009). Oxidative stress in cyanobacteria. FEMS Microbiol Rev **33,** 258-278.

Lea-Smith, D.J., Ross, N., Zori, M., Bendall, D.S., Dennis, J.S., Scott, S.A., Smith, A.G., and Howe, C.J. (2013). Thylakoid terminal oxidases are essential for the cyanobacterium *Synechocystis* sp. PCC 6803 to survive rapidly changing light intensities. Plant Physiol **162,** 484-495.

Letunic, I., and Bork, P. (2007). Interactive Tree Of Life (iTOL): an online tool for phylogenetic tree display and annotation. Bioinformatics **23,** 127-128.

Levi, C., and Preiss, J. (1976). Regulatory Properties of the ADP-Glucose Pyrophosphorylase of the Blue-Green Bacterium *Synechococcus* 6301. Plant Physiol **58,** 753-756.

Li, H., and Sherman, L.A. (2000). A redox-responsive regulator of photosynthesis gene expression in the cyanobacterium *Synechocystis* sp. Strain PCC 6803. J Bacteriol **182,** 4268-4277.

Li, M., Semchonok, D.A., Boekema, E.J., and Bruce, B.D. (2014). Characterization and evolution of tetrameric photosystem I from the thermophilic cyanobacterium Chroococcidiopsis sp TS-821. Plant Cell **26,** 1230-1245.

Liberton, M., Page, L.E., O'Dell, W.B., O'Neill, H., Mamontov, E., Urban, V.S., and Pakrasi, H.B. (2013). Organization and flexibility of cyanobacterial thylakoid membranes examined by neutron scattering. J Biol Chem **288,** 3632-3640.

Liberton, M., Saha, R., Jacobs, J.M., Nguyen, A.Y., Gritsenko, M.A., Smith, R.D., Koppenaal, D.W., and Pakrasi, H.B. (2016). Global Proteomic Analysis Reveals an Exclusive Role of Thylakoid Membranes in Bioenergetics of a Model Cyanobacterium. Mol Cell Proteomics **15,** 2021-2032.

Lindahl, M., and Florencio, F.J. (2003). Thioredoxin-linked processes in cyanobacteria are as numerous as in chloroplasts, but targets are different. Proc Natl Acad Sci U S A **100,** 16107-16112.

Lindahl, M., and Kieselbach, T. (2009). Disulphide proteomes and interactions with thioredoxin on the track towards understanding redox regulation in chloroplasts and cyanobacteria. J Proteomics **72,** 416-438.

Liu, H., Zhang, H., Niedzwiedzki, D.M., Prado, M., He, G., Gross, M.L., and Blankenship, R.E. (2013). Phycobilisomes supply excitations to both photosystems in a megacomplex in cyanobacteria. Science **342,** 1104-1107.

Llácer, J.L., Espinosa, J., Castells, M.A., Contreras, A., Forchhammer, K., and Rubio, V. (2010). Structural basis for the regulation of NtcA-dependent transcription by proteins PipX and PII. Proc Natl Acad Sci U S A **107,** 15397-15402.

Lyons, T.W., Reinhard, C.T., and Planavsky, N.J. (2014). The rise of oxygen in Earth's early ocean and atmosphere. Nature **506,** 307-315.

MacColl, R. (1998). Cyanobacterial phycobilisomes. J Struct Biol **124,** 311-334.

MacLean, B., Tomazela, D.M., Shulman, N., Chambers, M., Finney, G.L., Frewen, B., Kern, R., Tabb, D.L., Liebler, D.C., and MacCoss, M.J. (2010). Skyline: an open source document editor for creating and analyzing targeted proteomics experiments. Bioinformatics **26,** 966-968.

Mao, H.B., Li, G.F., Ruan, X., Wu, Q.Y., Gong, Y.D., Zhang, X.F., and Zhao, N.M. (2002). The redox state of plastoquinone pool regulates state transitions via cytochrome b6f complex in *Synechocystis* sp. PCC 6803. FEBS Lett **519,** 82-86.

Markson, J.S., Piechura, J.R., Puszynska, A.M., and O'Shea, E.K. (2013). Circadian control of global gene expression by the cyanobacterial master regulator RpaA. Cell **155,** 1396-1408.

Marreiros, B.C., Sena, F.V., Sousa, F.M., Batista, A.P., and Pereira, M.M. (2016). Type II NADH:quinone oxidoreductase family: phylogenetic distribution, structural diversity and evolutionary divergences. Environ Microbiol **18,** 4697-4709.

Marreiros, B.C., Sena, F.V., Sousa, F.M., Oliveira, A.S., Soares, C.M., Batista, A.P., and Pereira, M.M. (2017). Structural and Functional insights into the catalytic mechanism of the Type II NADH:quinone oxidoreductase family. Sci Rep **7,** 42303.

Matthijs, H.C., and Lubberding, H.J. (1988) Dark respiration in cyanobacteria. In Rogers, L.J., and Gallon, J.R. (eds) Biochemistry of the Algae and Cyanobacteria. Clarendon Press, Oxford, pp. 131–145.

Mazouni, K., Domain, F., Cassier-Chauvat, C., and Chauvat, F. (2004). Molecular analysis of the key cytokinetic components of cyanobacteria: FtsZ, ZipN and MinCDE. Mol Microbiol **52,** 1145-1158.

McConnell, M.D., Koop, R., Vasil'ev, S., and Bruce, D. (2002). Regulation of the distribution of chlorophyll and phycobilin-absorbed excitation energy in cyanobacteria. A structure-based model for the light state transition. Plant Physiol **130,** 1201-1212.

McDonald, A.E., Ivanov, A.G., Bode, R., Maxwell, D.P., Rodermel, S.R., and Hüner, N.P. (2011). Flexibility in photosynthetic electron transport: the physiological role of plastoquinol terminal oxidase (PTOX). Biochim Biophys Acta **1807,** 954-967.

Meeks, J.C., and Castenholz, R.W. (1971). Growth and photosynthesis in an extreme thermophile, *Synechococcus lividus* (Cyanophyta). Arch Mikrobiol **78,** 25-41.

Melo, A.M., Bandeiras, T.M., and Teixeira, M. (2004). New insights into type II NAD(P)H:quinone oxidoreductases. Microbiol Mol Biol Rev **68,** 603-616.

Mi, H., Endo, T., Schreiber, U., and Asada, K. (1992a). Donation of electrons from cytosolic components to the intersystem chain in the cyanobacterium *Synechococcus* sp. PCC 7002 as determined by the reduction of $P700^+$. Plant Cell Physiol **33,** 1099–1105.

Mi, H., Endo, T., Ogawa, T., and Kozi, A. (1992b). Thylakoid membrane-bound, NADPH-specific pyridine nucleotide dehydrogenase complex mediates cyclic electron transport in the cyanobacterium *Synechocystis* sp. PCC 6803. Plant Cell Physiol **36,** 661-668.

Miao, X., Wu, Q., Wu, G., and Zhao, N. (2003). Sucrose accumulation in salt-stressed cells of agp gene deletion-mutant in cyanobacterium *Synechocystis* sp PCC 6803. FEMS Microbiol Lett **218,** 71-77.

Michalecka, A.M., Svensson, A.S., Johansson, F.I., Agius, S.C., Johanson, U., Brennicke, A., Binder, S., and Rasmusson, A.G. (2003). Arabidopsis genes encoding mitochondrial type II NAD(P)H dehydrogenases have different evolutionary origin and show distinct responses to light. Plant Physiol **133,** 642-652.

Mimuro, M., and Katoh, T. (1991). Carotenoids in photostntheis-absorption, transfer and dissipation of light energy. Pure and Applied Chemistry **63,** 123-130.

Mitschke, J., Georg, J., Scholz, I., Sharma, C.M., Dienst, D., Bantscheff, J., Voss, B., Steglich, C., Wilde, A., Vogel, J., and Hess, W.R. (2011). An experimentally anchored map of transcriptional start sites in the model cyanobacterium *Synechocystis* sp. PCC6803. Proc Natl Acad Sci U S A **108,** 2124-2129.

Montgomery, B.L. (2015). Light-dependent governance of cell shape dimensions in cyanobacteria. Front Microbiol **6,** 514.

Montoya, J.P., Holl, C.M., Zehr, J.P., Hansen, A., Villareal, T.A., and Capone, D.G. (2004). High rates of N_2 fixation by unicellular diazotrophs in the oligotrophic Pacific Ocean. Nature **430,** 1027-1032.

Moroney, J.V., Jungnick, N., Dimario, R.J., and Longstreth, D.J. (2013). Photorespiration and carbon concentrating mechanisms: two adaptations to high O_2, low CO_2 conditions. Photosynth Res **117,** 121-131.

Mueller-Cajar, O., and Whitney, S.M. (2008). Evolving improved Synechococcus Rubisco functional expression in Escherichia coli. Biochem J **414,** 205-214.

Mullineaux, C.W. (2014a). Co-existence of photosynthetic and respiratory activities in cyanobacterial thylakoid membranes. Biochim Biophys Acta **1837,** 503-511.

Mullineaux, C.W. (2014b). Electron transport and light-harvesting switches in cyanobacteria. Front Plant Sci **5,** 7.

Mullineaux, C.W., and Allen, J.F. (1990). State 1-State 2 transitions in the cyanobacterium Synechococcus 6301 are controlled by the redox state of electron carriers between Photosystems I and II. Photosynth Res **23,** 297-311.

Mullineaux, C.W., and Emlyn-Jones, D. (2005). State transitions: an example of acclimation to low-light stress. J Exp Bot **56,** 389-393.

Muro-Pastor, A.M., Herrero, A., and Flores, E. (2001). Nitrogen-regulated group 2 sigma factor from *Synechocystis* sp. strain PCC 6803 involved in survival under nitrogen stress. J Bacteriol **183,** 1090-1095.

Mustila, H., Allahverdiyeva, Y., Isojärvi, J., Aro, E.M., and Eisenhut, M. (2014). The bacterial-type [4Fe-4S] ferredoxin 7 has a regulatory function under photooxidative stress conditions in the cyanobacterium *Synechocystis* sp. PCC 6803. Biochim Biophys Acta **1837,** 1293-1304.

Mustila, H., Paananen, P., Battchikova, N., Santana-Sánchez, A., Muth-Pawlak, D., Hagemann, M., Aro, E.M., and Allahverdiyeva, Y. (2016). The flavodiiron protein Flv3 functions as a homo-oligomer during stress acclimation and is distinct from the Flv1/Flv3 hetero-oligomer specific to the O_2 photoreduction pathway. Plant Cell Physiol **57,** 1468-1483.

Narainsamy, K., Cassier-Chauvat, C., Junot, C., and Chauvat, F. (2013). High performance analysis of the cyanobacterial metabolism via liquid chromatography coupled to a LTQ-Orbitrap mass spectrometer: evidence that glucose reprograms the whole carbon metabolism and triggers oxidative stress. Metabolomics **9,** 21-32.

Navarro, J.A., Durán, R.V., De la Rosa, M.A., and Hervás, M. (2005). Respiratory cytochrome c oxidase can be efficiently reduced by the photosynthetic redox proteins cytochrome c6 and plastocyanin in cyanobacteria. FEBS Lett **579,** 3565-3568.

Nelson, N., and Yocum, C.F. (2006). Structure and function of photosystems I and II. Annu Rev Plant Biol **57,** 521-565.

Nevo, R., Charuvi, D., Shimoni, E., Schwarz, R., Kaplan, A., Ohad, I., and Reich, Z. (2007). Thylakoid membrane perforations and connectivity enable intracellular traffic in cyanobacteria. EMBO J **26,** 1467-1473.

Nishimura, T., Takahashi, Y., Yamaguchi, O., Suzuki, H., Maeda, S., and Omata, T. (2008). Mechanism of low CO2-induced activation of the cmp bicarbonate transporter operon by a LysR family protein in the cyanobacterium Synechococcus elongatus strain PCC 7942. Mol Microbiol **68,** 98-109.

Noctor, G., Queval, G., and Gakière, B. (2006). NAD(P) synthesis and pyridine nucleotide cycling in plants and their potential importance in stress conditions. J Exp Bot **57,** 1603-1620.

Ogawa, T. (1991). A gene homologous to the subunit-2 gene of NADH dehydrogenase is essential to inorganic carbon transport of *Synechocystis* PCC6803. Proc Natl Acad Sci U S A **88,** 4275-4279.

Ohkawa, H., Pakrasi, H.B., and Ogawa, T. (2000). Two types of functionally distinct NAD(P)H dehydrogenases in *Synechocystis* sp. strain PCC6803. J Biol Chem **275,** 31630-31634.

Omata, T., Gohta, S., Takahashi, Y., Harano, Y., and Maeda, S. (2001). Involvement of a CbbR homolog in low CO_2-induced activation of the bicarbonate transporter operon in cyanobacteria. J Bacteriol **183,** 1891-1898.

Omata, T., Price, G.D., Badger, M.R., Okamura, M., Gohta, S., and Ogawa, T. (1999). Identification of an ATP-binding cassette transporter involved in bicarbonate uptake in the cyanobacterium *Synechococcus* sp. strain PCC 7942. Proc Natl Acad Sci U S A **96,** 13571-13576.

Orf, I., Schwarz, D., Kaplan, A., Kopka, J., Hess, W.R., Hagemann, M., and Klähn, S. (2016). CyAbrB2 Contributes to the Transcriptional Regulation of Low CO2 Acclimation in *Synechocystis* sp. PCC 6803. Plant Cell Physiol **57,** 2232-2243.

Osanai, T., Azuma, M., and Tanaka, K. (2007). Sugar catabolism regulated by light- and nitrogen-status in the cyanobacterium *Synechocystis* sp. PCC 6803. Photochem Photobiol Sci **6,** 508-514.

Osanai, T., Imamura, S., Asayama, M., Shirai, M., Suzuki, I., Murata, N., and Tanaka, K. (2006). Nitrogen induction of sugar catabolic gene expression in *Synechocystis* sp. PCC 6803. DNA Res **13,** 185-195.

Osanai, T., Imashimizu, M., Seki, A., Sato, S., Tabata, S., Imamura, S., Asayama, M., Ikeuchi, M., and Tanaka, K. (2009). ChlH, the H subunit of the Mg-chelatase, is an anti-sigma factor for SigE in *Synechocystis* sp. PCC 6803. Proc Natl Acad Sci U S A **106,** 6860-6865.

Osanai, T., Kuwahara, A., Iijima, H., Toyooka, K., Sato, M., Tanaka, K., Ikeuchi, M., Saito, K., and Hirai, M.Y. (2013). Pleiotropic effect of sigE over-expression on cell morphology, photosynthesis and hydrogen production in *Synechocystis* sp. PCC 6803. Plant J **76,** 456-465.

Osanai, T., Kanesaki, Y., Nakano, T., Takahashi, H., Asayama, M., Shirai, M., Kanehisa, M., Suzuki, I., Murata, N., and Tanaka, K. (2005). Positive regulation of sugar catabolic pathways in the cyanobacterium *Synechocystis* sp. PCC 6803 by the group 2 sigma factor sigE. J Biol Chem **280,** 30653-30659.

Paumann, M., Bernroitner, M., Lubura, B., Peer, M., Jakopitsch, C., Furtmüller, P.G., Peschek, G.A., and Obinger, C. (2004). Kinetics of electron transfer between plastocyanin and the soluble CuA domain of cyanobacterial cytochrome c oxidase. FEMS Microbiol Lett **239,** 301-307.

Peltier, G., Aro, E.M., and Shikanai, T. (2016). NDH-1 and NDH-2 Plastoquinone Reductases in Oxygenic Photosynthesis. Annu Rev Plant Biol **67,** 55-80.

Perkins, D.N., Pappin, D.J., Creasy, D.M., and Cottrell, J.S. (1999). Probability-based protein identification by searching sequence databases using mass spectrometry data. Electrophoresis **20,** 3551-3567.

Peschek, G.A., Obinger, C., and Paumann, M. (2004). The respiratory chain of blue-green algae (cyanobacteria). Physiol Plant **120,** 358-369.

Pettersen, E.F., Goddard, T.D., Huang, C.C., Couch, G.S., Greenblatt, D.M., Meng, E.C., and Ferrin, T.E. (2004). UCSF Chimera--a visualization system for exploratory research and analysis. J Comput Chem **25,** 1605-1612.

Pils, D., and Schmetterer, G. (2001). Characterization of three bioenergetically active respiratory terminal oxidases in the cyanobacterium *Synechocystis* sp. strain PCC 6803. FEMS Microbiol Lett **203,** 217-222.

Pils, D., Gregor, W., and Schmetterer, G. (1997). Evidence for in vivo activity of three distinct respiratory terminal oxidases in the cyanobacterium *Synechocystis* sp strain PCC6803. Fems Microbiology Letters **152,** 83-88.

Pisareva, T., Kwon, J., Oh, J., Kim, S., Ge, C., Wieslander, A., Choi, J.S., and Norling, B. (2011). Model for membrane organization and protein sorting in the cyanobacterium *Synechocystis* sp. PCC 6803 inferred from proteomics and multivariate sequence analyses. J Proteome Res **10,** 3617-3631.

Pitt, F.D., Mazard, S., Humphreys, L., and Scanlan, D.J. (2010). Functional characterization of *Synechocystis* sp. strain PCC 6803 pst1 and pst2 gene clusters reveals a novel strategy for phosphate uptake in a freshwater cyanobacterium. J Bacteriol **192,** 3512-3523.

Plohnke, N., Seidel, T., Kahmann, U., Rögner, M., Schneider, D., and Rexroth, S. (2015). The proteome and lipidome of *Synechocystis* sp. PCC 6803 cells grown under light-activated heterotrophic conditions. Mol Cell Proteomics **14,** 572-584.

Price, G.D. (2011). Inorganic carbon transporters of the cyanobacterial CO2 concentrating mechanism. Photosynth Res **109,** 47-57.

Pétriacq, P., de Bont, L., Tcherkez, G., and Gakière, B. (2013). NAD: not just a pawn on the board of plant-pathogen interactions. Plant Signal Behav **8,** e22477.

Pétriacq, P., de Bont, L., Genestout, L., Hao, J., Laureau, C., Florez-Sarasa, I., Rzigui, T., Queval, G., Gilard, F., Mauve, C., Guérard, F., Lamothe-Sibold, M., Marion, J., Fresneau, C., Brown, S., Danon, A., Krieger-Liszkay, A., Berthomé, R., Ribas-Carbo, M., Tcherkez, G., Cornic, G., Pineau, B., Gakière, B., and De Paepe, R. (2017). Photoperiod Affects the Phenotype of Mitochondrial Complex I Mutants. Plant Physiol **173,** 434-455.

Rasmussen, B., Fletcher, I.R., Brocks, J.J., and Kilburn, M.R. (2008). Reassessing the first appearance of eukaryotes and cyanobacteria. Nature **455,** 1101-1104.

Rees, D.C., and Howard, J.B. (2003). The interface between the biological and inorganic worlds: iron-sulfur metalloclusters. Science **300,** 929-931.

Richaud, C., Zabulon, G., Joder, A., and Thomas, J. (2001). Nitrogen or sulfur starvation differentially affects phycobilisome degradation and expression of the nblA gene in *Synechocystis* strain PCC 6803. Journal of Bacteriology **183,** 2989-2994.

Rippka, R., Deruelles, J., Waterbury, J., Herdman, M., and Stanier , R. (1979). Generic assignments, strain histories and properties of pure cultures of cyanobacteria. J Gen Microbiol **111,** 1-61.

Sali, A., and Blundell, T.L. (1993). Comparative protein modelling by satisfaction of spatial restraints. J Mol Biol **234,** 779-815.

Salomon, E., and Keren, N. (2011) Manganese limitation induces changes in the activity and in the organization of photosynthetic complexes in the cyanobacterium *Synechocystis* sp. strain PCC 6803. Plant Phys **155,** 571-579.

Sarsekeyeva, F., Zayadan, B.K., Usserbaeva, A., Bedbenov, V.S., Sinetova, M.A., and Los, D.A. (2015). Cyanofuels: biofuels from cyanobacteria. Reality and perspectives. Photosynth Res **125,** 329-340.

Sauer, U., Canonaco, F., Heri, S., Perrenoud, A., and Fischer, E. (2004). The soluble and membrane-bound transhydrogenases UdhA and PntAB have divergent

functions in NADPH metabolism of *Escherichia coli*. J Biol Chem **279,** 6613-6619.

Scherer, S. (1990). Do photosynthetic and respiratory electron transport chains share redox proteins? Trends Biochem Sci **15,** 458-462.

Schneegurt, M.A., Sherman, D.M., Nayar, S., and Sherman, L.A. (1994). Oscillating behavior of carbohydrate granule formation and dinitrogen fixation in the cyanobacterium *Cyanothece* sp. strain ATCC 51142. J Bacteriol **176,** 1586-1597.

Schneider, D., Berry, S., Rich, P., Seidler, A., and Rögner, M. (2001). A regulatory role of the PetM subunit in a cyanobacterial cytochrome b6f complex. J Biol Chem **276,** 16780-16785.

Schopf, J.W. (1993). Microfossils of the Early Archean Apex chert: new evidence of the antiquity of life. Science **260,** 640-646.

Schultze, M., Forberich, B., Rexroth, S., Dyczmons, N.G., Roegner, M., and Appel, J. (2009). Localization of cytochrome b6f complexes implies an incomplete respiratory chain in cytoplasmic membranes of the cyanobacterium *Synechocystis* sp. PCC 6803. Biochim Biophys Acta **1787,** 1479-1485.

Seedorf, H., Hagemeier, C.H., Shima, S., Thauer, R.K., Warkentin, E., and Ermler, U. (2007). Structure of coenzyme F420H2 oxidase (FprA), a di-iron flavoprotein from methanogenic Archaea catalyzing the reduction of O2 to H2O. FEBS J **274,** 1588-1599.

Sena, F.V., Batista, A.P., Catarino, T., Brito, J.A., Archer, M., Viertler, M., Madl, T., Cabrita, E.J., and Pereira, M.M. (2015). Type-II NADH:quinone oxidoreductase from Staphylococcus aureus has two distinct binding sites and is rate limited by quinone reduction. Mol Microbiol **98,** 272-288.

Sharma, V., Eckels, J., Taylor, G.K., Shulman, N.J., Stergachis, A.B., Joyner, S.A., Yan, P., Whiteaker, J.R., Halusa, G.N., Schilling, B., Gibson, B.W., Colangelo, C.M., Paulovich, A.G., Carr, S.A., Jaffe, J.D., MacCoss, M.J., and MacLean, B. (2014). Panorama: a targeted proteomics knowledge base. J Proteome Res **13,** 4205-4210.

Shen, G., Boussiba, S., and Vermaas, W.F. (1993). *Synechocystis* sp PCC 6803 strains lacking photosystem I and phycobilisome function. Plant Cell **5,** 1853-1863.

Shen, J.R. (2015). The Structure of Photosystem II and the Mechanism of Water Oxidation in Photosynthesis. Annu Rev Plant Biol **66,** 23-48.

Shevchenko, A., Wilm, M., Vorm, O., and Mann, M. (1996). Mass spectrometric sequencing of proteins silver-stained polyacrylamide gels. Anal Chem **68,** 850-858.

Shevchenko, A., Tomas, H., Havlis, J., Olsen, J.V., and Mann, M. (2006). In-gel digestion for mass spectrometric characterization of proteins and proteomes. Nat Protoc **1,** 2856-2860.

Shibata, M., Ohkawa, H., Katoh, H., Shimoyama, M., and Ogawa, T. (2002a). Two CO2 uptake systems in cyanobacteria: four systems for inorganic carbon acquisition in *Synechocystis* sp strain PCC6803. Functional Plant Biology **29,** 123-129.

Shibata, M., Katoh, H., Sonoda, M., Ohkawa, H., Shimoyama, M., Fukuzawa, H., Kaplan, A., and Ogawa, T. (2002b). Genes essential to sodium-dependent bicarbonate transport in cyanobacteria: function and phylogenetic analysis. J Biol Chem **277,** 18658-18664.

Schmetterer, G. (2016) The respiratory terminal oxidases (RTOs) of cyanobacteria. In Cramer W., and Kallas, T. (eds) Cytochrome Complexes: Evolution, Structures, Energy Transduction, and Signaling. Advances in Photosynthesis and Respiration (Including Bioenergy and Related Processes), vol 41. Springer, Dordrecht, pp. 331-355.

Sievers, F., Wilm, A., Dineen, D., Gibson, T.J., Karplus, K., Li, W., Lopez, R., McWilliam, H., Remmert, M., Söding, J., Thompson, J.D., and Higgins, D.G. (2011). Fast, scalable generation of high-quality protein multiple sequence alignments using Clustal Omega. Mol Syst Biol **7,** 539.

Silaghi-Dumitrescu, R., Kurtz, D.M., Ljungdahl, L.G., and Lanzilotta, W.N. (2005). X-ray crystal structures of Moorella thermoacetica FprA. Novel diiron site structure and mechanistic insights into a scavenging nitric oxide reductase. Biochemistry **44,** 6492-6501.

Singh, A.K., and Sherman, L.A. (2005). Pleiotropic effect of a histidine kinase on carbohydrate metabolism in *Synechocystis* sp. strain PCC 6803 and its requirement for heterotrophic growth. J Bacteriol **187,** 2368-2376.

Singh, R., Parihar, P., Singh, M., Bajguz, A., Kumar, J., Singh, S., Singh, V.P., and Prasad, S.M. (2017). Uncovering Potential Applications of Cyanobacteria and Algal Metabolites in Biology, Agriculture and Medicine: Current Status and Future Prospects. Front Microbiol **8,** 515.

Smith, A. (1982). Modes of cyanobacterial carbon metabolism. In Carr, N.G., and Whitton, B.A. (eds) The Biology of the Cyanobacteria, Oxford, Blackwell, pp. 47-86.

Stal, L.J. (2009). Is the distribution of nitrogen-fixing cyanobacteria in the oceans related to temperature? Environ Microbiol **11,** 1632-1645.

Stanier, R.Y., Kunisawa, R., Mandel, M., and Cohen-Bazire, G. (1971). Purification and properties of unicellular blue-green algae (order *Chroococcales*). Bacteriol Rev **35,** 171-205.

Steinhauser, D., Fernie, A.R., and Araújo, W.L. (2012). Unusual cyanobacterial TCA cycles: not broken just different. Trends Plant Sci **17,** 503-509.

Stoitchkova, K., Zsiros, O., Jávorfi, T., Páli, T., Andreeva, A., Gombos, Z., and Garab, G. (2007). Heat- and light-

induced reorganizations in the phycobilisome antenna of *Synechocystis* sp. PCC 6803. Thermo-optic effect. Biochim Biophys Acta **1767,** 750-756.

Strand, D.D., Fisher, N., and Kramer, D.M. (2017). The higher plant plastid NAD(P)H dehydrogenase-like complex (NDH) is a high efficiency proton pump that increases ATP production by cyclic electron flow. J Biol Chem **292,** 11850-11860.

Summerfield, T.C., Crawford, T.S., Young, R.D., Chua, J.P., Macdonald, R.L., Sherman, L.A., and Eaton-Rye, J.J. (2013). Environmental pH affects photoautotrophic growth of *Synechocystis* sp. PCC 6803 strains carrying mutations in the lumenal proteins of PSII. Plant Cell Physiol **54,** 859-874.

Suzuki, E., Ohkawa, H., Moriya, K., Matsubara, T., Nagaike, Y., Iwasaki, I., Fujiwara, S., Tsuzuki, M., and Nakamura, Y. (2010). Carbohydrate metabolism in mutants of the cyanobacterium *Synechococcus elongatus* PCC 7942 defective in glycogen synthesis. Appl Environ Microbiol **76,** 3153-3159.

Terashima, M., Specht, M., Naumann, B., and Hippler, M. (2010). Characterizing the anaerobic response of *Chlamydomonas reinhardtii* by quantitative proteomics. Mol Cell Proteomics **9,** 1514-1532.

Thomas, J.C., Ughy, B., Lagoutte, B., and Ajlani, G. (2006). A second isoform of the ferredoxin:NADP oxidoreductase generated by an in-frame initiation of translation. Proc Natl Acad Sci U S A **103,** 18368-18373.

Tyystjärvi, E., and Aro, E.M. (1996). The rate constant of photoinhibition, measured in lincomycin-treated leaves, is directly proportional to light intensity. Proc Natl Acad Sci U S A **93,** 2213-2218.

Tyystjärvi, T., Herranen, M., and Aro, E.M. (2001). Regulation of translation elongation in cyanobacteria: membrane targeting of the ribosome nascent-chain complexes controls the synthesis of D1 protein. Mol Microbiol **40,** 476-484.

Umena, Y., Kawakami, K., Shen, J.R., and Kamiya, N. (2011). Crystal structure of oxygen-evolving photosystem II at a resolution of 1.9 Å. Nature **473,** 55-60.

van Thor, J., Mullineaux, C., Matthijs, H., and Hellingwert, K. (1998). Light harvesting and state transitions in cyanobacteria. Botanica Acta **111,** 430-443.

van Thor, J.J., Jeanjean, R., Havaux, M., Sjollema, K.A., Joset, F., Hellingwerf, K.J., and Matthijs, H.C. (2000). Salt shock-inducible photosystem I cyclic electron transfer in *Synechocystis* PCC6803 relies on binding of ferredoxin:NADP(+) reductase to the thylakoid membranes via its CpcD phycobilisome-linker homologous N-terminal domain. Biochim Biophys Acta **1457,** 129-144.

Vass, I., Kirilovsky, D., and Etienne, A.L. (1999). UV-B radiation-induced donor- and acceptor-side modifications of photosystem II in the cyanobacterium *Synechocystis* sp. PCC 6803. Biochemistry **38,** 12786-12794.

Vermaas, W. (2001) Photosynthesis and respiration in cyanobacteria. In eLS, John Wiley & Sons, London, United Kingdom.

Vicente, J.B., Gomes, C.M., Wasserfallen, A., and Teixeira, M. (2002). Module fusion in an A-type flavoprotein from the cyanobacterium *Synechocystis* condenses a multiple-component pathway in a single polypeptide chain. Biochem Biophys Res Commun **294,** 82-87.

Vuorijoki, L., Isojärvi, J., Kallio, P., Kouvonen, P., Aro, E.M., Corthals, G.L., Jones, P.R., and Muth-Pawlak, D. (2016). Development of a quantitative SRM-based proteomics method to study iron metabolism of *Synechocystis* sp. PCC 6803. J Proteome Res **15,** 266-279.

Wan, N., DeLorenzo, D.M., He, L., You, L., Immethun, C.M., Wang, G., Baidoo, E.E.K., Hollinshead, W., Keasling, J.D., Moon, T.S., and Tang, Y.J. (2017). Cyanobacterial carbon metabolism: Fluxome plasticity and oxygen dependence. Biotechnol Bioeng **114,** 1593-1602.

Wang, H.L., Postier, B.L., and Burnap, R.L. (2004). Alterations in global patterns of gene expression in *Synechocystis* sp. PCC 6803 in response to inorganic carbon limitation and the inactivation of ndhR, a LysR family regulator. J Biol Chem **279,** 5739-5751.

Whitehead, L., Long, B.M., Price, G.D., and Badger, M.R. (2014). Comparing the in vivo function of α-carboxysomes and β-carboxysomes in two model cyanobacteria. Plant Physiol **165,** 398-411.

Whitney, S.M., Houtz, R.L., and Alonso, H. (2011). Advancing our understanding and capacity to engineer nature's CO_2-sequestering enzyme, Rubisco. Plant Physiol **155,** 27-35.

Wierenga, R.K., Terpstra, P., and Hol, W.G. (1986). Prediction of the occurrence of the ADP-binding beta alpha beta-fold in proteins, using an amino acid sequence fingerprint. J Mol Biol **187,** 101-107.

Williams, J.K.G. (1988) Construction of specific mutations in Photosystem-II photosynthetic reaction center by genetic-engineering methods in *Synechocystis* 6803. Method Enzymol **167,** 766–778.

Wilson, A., Boulay, C., Wilde, A., Kerfeld, C.A., and Kirilovsky, D. (2007). Light-induced energy dissipation in iron-starved cyanobacteria: roles of OCP and IsiA proteins. Plant Cell **19,** 656-672.

Wilson, A., Ajlani, G., Verbavatz, J.M., Vass, I., Kerfeld, C.A., and Kirilovsky, D. (2006). A soluble carotenoid protein involved in phycobilisome-related energy dissipation in cyanobacteria. Plant Cell **18,** 992-1007.

Wilson, W.A., Roach, P.J., Montero, M., Baroja-Fernández, E., Muñoz, F.J., Eydallin, G., Viale, A.M.,

and Pozueta-Romero, J. (2010). Regulation of glycogen metabolism in yeast and bacteria. FEMS Microbiol Rev **34,** 952-985.

Wolfe, G., Cunningham, F., Durnford, D., Green, B., and Gantt, E. (1994). Evidence for a common origin of chloroplast with light-harvesting complexes of different pigmentation. Nature **367,** 566-568.

Xu, L., Law, S.R., Murcha, M.W., Whelan, J., and Carrie, C. (2013a). The dual targeting ability of type II NAD(P)H dehydrogenases arose early in land plant evolution. BMC Plant Biol **13,** 100.

Xu, Y., Guerra, L.T., Li, Z., Ludwig, M., Dismukes, G.C., and Bryant, D.A. (2013b). Altered carbohydrate metabolism in glycogen synthase mutants of *Synechococcus* sp. strain PCC 7002: Cell factories for soluble sugars. Metab Eng **16,** 56-67.

Yagi, T. (1991). Bacterial NADH-quinone oxidoreductases. J Bioenerg Biomembr **23,** 211-225.

Yamauchi, Y., Kaniya, Y., Kaneko, Y., and Hihara, Y. (2011). Physiological roles of the cyAbrB transcriptional regulator pair Sll0822 and Sll0359 in *Synechocystis* sp. strain PCC 6803. J Bacteriol **193,** 3702-3709.

Yamori, W., and Shikanai, T. (2016). Physiological functions of cyclic electron transport around Photosystem I in sustaining photosynthesis and plant growth. Annu Rev Plant Biol **67,** 81-106.

Yan, J., Kurisu, G., and Cramer, W.A. (2006). Intraprotein transfer of the quinone analogue inhibitor 2,5-dibromo-3-methyl-6-isopropyl-p-benzoquinone in the cytochrome b_6f complex. Proc Natl Acad Sci U S A **103,** 69-74.

Yang, C., Hua, Q., and Shimizu, K. (2002). Metabolic flux analysis in *Synechocystis* using isotope distribution from 13C-labeled glucose. Metab Eng **4,** 202-216.

Yeremenko, N., Jeanjean, R., Prommeenate, P., Krasikov, V., Nixon, P.J., Vermaas, W.F., Havaux, M., and Matthijs, H.C. (2005). Open reading frame ssr2016 is required for antimycin A-sensitive photosystem I-driven cyclic electron flow in the cyanobacterium *Synechocystis* sp. PCC 6803. Plant Cell Physiol **46,** 1433-1436.

Yoon, H.S., Hackett, J.D., Ciniglia, C., Pinto, G., and Bhattacharya, D. (2004). A molecular timeline for the origin of photosynthetic eukaryotes. Mol Biol Evol **21,** 809-818.

You, L., Berla, B., He, L., Pakrasi, H.B., and Tang, Y.J. (2014) 13C-MFA delineates the photomixotrophic metabolism of *Synechocystis* sp. PCC 6803 under light- and carbon-sufficient conditions. Biotechnol J **9,** 684–692.

Young, J.D., Shastri, A.A., Stephanopoulos, G., and Morgan, J.A. (2011). Mapping photoautotrophic metabolism with isotopically nonstationary (13)C flux analysis. Metab Eng **13,** 656-665.

Zerulla, K., Ludt, K., and Soppa, J. (2016). The ploidy level of *Synechocystis* sp. PCC 6803 is highly variable and is influenced by growth phase and by chemical and physical external parameters. Microbiology **162,** 730-739.

Zhang, L.F., Yang, H.M., Cui, S.X., Hu, J., Wang, J., Kuang, T.Y., Norling, B., and Huang, F. (2009a). Proteomic analysis of plasma membranes of cyanobacterium *Synechocystis* sp. Strain PCC 6803 in response to high pH stress. J Proteome Res **8,** 2892-2902.

Zhang, P., Allahverdiyeva, Y., Eisenhut, M., and Aro, E.M. (2009b). Flavodiiron proteins in oxygenic photosynthetic organisms: photoprotection of photosystem II by Flv2 and Flv4 in *Synechocystis* sp. PCC 6803. PLoS One **4,** e5331.

Zhang, P., Battchikova, N., Jansen, T., Appel, J., Ogawa, T., and Aro, E.M. (2004). Expression and functional roles of the two distinct NDH-1 complexes and the carbon acquisition complex NdhD3/NdhF3/CupA/Sll1735 in *Synechocystis* sp PCC 6803. Plant Cell **16,** 3326-3340.

Zhang, P., Eisenhut, M., Brandt, A.M., Carmel, D., Silén, H.M., Vass, I., Allahverdiyeva, Y., Salminen, T.A., and Aro, E.M. (2012). Operon flv4-flv2 provides cyanobacterial photosystem II with flexibility of electron transfer. Plant Cell 24, 1952-1971.

Zhang, S., and Bryant, D.A. (2011). The tricarboxylic acid cycle in cyanobacteria. Science **334,** 1551-1553.

Zilliges, Y. (2014) Glycogen: a dynamic cellular sink and reservoir for carbon. In Flores, E., and Herrero, A. (eds) The Cell Biology of Cyanobacteria. Caister Academic Press, U.K., pp. 189.

Annales Universitatis Turkuensis

Turun yliopisto
University of Turku

Painosalama Oy, Turku, Finland 2018

ISBN 978-951-29-7146-6 (PRINT)
ISBN 978-951-29-7147-3 (PDF)
ISSN 0082-7002 (PRINT) | ISSN 2343-3175 (PDF)